INFORMATION TO USERS

This material was produced from a microfilm copy of the original document. While the most advanced technological means to photograph and reproduce this document have been used, the quality is heavily dependent upon the quality of the original submitted.

The following explanation of techniques is provided to help you understand markings or patterns which may appear on this reproduction.

1. The sign or "target" for pages apparently lacking from the document photographed is "Missing Page(s)". If it was possible to obtain the missing page(s) or section, they are spliced into the film along with adjacent pages. This may have necessitated cutting thru an image and duplicating adjacent pages to insure you complete continuity.

2. When an image on the film is obliterated with a large round black mark, it is an indication that the photographer suspected that the copy may have moved during exposure and thus cause a blurred image. You will find a good image of the page in the adjacent frame.

3. When a map, drawing or chart, etc., was part of the material being photographed the photographer followed a definite method in "sectioning" the material. It is customary to begin photoing at the upper left hand corner of a large sheet and to continue photoing from left to right in equal sections with a small overlap. If necessary, sectioning is continued again — beginning below the first row and continuing on until complete.

4. The majority of users indicate that the textual content is of greatest value, however, a somewhat higher quality reproduction could be made from "photographs" if essential to the understanding of the dissertation. Silver prints of "photographs" may be ordered at additional charge by writing the Order Department, giving the catalog number, title, author and specific pages you wish reproduced.

5. PLEASE NOTE: Some pages may have indistinct print. Filmed as received.

Xerox University Microfilms
300 North Zeeb Road
Ann Arbor, Michigan 48106

Downloaded from SHAREOK. Persistent Handle URL: https://hdl.handle.net/11244/4390

7815376

OWENS, JAMES LARRY
I. ELECTROCHEMICAL REDUCTION OF TETRAKETOPIPERAZINE. II. SPECTROELECTROCHEMICAL INVESTIGATIONS OF SOME BIOLOGICALLY IMPORTANT PURINES.

THE UNIVERSITY OF OKLAHOMA, PH.D., 1977

University Microfilms International 300 N. ZEEB ROAD, ANN ARBOR, MI 48106

THE UNIVERSITY OF OKLAHOMA

GRADUATE COLLEGE

I. ELECTROCHEMICAL REDUCTION OF TETRAKETOPIPERAZINE

II. SPECTROELECTROCHEMICAL INVESTIGATIONS OF SOME BIOLOGICALLY IMPORTANT PURINES

A DISSERTATION

SUBMITTED TO THE GRADUATE FACULTY

in partial fulfillment of the requirements for the degree of

DOCTOR OF PHILOSOPHY

By

James Larry Owens

Norman, Oklahoma

1977

I. ELECTROCHEMICAL REDUCTION OF TETRAKETO-PIPERAZINE

II. SPECTROELECTROCHEMICAL INVESTIGATIONS OF SOME BIOLOGICALLY IMPORTANT PURINES

APPROVED BY

DISSERTATION COMMITTEE

DEDICATION

To the gentleman on the review board of the Petroleum Research Fund of the American Chemical Society who thought that the study of purine electrooxidation intermediates by spectroelectrochemistry was impossible. Well, sir, it was possible, and it has been done!

ACKNOWLEDGEMENTS

Appreciation is expressed to Dr. Glenn Dryhurst for providing the problems discussed herein, for guidance and support during the course of this research, and for his excellence as a teacher and researcher.

Special thanks go to Dr. C. LeRoy Blank for his electronics expertise and for many helpful discussions. The friendship of Dr. Arnulf P. Hagen and Dr. Eddie C. Smith are gratefully appreciated.

Financial assistance from the Chemistry Department of the University of Oklahoma in the form of teaching assistantships and from Dr. Glenn Dryhurst in the form of research assistantships are acknowledged. Appreciation is also extended to the U.S. Naval Reserve and to the Veterans Administration for further financial support.

Much technical assistance, advice, and moral support has been given me by Dr. David L. McAllister, the senior graduate student in our lab during my early electrochemistry days. I am very grateful for his time and assistance, and for the friendship offered by him and his wife, Cathie. Discussions with chemistry faculty

members, postdoctoral fellows, and my fellow graduate students have been very helpful. Special thanks are accorded Mr. Michael T. Cleary and Mr. Henry A. Marsh, Jr.

Gratitude is also due the various departmental staffs including secretarial, library, technical, and supply. However, I must personally acknowledge the assistance of Mr. Ron Stermer, Mr. Joe Earls, and Mr. Fred Dillon in their timely preparation and repair of research equipment, and to Ms. Nancy Heinicke for the beautiful typing of this dissertation.

These acknowledgements would be incomplete without thanking Mr. and Mrs. Roy A. Good, Jr., who made my undergraduate years possible.

The ability and inspiration of my high school chemistry teacher, Mrs. Glenda Jane Phelps, provided the foundation upon which this degree was built. To her, I express my sincerest thanks.

How can I adequately thank my parents for all they have done for me? I am most indebted to them for their love and understanding, and their encouragement given me in my youth to read, inquire, and learn.

Finally, this work would not have been brought to completion without the firm understanding, love, patience, and encouragement of my wife, Barbara. Without her, the effort would not have been worth it.

TABLE OF CONTENTS

Page

LIST OF TABLES ix

LIST OF ILLUSTRATIONS xii

PART I. ELECTROCHEMICAL REDUCTION OF TETRAKETO-PIPERAZINE 1

Chapter

1. INTRODUCTION 1

2. RESULTS AND DISCUSSION 4

3. EXPERIMENTAL 45

4. SUMMARY 58

5. REFERENCES 60

PART II. SPECTROELECTROCHEMICAL INVESTIGATIONS OF SOME BIOLOGICALLY IMPORTANT PURINES 64

Chapter

1. INTRODUCTION 64

2. THIN-LAYER SPECTROELECTROCHEMICAL OXIDATION OF 5,6-DIAMINOURACIL 77

Introduction 77

Results 80

Discussion 96

Experimental 98

TABLE OF CONTENTS (continued)

Page

Summary 104

3. SPECTROELECTROCHEMICAL OXIDATION OF URIC ACID AND XANTHINE 106

Introduction 106

Results 107

Discussion 128

Experimental 131

Summary 134

4. EFFECT OF 9-METHYL SUBSTITUTION ON THE ELECTROCHEMICAL OXIDATION OF URIC ACID AND XANTHINE . 136

Introduction 136

Results and Discussion 137

Experimental 173

Summary 174

5. ELECTROCHEMICAL OXIDATION OF XANTHOSINE (9-RIBOSYLXANTHINE) 176

Introduction 176

Results and Discussion 177

Experimental 189

Summary 190

6. ANALYTICAL APPLICATIONS 192

A. Detection and Determination of Xanthine in Xanthosine by Electrochemical Methods . 193

Introduction 193

TABLE OF CONTENTS (continued)

		Page
	Results and Discussion	195
	Experimental	201
	Summary	207
B.	Separation of Some Low Molecular Weight Organic Compounds from Phosphate Buffers	208
	Introduction	208
	Results and Discussion	210
	Experimental	220
	Summary	227
7.	SUMMARY	229
8.	REFERENCES	232

LIST OF TABLES

Table — Page

PART I.

1. Variation of $E_{1/2}$ with Drop Time and Mercury Column Height at pH 2 for Tetraketopiperazine . 12
2. Separation of Anodic and Cathodic Peak Potentials for Peak I of Tetraketopiperazine at the HMDE 19
3. Variation of Peak Current Function with Voltage Scan Rate for Peak I_c of Tetraketopiperazine 24
4. Coulometric n-Values for the Electrochemical Reduction of Tetraketopiperazine 34
5. Limiting Current Values of Wave II as a Function of Electrolysis Time for Reduction of Tetraketopiperazine on Wave I 37

PART II.

1. Experimental n-Values for Electrochemical Oxidation of 5,6-Diaminouracil at Gold Minigrid Electrode 84

LIST OF TABLES (continued)

Page

2. First-Order Rate Constants for Hydrolysis of the Intermediate Formed on Electrochemical Oxidation of 5,6-Diaminouracil at a Gold Minigrid Electrode 91

3. Experimental n-Values for Electrochemical Oxidation of Uric Acid and Xanthine at a Gold Minigrid Electrode 121

4. Observed First-Order Rate Constants for the U.v.-absorbing Intermediate Formed on Electrochemical Oxidation of Uric Acid at a Gold Minigrid Electrode 127

5. Comparison of pK_a Values for Uric Acid, Xanthine, and Their 9-Methyl Derivatives . . . 139

6. Experimental n-Values Observed for Electrochemical Oxidation of 9-Methyluric Acid and 9-Methylxanthine at a Gold Minigrid Electrode . 149

7. Comparison of (A_{max}) intermediate/$(A_{initial})$ for Uric Acid and 9-Methylxanthine 158

8. Observed First-Order Rate Constants of U.v.-absorbing Intermediate Formed on Electrochemical Oxidation of 9-Methyluric Acid at a Gold Minigrid Electrode 164

LIST OF TABLES (continued)

Page

9. Observed First-Order Rate Constants for Reaction of the Intermediate (340 nm) on Electrochemical Oxidation of 9-Methylxanthine at a Gold Minigrid Electrode 166
10. Coulometric n-Values for the Electrochemical Oxidation of Xanthosine at the PGE 182
11. Typical Results for Coulometric Determination of Xanthine in Xanthosine 200
12. Coulometric Determination of Xanthine in Commercial Xanthosine Samples 202
13. Resolution Between Phosphate and Organic Component Chromatographic Peaks on Sephadex G-10 Column 216
14. Retention Volumes for Methanol AG 50W-X8 Column 218

LIST OF ILLUSTRATIONS

Figure Page

PART I.

1. D.C. Polarogram of Tetraketopiperazine at pH 2.0 6
2. Dependence of $E_{1/2}$ on pH for Tetraketopiperazine Waves I, II, and III 7
3. Variation of the Diffusion Current Constant, I, with pH for Tetraketopiperazine Waves I, II, and III 8
4. Linear Relationship Between Limiting Current and Concentration of Tetraketopiperazine at pH 2.0 11
5. Cyclic Voltammogram of Tetraketopiperazine at pH 2.0 at the PGE 16
6. Variation of E_p with pH for Tetraketopiperazine at the PGE 17
7. Cyclic Voltammograms of Tetraketopiperazine at pH 2.0 at the HMDE 26
8. Comparison of Experimental with Theoretical Current-Time Curves for the Electrochemical Reduction of Tetraketopiperazine at Wave III Potentials at the HMDE 32

LIST OF ILLUSTRATIONS (continued)

Figure		Page
9.	Proposed Reaction Scheme for the Electrochemical Reduction of Tetraketopiperazine . . .	41
10.	Mass Spectrum of Tetraketopiperazine Wave I Reduction Product	54
11.	Mass and i.r. Spectra of 2,5-Diketopiperazine	56
PART II.		
1.	Effect of pH and Nature of Electrode on Cyclic Voltammograms of 5,6-Diaminouracil at the PGE and Gold Foil Electrode	82
2.	Spectra of 5,6-Diaminouracil Electrolyzing at 0.35 V at pH 5 at a Gold Minigrid Electrode.	86
3.	Variation of Absorbance with Time for Intermediate Species ($A_{320\ nm}$) during Electrooxidation of 5,6-Diaminouracil at 0.35 V at pH 5 at a Gold Minigrid Electrode	90
4.	Kinetic Plot of Time versus Absorbance at 330 nm for Intermediate Species formed on Electrooxidation of 5,6-Diaminouracil	92
5.	Log of Rate Constant k_{obs} versus pH for Follow-up Hydrolysis Reaction of 5,6-Diaminouracil	95

LIST OF ILLUSTRATIONS (continued)

Figure		Page
6.	Cyclic Voltammograms of Uric Acid at pH 7.0 at RPGE, SPGE, and Gold Foil Electrode	109
7.	Cyclic Voltammograms of Uric Acid at pH 7.0 at Rough Spectroscopic Graphite, Rough WISGE, and Smooth WISGE	112
8.	Cyclic Voltammograms of Xanthine at pH 7.0 at RPGE, SPGE, Rough WISGE, and Smooth WISGE .	114
9A.	Cyclic Voltammograms of Uric Acid Between pH 4 and 9 at RPGE	117
9B.	Cyclic Voltammograms of Uric Acid Between pH 4 and 9 at SPGE	118
10.	Spectrum of Uric Acid Electrolyzing at 0.9 V at pH 7 at a Gold Minigrid Electrode	122
11.	(A) Variation of Absorbance with Time and (B) Kinetic Plot of Time versus Log Absorbance at 320 nm during Electrooxidation of Uric Acid at pH 7 at a Gold Minigrid Electrode . . .	126
12.	Wavelength vs. pH for the Two U.v.-absorbing Peaks of 9-Methyluric Acid and 9-Methyl-xanthine	138
13.	Cyclic Voltammograms of 9-Methyluric Acid at pH 7 at the RPGE and SPGE	141
14A.	Cyclic Voltammogram of 9-Methylxanthine at pH 8 at the RPGE	144

LIST OF ILLUSTRATIONS (continued)

Figure Page

14B. Cyclic Voltammogram of 20 mM 9-Methylxanthine at pH 8 at the RPGE 145

15. Cyclic Voltammograms at Various Stages during Electrolysis of 9-Methylxanthine at pH 7 at PGE 151

16. Spectrum of 9-Methyluric Acid Electrolyzing at 0.8 V at pH 7 at a Gold Minigrid Electrode 154

17. Spectrum of 9-Methylxanthine Electrolyzing at 1.2 V at pH 8 at a Gold Minigrid Electrode 157

18. Absorbance vs. Time for Electrooxidation of 9-Methyluric Acid at pH 7 at 284 nm 162

19. Kinetic Plot of Time vs. Log Absorbance at 284 nm for 9-Methyluric Acid 163

20. Absorbance vs. Time for Electrooxidation of 9-Methylxanthine at pH 8 at ca. 340 nm 165

21. Wavelength vs. pH for the Two U.v-absorbing Peaks of Xanthosine 178

22. Cyclic Voltammogram of Xanthosine at pH 7 at the RPGE 179

LIST OF ILLUSTRATIONS (continued)

Figure		Page
23.	Spectrum of Xanthosine Electrolyzing at 1.2 V at pH 8 at a Gold Minigrid Electrode . .	186
24.	Variation of E_p with pH for Xanthine and Xanthosine at PGE	197
25.	Linear Sweep Voltammogram of Xanthosine plus Xanthine at pH 7 at PGE	198
26.	Chromatograms of D-ribose, Allantoin and Urea in 1 M KH_2PO_4 with Water as Eluant	211
27.	Chromatograms of Alloxan and Parabanic Acid in 1 M KH_2PO_4 with Water as Eluant	212
28.	Chromatograms of Alloxan, Parabanic Acid, and Oxaluric Acid in 1 M KH_2PO_4 with 0.001 M HCl as Eluant	214

PART I

THE ELECTROCHEMICAL REDUCTION OF TETRAKETOPIPERAZINE

CHAPTER I

INTRODUCTION

Piperazine (I) and many of its derivatives have been known for some time to possess interesting pharmacological properties.[1] Piperazine and 2,5-dimethyl-

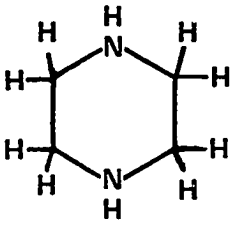

(I)

piperazine have been utilized in the treatment of rheumatism.[2] Other derivatives, such as the β-hydroxyethyl compounds[3] and their esters,[4] act as anesthetics or sedatives. Filariosis, a tropical parasitic disease, is often treated by various derivatives of N-carboxypiperazine.[5,6,7] Many piperazine derivatives display antihistamine activity.[8,9,10]

One group of derivatives of piperazine display quite different chemical properties from the simpler, more reduced piperazines.[11] These are the various forms of the ketopiperazines, including the monoketo-, 2,3-diketo, and 2,6-diketopiperazines. Another, the 2,5-diketopiperazines, have been rather extensively studied because of their close relationship to amino acids and their possible existence in various protein structures.[12] The 2,5-diketopiperazines can be considered to be anhydride derivatives of their respective amino acids. For example, the parent member of this group can be referred to as diketopiperazine, 2,5-diketopiperazine, or glycine anhydride (resulting from the elimination of water between two molecules of the amino acid glycine).

A final group of the ketopiperazines are the derivatives of tetraketopiperazine (II). This compound is one of a number of products resulting from the electrochemical oxidation of 6,7-dihydroxypteridine (III) at the pyrolytic graphite electrode (PGE) in acidic solution.[13]

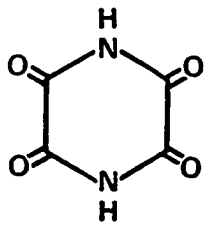

(II)

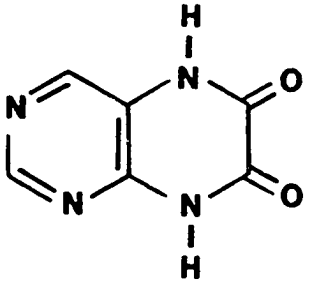

(III)

The yield of tetraketopiperazine was measured by a d.c. polarographic method (since it is electrochemically reducible at both the dropping mercury electrode (DME) and the PGE) based on the height of the first of its three polarographic reduction waves observed between pH 0-4. As this appears to give a simple, sensitive, quantitative, and qualitative procedure for tetraketopiperazine, a more detailed investigation of the electrochemical reduction mechanism was carried out.

CHAPTER 2

RESULTS AND DISCUSSION

Determinations of pK_a Values of Tetraketopiperazine

Values for the first and second pK_a of tetraketopiperazine were determined by potentiometric titration (see Experimental). The pK_a values so measured were 4.8 and 8.2. The first pK_a corresponds to a neutral molecule/anion equilibrium; the second pK_a corresponds to formation of a dianion.[14] Spectrophotometric determination of the pK_a values is not possible since tetraketopiperazine does not exhibit any significant absorption in the u.v.-visible region at concentrations up to 5.0 mM. (Only in pH 0.5 chloride buffer is there a small peak at ca. 230 nm. However, this peak is very near the solvent cutoff region and thus not well defined enough for absorption studies).

Stability of Tetraketopiperazine

D.c. polarography was used to study the stability of tetraketopiperazine as a function of pH and time because of the reported hydrolysis of this compound to

oxamide, oxalic acid, and oxamic acid in neutral aqueous solution.[13,15] In these studies, d.c. polarograms of solutions at a particular pH were run at intervals of ca. 30 minutes, and the decrease in the height of all three polarographic waves of tetraketopiperazine was observed. At pH 2 the polarographic wave height decreased only 15-20 percent over a period of 24 hours. However, at pH 3, hydrolysis was complete in about 4-5 hours, and above pH 4, complete hydrolysis occurred within a few minutes. Accordingly, detailed electrochemical studies of tetraketopiperazine above pH 3 were not undertaken.

D.C. Polarography

Over the pH range 0-6, tetraketopiperazine exhibits three polarographic waves (Fig. 1), the $E_{1/2}$ of which shift linearly more negative with increasing pH (Fig. 2). The dependence of $E_{1/2}$ on pH for these waves can be expressed as follows:

Wave I (pH 0-6); $E_{1/2} = -0.275-0.054$ pH

Wave II (pH 0-6); $E_{1/2} = -0.600-0.069$ pH

Wave III (pH 0-6); $E_{1/2} = -0.89-0.059$ pH

The variation of the diffusion current constant ($I = i_\ell/Cm^{2/3}t^{1/6}$) with pH is shown in Fig. 3. For Wave I, I is essentially constant (I = 2.8) above pH 1.0, and closely approximates the theoretical value for a 2e process (I = 3.2; $I = 607\ nD^{1/2}$, where $D = 7.24 \times 10^{-6}$ cm^2

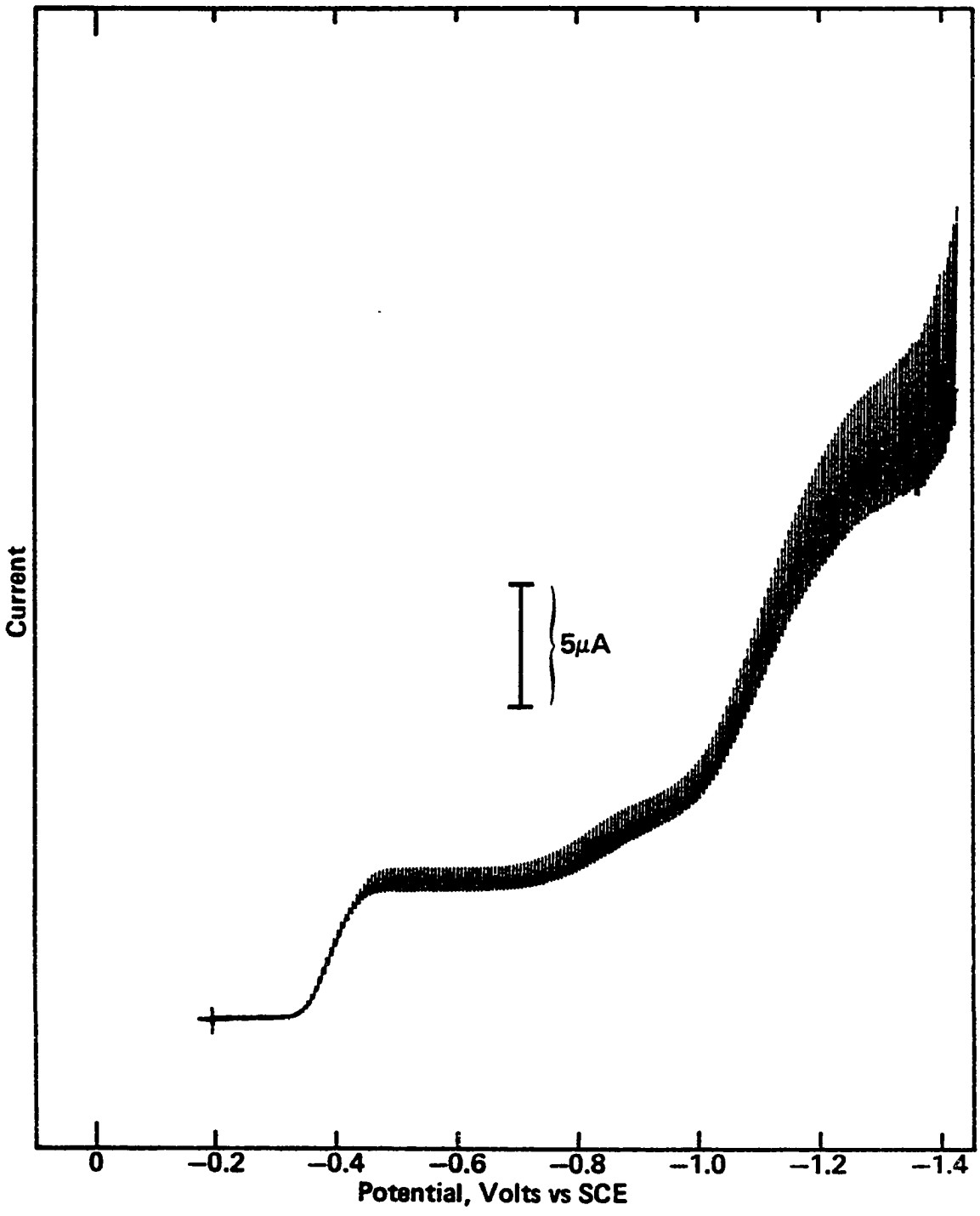

Figure 1. Typical d.c. polarogram of ca. 1 mM tetraketopiperazine in pH 2.0 McIlvaine buffer. Scan rate 2.5 mV sec^{-1}.

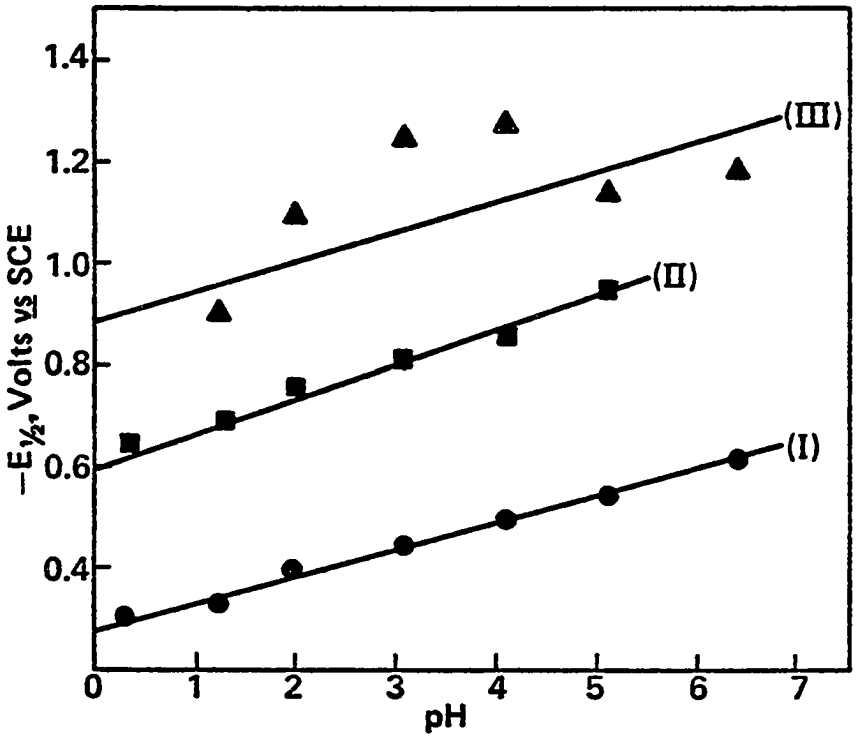

Figure 2. Dependence of $E_{1/2}$ on pH for tetraketopiperazine wave I (●—●), wave II (■—■), and wave III (▲—▲). Solutions ca. 1 mM. Scan rate 5 mV sec^{-1}.

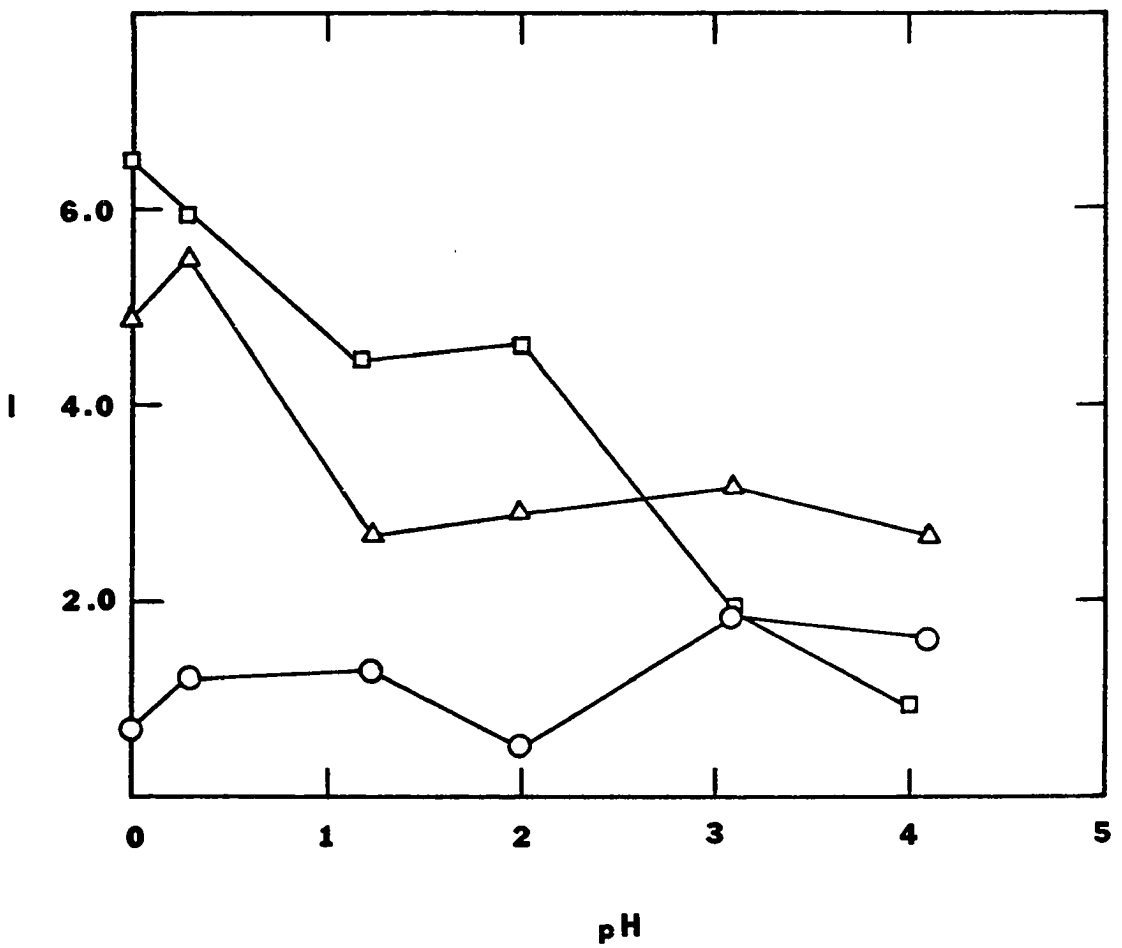

Figure 3. Variation of the diffusion current constant, I, with pH for tetraketopiperazine wave I (△—△), wave II (○—○), and wave III (□—□). Solutions ca. 1 mM. Scan rate 5 mV sec^{-1}.

sec^{-1} [a]). Below pH 1, Wave I becomes distorted due to a large maximum which results in a large variation in I below pH 1.

For Wave II, I was always appreciably smaller than for Wave I and had an average value of 1.6. Wave III, on the other hand, generally had a larger value of I (5-7 at low pH values) than for Wave I. As pH increased, Wave III appeared closer to background discharge potentials, making the determination of i_d difficult. It is likely that this effect is responsible for the apparent decrease in I.

A diffusion controlled process for Wave I is indicated by the dependence of the limiting current on the square root of the corrected mercury column height,[17] i.e., $i_\ell/h_{corr}^{1/2} = k$,[b] and from the value of the temperature coefficient[18] (1.5%/°C) at pH 2.[c] Likewise, a con-

---

[a] D for 5,6-diaminouracil,[16] a molecule similar in structure and size to tetraketopiperazine, was used because the diffusion coefficient of tetraketopiperazine is unobtainable from normal polarographic and potentiostatic means because the Wave I process is not entirely under diffusion control (vide infra).

[b] h_{corr}, also called "net" or "effective" height, is defined as the difference between the measured or experimental height and a term giving the interfacial back pressure at the mercury drop surface (i.e., $h_{corr} = h_{measured} - \frac{3.1}{(mt)^{1/3}}$). See reference 17 for more details.

[c] Temperature coefficient, T.C. $= \frac{2.3}{T_2-T_1} \log \frac{i_2}{i_1}$ where i is the diffusion current and T is the temperature (reference 18).

centration study over the range 0.1 to 2.0 m*M*, revealed a direct relationship between i_ℓ and concentration, which implies a diffusion controlled process[19] (Fig. 4). However, voltammetric and potentiostatic results (see later discussion) will indicate that the Wave I process is not entirely diffusion controlled and is partially under kinetic control.

Polarographic Wave II of tetraketopiperazine is under kinetic control as shown by its large temperature coefficient[18] (6.3%/°C at pH 2). In addition, at pH 0.5, for example, the limiting current for Wave II was independent of h_{corr} as expected for a kinetically controlled process.[20] Kinetic control is further supported by controlled potential coulometry and cyclic voltammetry (*vide infra*).

Owing to the closeness of Wave III to background discharge potentials, the type of controlling process involved could not be determined with any real confidence by means of i_ℓ *vs.* h_{corr} and temperature studies. However, potentiostatic methods, to be discussed later, will address this point.

The independence of the half-wave potential on the mercury drop time[21] indicated that Wave I is a reversible process (Table 1). However, the more common criterion for reversibility, the log plot method[22] (E_{dme} *vs.* log i/i_d-i), yielded a slope of 42.7 mV, a

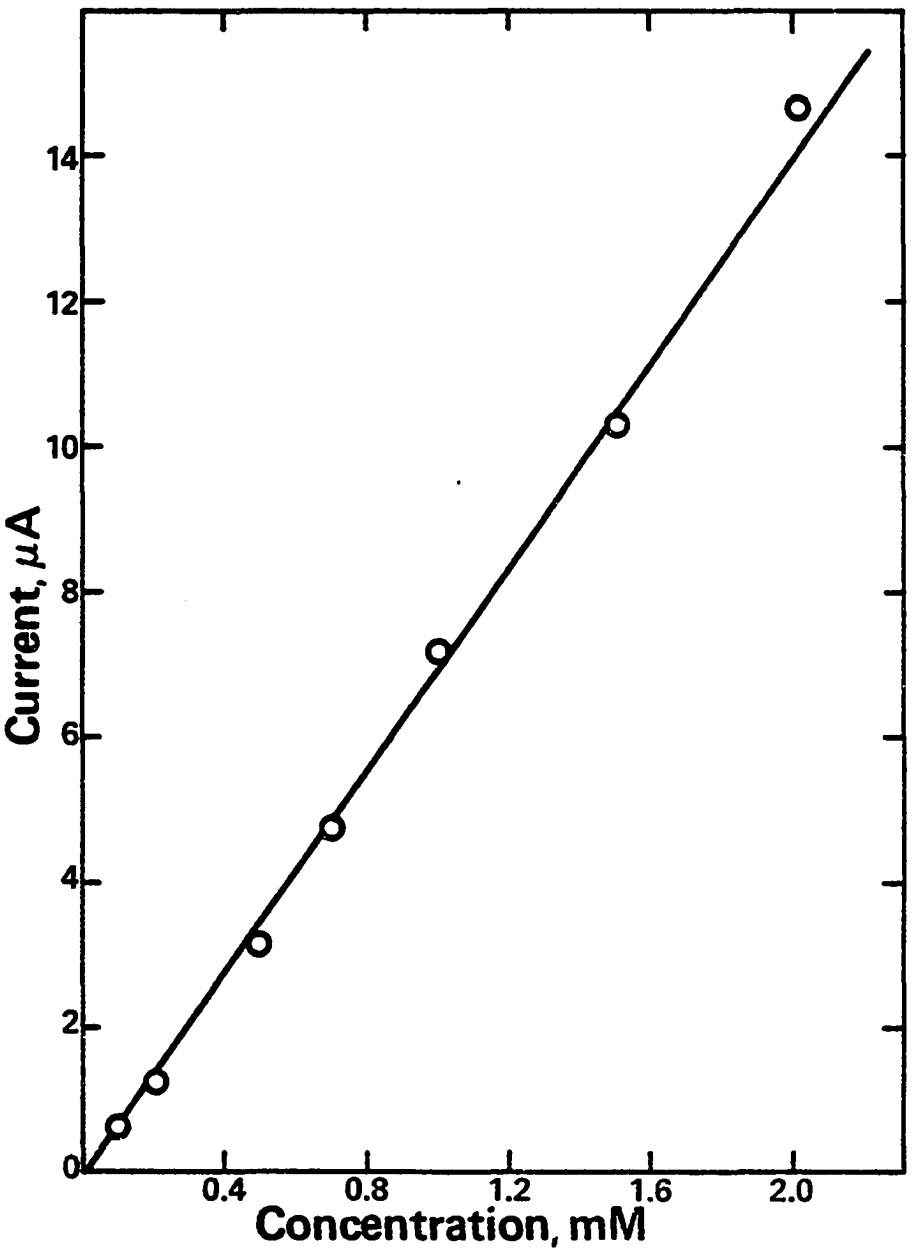

Figure 4. Linear relationship between limiting current (μA) and concentration of tetraketopiperazine in pH 2.0 McIlvaine buffer at the DME. Scan rate 5 mV sec^{-1}

TABLE 1

Variation of $E_{1/2}$ with Drop Time and Mercury Column Height at pH 2[a] for Tetraketopiperazine

Wave	Hg h_{corr},[b] cm	Drop time, t, sec.	$E_{1/2}$, Volts	$\Delta E_{1/2}/\Delta \log t$
I	28.8	7.52	-0.44	0.00
	40.0	5.44	-0.44	0.00
	49.6	4.40	-0.44	0.00
	59.8	3.64	-0.44	0.00
	71.4	3.05	-0.44	0.00
	79.9	2.71	-0.44	0.00
	89.6	2.44	-0.44	0.00
	99.6	2.18	-0.44	0.00
II	28.8	7.30	-0.76	-
	40.0	5.26	-0.79	0.21
	49.6	4.26	-0.79	0.00
	59.8	3.54	-0.80	0.12
	71.4	2.96	-0.81	0.13
	79.9	2.64	-0.82	0.10
	89.6	2.35	-0.825	0.10
	99.9	2.10	-0.83	0.10

[a] McIlvaine buffer

[b] $h_{corr} = h_{meas} - \frac{3.1}{(mt)^{1/3}}$

deviation from the theoretically predicted value of 30 mV for a perfectly reversible uncomplicated 2e process, and thus indicates some departure from reversibility, i.e., quasi-reversible.

Wave II is an irreversible process as evidenced by the dependence of $E_{1/2}$ on the mercury electrode drop time;[21] that is, $E_{1/2}$ becomes more negative as the drop time decreases (Table 1). Values of $\Delta E_{1/2}/\Delta$ log t for irreversible processes normally range from 15 to 300 mV.[21] From Table 1 it can be seen that the experimental value of $\Delta E_{1/2}/\Delta$ log t for Wave II lies between ca. 100-200 mV, well within the range expected for an irreversible system.

Adsorption Studies

Studies were undertaken to investigate the possibility of tetraketopiperazine being adsorbed at the DME. An electrocapillary curve was constructed by plotting drop time as a function of potential for both the background solution and a solution of tetraketopiperazine (ca. 1 mM). This curve has an almost parabolic shape in the absence of any adsorption, but adsorbed substances lower the drop time and therefore depress the curve.[23] However, for tetraketopiperazine no electrocapillary curve depression was observed. In addition, a.c. polarograms at various concentrations of tetraketopiperazine over the pH range 0.5 to 2 showed no indications of any

adsorption processes.[24]

Cyclic and Linear Scan Voltammetry

Linear scan voltammetry utilizes a linearly changing d.c. voltage ramp applied to a working electrode (pyrolytic graphite electrode, PGE, or hanging mercury drop electrode, HMDE, for example) with the current being monitored during the entire voltage scan or sweep. Cyclic voltammetry employs a triangular wave-form voltage applied to the electrode and again the current is recorded as a function of the applied potential. Voltage sweep rates normally range from 1 mV sec^{-1} to >1 V sec^{-1}. Since voltammetry is performed at a stationary electrode in a quiet solution and the time interval between reverse sweeps is relatively short, the products of a reduction, for example, are still in the vicinity of the electrode surface and thus, available for reoxidation on the positive-going segment of the voltage sweep. Cyclic voltammetry can thus provide information on the reversibility of the electron transfer process. In addition, cyclic voltammetry is a very useful technique for calculating electrode (heterogeneous) and coupled chemical (homogeneous) kinetic parameters which are important in mechanistic studies. Most importantly, cyclic voltammetry is used for qualitative evaluation of electrode processes (e.g., intermediates, follow-up reactions, etc.).

At both the PGE and HMDE, tetraketopiperazine exhibits three reduction peaks, I_c, II_c, and III_c (Figure 5), corresponding to polarographic waves I, II, and III, respectively. No oxidation peaks are observed on the initial positive-going scan at a clean PGE. However, once having scanned past peak I_c, and then reversing the scan (positive-going), one anodic peak, I_a, is observed just slightly positive of peak I_c. Figure 6 shows the dependence of the peak potentials on pH for peaks I_c, I_a, II_c, and III_c at the PGE. The variation of E_p with pH at 200 mV sec^{-1} (at the PGE) for the four peaks can be represented as follows:

peak I_c (pH 0-6); E_p = -0.3-0.061 pH

peak I_a (pH 0-6); E_p = -0.285-0.048 pH

peak II_c (pH 0-6); E_p = -0.7-0.075 pH

peak III_c (pH 0-6); E_p = -0.9-0.082 pH

Theoretically, for an uncomplicated reversible system the potential increment between the cathodic and anodic peaks, at sweep rates slow with respect to the rate of electron transfer, is given by[25]

$$E_p = (E_p)_a - (E_p)_c = \frac{58}{n} \text{ mV} \qquad (1)$$

where $(E_p)_a$ = anodic peak potential

$(E_p)_c$ = cathodic peak potential

n = number of electrons involved in electrode reaction

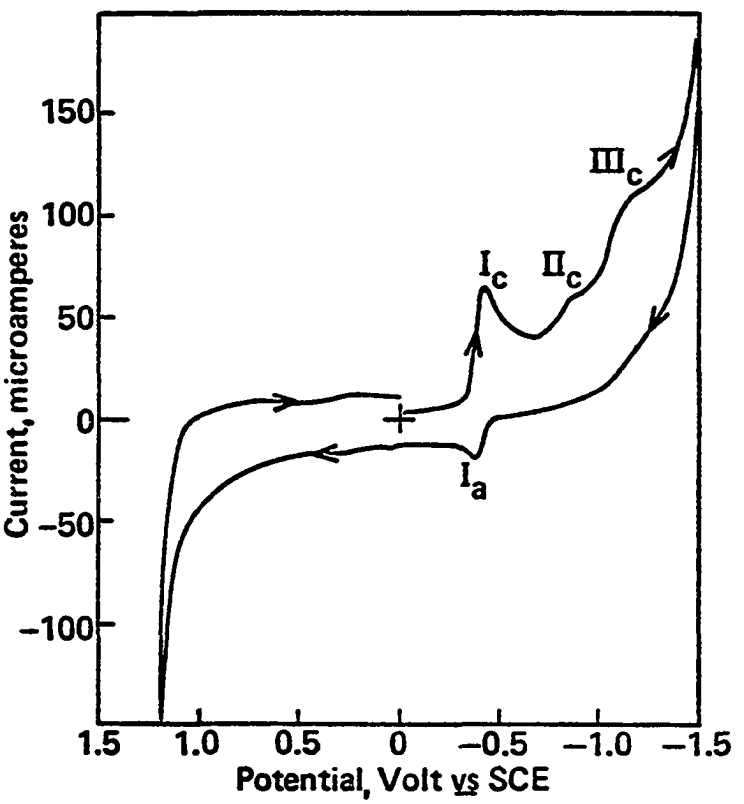

Figure 5. Cyclic voltammogram of 1 mM tetraketopiperazine in pH 2.0 McIlvaine buffer at the PGE. Voltage sweep pattern, 0.00 V → -1.50 V → 1.20 V → 0.00 V. Scan rate 200 mV sec^{-1}.

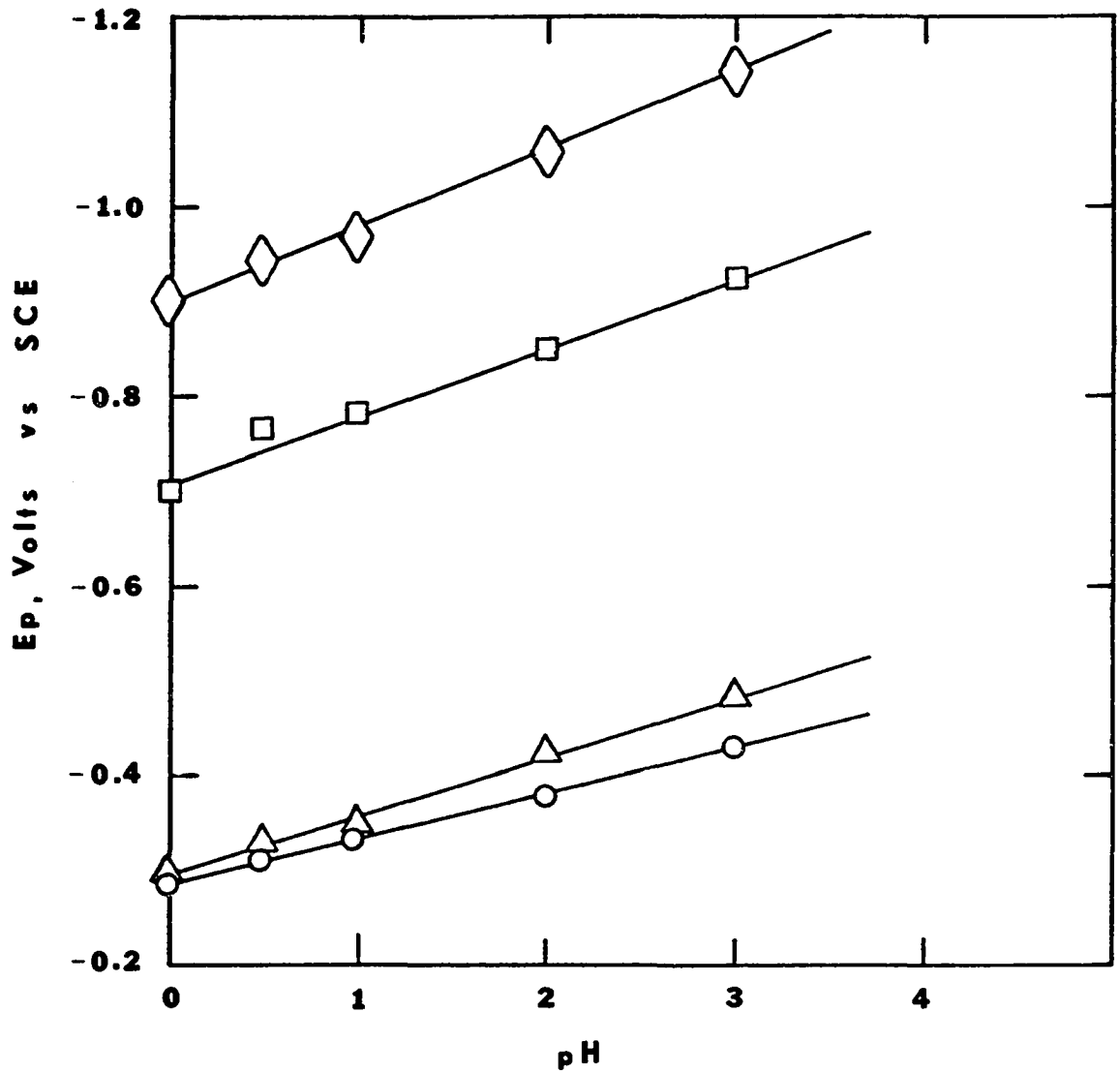

Figure 6. Variation of E_p with pH for tetraketopiperazine at the PGE. Cathodic peak I_c (△—△), peak II_c (□—□), peak III_c (◇—◇). Anodic peak I_a (○—○). Solutions ca. 1 mM. Scan rate 5 mV sec^{-1}.

Constant potential coulometry established that the electroreduction of tetraketopiperazine via the peak I_c process involves two electrons (vide infra). Therefore, if peaks I_c and I_a form a reversible couple, their expected peak potential separation should be close to 30 mV. Experimental values of ΔE_p for the I_c-I_a couple as a function of voltage sweep rate at the HMDE at pH 2 are given in Table 2. The peak potential separation initially decreases, then levels off and remains essentially constant (40 mV) as the sweep rate increases. Only at sweep rates greater than 0.2 V sec^{-1} are the experimental values of ΔE_p close to the theoretical value for an uncomplicated, 2e reversible process calculated from equation 1. This behavior suggests that the overall I_c-I_a electrode reaction is most probably affected by one or more complicating chemical processes.

Nicholson and Shain[26] have developed several diagnostic criteria to help characterize unknown systems in which preceding, following, or catalytic chemical reactions are coupled with reversible or irreversible charge transfer processes. Among these criteria is the examination of peak potential separation as a function of voltage sweep rate. Of six possible cases discussed by Nicholson and Shain (no evidence was found for two cases, involving catalytic reactions, and will thus not be considered) only two demonstrate behavior somewhat similar to that observed for the peak I_c-I_a system

TABLE 2

Separation of Anodic and Cathodic Peak Potentials for the Peak I System of Tetraketopiperazine at Various Sweep Rates at pH 2[a] at the HMDE

Voltage Sweep Rate, V sec^{-1}	$(E_p)_c$, Volts	$(E_p)_a$, Volts	ΔE_p[b], mV
0.01	-0.45	-0.365	85
0.02	-0.45	-0.37	80
0.05	-0.445	-0.375	70
0.10	-0.44	-0.38	60
0.20	-0.43	-0.38	50
0.50	-0.43	-0.39	40
1.0	-0.44	-0.40	40
2.0	-0.46	-0.42	40
5.0	-0.46	-0.42	40
10.0	-0.47	-0.43	40
20.0	-0.47	-0.43	40

[a] McIlvaine buffer

[b] $\Delta E_p = (E_p)_a - (E_p)_c$

(Table 2). One of these is a reversible chemical reaction preceding a reversible charge transfer (Case A). The other is a reversible charge transfer followed by an irreversible chemical reaction (Case B). It can be inferred from reference 26 that ΔE_p should continue to decrease as the sweep rate is increased for Case A while for Case B, the peak separation should decrease and then approach the constant, theoretical value of 30 mV. The experimental results imply, then, that the peak I_c process of tetraketopiperazine is probably a quasi-reversible charge transfer followed by an irreversible chemical reaction and may also involve a small, preceding kinetic contribution.

Another criterion is the direction in which the peak potential (here, the cathodic peak) shifts, positive or negative, as the voltage scan rate is increased.[26] Table 2 shows that the cathodic peak potential, $(E_p)_c$, shifts positive as the scan rate increases to ca. 1 V sec^{-1}, then shifts negative as the scan rate is further increased. For Case A, $(E_p)_c$ should shift positive as the voltage sweep rate increases which is observed experimentally for the slower sweep rates. $(E_p)_c$ should shift negative as the sweep rate increases for Case B, and at faster sweep rates (>1 V sec^{-1}) this is observed for peak I_c of tetraketopiperazine. Therefore, the electron transfer reaction for the peak I_c process is

most probably complicated by both a preceding and a follow-up chemical reaction.

By application of absolute rate theory, Nicholson[27] has developed a method for determining the heterogeneous rate constant for the electron transfer reaction from the separation of cathodic and anodic peak potentials. Numerical solution of an integral equation provides a correlation of this separation, ΔE_p, with a function ψ given by

$$\psi = \gamma^{\alpha} k_s / \pi^{1/2} D_o (nF/RT)^{1/2} v^{1/2} \qquad (2)$$

where $\gamma = (D_o/D_r)^{1/2}$

D_o = diffusion coefficient of oxidized species $cm^2\ sec^{-1}$

D_r = diffusion coefficient of reduced species, cm^2/sec

α = electron transfer coefficient

k_s = heterogeneous rate constant at E = E°' (formal potential)

n = number of electrons involved in electrode reaction

F = 96,500 coulombs

R = gas constant = 8.31 joules deg^{-1} mol

T = absolute temperature, °K

v = voltage sweep rate, Volts sec^{-1}

The variation of ψ with ΔE_p is presented in tables and

working curves in reference 27. To determine k_s, ΔE_p is measured at sweep rates where the system shows peak separation in excess of reversible behavior, i.e., $>\frac{59}{n}$ mV, and ψ is determined from the working curve. Since all other parameters are known, k_s can be calculated from equation 2. It is apparent after examining the working curve, however, that in order to calculate k_s by this method, the value of $\Delta E_p x$ n must increase as the voltage sweep rate increases. The data in Table 2 shows this is clearly not the case. Therefore, it appears that the combined effects of Case A and Case B type processes prevent the calculation of k_s by the method of Nicholson.

In order to obtain further information on the nature of the peak I_c process, the experimentally determined peak current function, $i_p/ACv^{1/2}$, was compared to the theoretical value for a 2e uncomplicated perfectly reversible electrode reaction calculated from the following equation:[28]

$$i_p = 2.69 \times 10^5 \, AD^{1/2} v^{1/2} n^{3/2} C \qquad (3)$$

where i_p = peak current, μA

A = electrode area, cm^2

D = diffusion coefficient, cm^2 sec^{-1}

v = sweep rate, V sec^{-1}

n = number of electrons involved in electrode

reaction

C = bulk concentration of electroactive species, m$\underline{M}$.

According to equation 3, the peak current function should be independent of voltage sweep rate. For a variation of sweep rate from 0.001 V sec^{-1} to 50 V sec^{-1}, the peak current function for peak I_c at pH 2 at the HMDE decreases and then remains essentially constant (Table 3), and is of a smaller magnitude than the theoretical value for an uncomplicated, 2$\underline{e}$ reversible reaction (1801 μA cm^{-2} m$\underline{M}^{-1}$ $v^{-1/2}$ $s^{1/2}$). Consideration of the diagnostic criterion in reference 26 shows that either a preceding chemical step (Case A), a follow-up chemical reaction (Case B), or both, could account for these observed experimental results. For Case B, the peak current function should decrease as the sweep rate increases and approach the theoretical value for an uncomplicated 2$\underline{e}$ reversible process (1801), while for Case A, the peak current function should steadily decrease and be of a smaller magnitude than that for the corresponding uncomplicated reversible process. Evaluation of the trends in the peak current function data for the peak I_c process indicates that both a preceding and a following chemical reaction are most probably affecting the electron transfer reaction.

Studies of the cyclic voltammetry of tetraketo-

TABLE 3

The Variation of Peak Current Function with Voltage Scan Rate for Peak I_c of Tetraketopiperazine at pH 2[a] at the HMDE

Scan rate V sec^{-1}	Theoretical Peak Current Function[b]	Experimental Peak Current Function[c]
0.001		2917
0.002		2562
0.005		2182
0.0075		1892
0.010		1724
0.020		1753
0.050		1710
0.10	1801	1715
0.20		1696
0.50		1743
1.0		1706
2.0		1723
5.0		1744
10.0		1734
20.0		1744
50.0		1741

[a] McIlvaine buffer

[b] $2.69 \times 10^5 D^{1/2} n^{3/2}$

[c] $i_p/AC\ v^{1/2}$, $\mu A\ cm^{-2}\ (m\underline{M}\ \ell^{-1})^{-1}\ V^{-1/2}\ sec^{1/2}$

piperazine as a function of voltage sweep rate disclosed a variation in the relative magnitude of the currents for peaks I_c and I_a with changing sweep rate. In a perfectly reversible, totally uncomplicated electrode reaction, i.e., no adsorption of product or reactant, or no preceding or following chemical reactions the peak heights of the I_c-I_a couple should be equal at any given sweep rate. If, however, a chemical reaction consumes some of the peak I_c product so that it is unavailable for oxidation in the peak I_a process, then peak I_a would be smaller than peak I_c. This effect would be more pronounced at slow sweep rates, where there is more time for the peak I_c product to be consumed. As the voltage sweep rate increases, the smaller amount of time between formation of the peak I_c product and its subsequent oxidation in the peak I_a process does not permit as much of the peak I_c product to be available for consumption in a follow-up chemical step and this, then, results in a larger peak I_a current. This behavior is indeed observed experimentally for tetraketopiperazine (Fig. 7) and is characteristic of an EC mechanism,[26] i.e., a charge transfer step followed by a chemical reaction (Case B).

Calculation of the homogeneous rate constant for an EC process from cyclic voltammetric data like that above (ratios of peak I_a to I_c as a function of sweep rate) as presented by Nicholson and Shain in reference 26

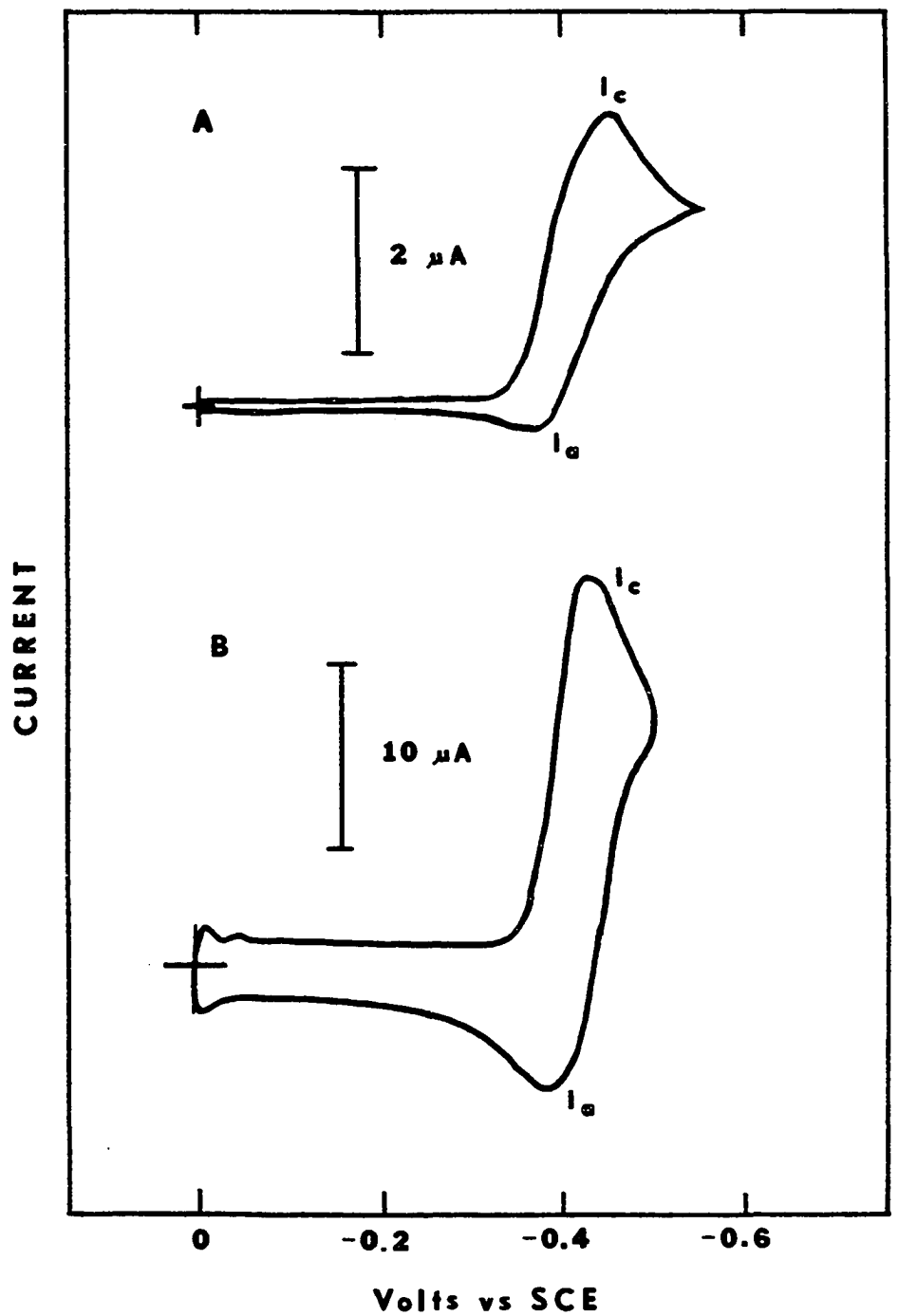

Figure 7. Cyclic voltammograms of 1 mM tetraketopiperazine in pH 2.0 McIlvaine buffer at the HMDE illustrating the effect of voltage sweep rate on the ratio of Peak I_c to Peak I_a. Sweep rate (A) 10 mV sec^{-1}, (B) 500 mV sec^{-1}.

is not possible with the tetraketopiperazine system because of the apparent preceding kinetic contribution to peak I_c, which causes a departure from diffusion control.

Peaks II_c and III_c of tetraketopiperazine gave no evidence for any reverse peaks on cyclic voltammetry at sweep rates up to 50 V sec^{-1}.

Potentiostatic Studies

To further clarify the nature of the Wave I and peak I_c process, potentiostatic current-time curves were measured over the pH range 0.5 to 2 in 0.05 to 5 mM solutions of tetraketopiperazine at potentials somewhat negative of E_p for peak I_c. The expression for the instantaneous current at a plane electrode under semi-infinite linear diffusion control is given by the Cottrell equation:[29]

$$i_t = \frac{nFAD^{1/2}C}{\pi^{1/2}t^{1/2}} \qquad (4)$$

where i_t = current at time (t) in amperes

n = total number of electrons

A = electrode area, cm^2

D = diffusion coefficient of electroactive species, $cm^2\ sec^{-1}$

C = concentration of electroactive species in moles ml^{-1}

For a particular value of concentration the value of $it^{1/2}$ should remain constant if the system is under diffusion control. In the case of tetraketopiperazine for periods up to 6-8 seconds, the product $it^{1/2}$ increased somewhat (as much as 15-20%) with increasing time at both the PGE and HMDE. (In the case of the HMDE, the Cottrell equation for a spherical electrode is adjusted by the term $4\pi rnFDC$ where r is the radius of the sphere. At times <10 seconds, linear diffusion to a planar electrode, i.e., equation 4, can be used with little error.[30]) At times greater than 8-10 seconds, linear diffusion is no longer the sole mode of mass transport and hence the Cottrell equation is no longer truly applicable.[30]

The potentiostatic current-time data was compared to that for alloxan (IV),

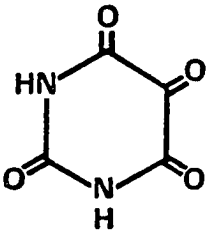

(IV)

a molecule structurally similar to tetraketopiperazine. The electroreduction of alloxan is reported to involve a carbonyl dehydration step prior to electron transfer[31] and the continual production of electroactive alloxan from the hydrated molecule apparently causes the value

of $it^{1/2}$ to increase with time rather than remain constant, for the value of $it^{1/2}$ for alloxan at pH 2 increased ca. 70 percent over a period of eight seconds. Because of the similarities in structure and current-time behavior between alloxan and tetraketopiperazine, it is quite reasonable to assume that a small, but significant preceding chemical reaction such as carbonyl hydration is also affecting the peak I_c electroreduction of tetraketopiperazine.

Owing to this apparent kinetic contribution to the peak I_c/Wave I process, double potential step chronoamperometry after the method of Bard, et al.,[32] could not be employed to investigate further the nature of the follow-up chemical reaction affecting the peak I_c process and to calculate a homogeneous rate constant for this reaction. This method depends upon complete diffusion control, i.e., constant values of $it^{1/2}$.

Potentiostatic current-time curves were measured at pH 0.5 and pH 2 for the Wave III/peak III_c process in order to obtain the n-value since constant potential coulometry proved rather difficult because these processes occur very near background discharge potentials. The value of n, however, was found to be both pH and time dependent. At short times, n = 4 seemed to fit the Cottrell equation while at longer times, n = 8 provided a better solution. Also, at the lower pH, less time was

required for the n-value of 8 to fit the equation better than at the higher pH. These results can be explained if the Wave III process proceeds via an ECE mechanism, that is, a process in which a chemical reaction is interposed between two charge transfer steps.

Alberts and Shain[33] have developed a potentiostatic method for studying an ECE process. In short, an ECE process can be depicted as: $A \xrightarrow{n_1 e} B \xrightarrow{k_f} C \xrightarrow{n_2 e} D.$ Regardless of the reversibility of the coupled chemical reaction, the normalized current is given to a first approximation by the equation:

$$i/FAD^{1/2}C = \frac{n_1 + n_2 (1-e^{-k_f t})}{t^{1/2}\pi^{1/2}} \qquad (5)$$

where n_1 = number of electrons in the first charge transfer step

n_2 = number of electrons in the second charge transfer step

k_f = homogeneous rate constant for the interposed chemical reaction, sec^{-1}

All other terms have their usual significance. There are two limiting cases: $k_f = \infty$ and $k_f = 0$. When k_f is infinitely large the interposed chemical reaction is so rapid that an $n_1 + n_2$ electron process is observed; when k_f is zero the rate of the chemical reaction is very slow so that only an n_1 electron process takes place. For each limiting case, equation 5 reduces to the Cottrell equation

for a $(n_1 + n_2)\underline{e}$ and $n_1\underline{e}$ process, respectively. In practice the potential of a stationary microelectrode (e.g., HMDE) is stepped to a value corresponding to the plateau of a polarographic wave (a region where all molecules of the electroactive substance reaching the electrode surface are immediately reduced) and the resulting current is monitored as a function of time. At short times the current corresponds to the first charge transfer step, but at longer times there is a transition to the current corresponding to both charge transfer steps. The time at which the transition occurs depends upon the rate of the interposed chemical reaction. Theoretical normalized current ($i_t/FAD^{1/2}C$) *vs.* time (or $t^{-1/2}$) curves were calculated for n = 4 and n = 8 for $k_f = 0$ and $k_f = \infty$, respectively. Experimental curves revealed that at very short times the normalized current was close to that expected for a $4\underline{e}$, diffusion controlled reaction while at longer times the curve deviated and approached the theoretical $8\underline{e}$ curve (Figure 8A,B). The transition from the $4\underline{e}$ to $8\underline{e}$ reaction took somewhat longer at pH 2 than at pH 0.5. This implies that the value of k_f becomes smaller as the pH increases. The value of k_f at each pH can be obtained from data of the type shown in Figure 8 by use of the working curves prepared by Alberts and Shain.[33] The experimental normalized current *vs.* $t^{-1/2}$ curves for $k_f = 4$ sec^{-1} (pH 0.5) and $k_f = 1$

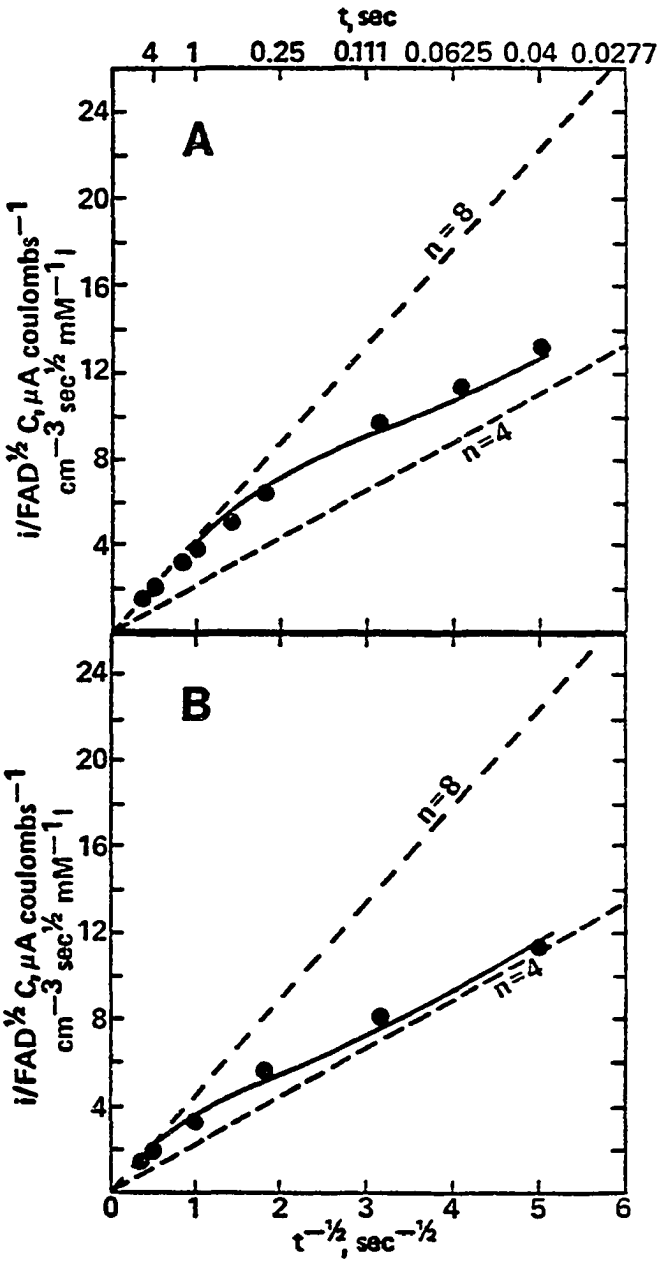

Figure 8. Comparison of the experimental with the theoretical normalized current-time curves for the electrochemical reduction of tetraketopiperazine at polarographic wave III potentials at the HMDE; (A) pH 0.5 KCl/HCl supporting electrolyte, k_f = 4 sec^{-1}; (B) pH 2.0 McIlvaine buffer, k_f = 1 sec^{-1}. Circles represent experimental values, solid lines are theoretical curves for the given rate constants calculated from equation 5. Dotted lines represent theoretical curves for uncomplicated 4e and 8e processes calculated from the Cottrell equation.

sec^{-1} (pH 2) agree quite well with the theoretical curves for k_f = 4 and 1 sec^{-1}, respectively (Figure 8).

Controlled Potential Electrolysis and Coulometry

Electrochemical reduction of tetraketopiperazine on the plateau of Wave I at pH 0.5 and 2.0 yielded a faradaic n-value of 2.0 ± 0.1 (Table 4). Electrolyses were done at both the stirred mercury pool and pyrolytic graphite electrodes. After completion of each electrolysis, d.c. polarography and voltammetry at the PGE revealed only the presence of Wave II or peak II_c. This indicated that the Wave III and peak III_c process represents another reduction pathway of the initial tetraketopiperazine in addition to the Wave I and peak I_c process. The u.v. spectrum after electrolysis at pH 2 revealed a small, broad peak at ca. 260 nm while that at pH 0.5 showed, in addition to the peak at 260 nm, a peak at ca. 215-220 nm. This peak occurs at or very near the background cutoff wavelength.

Electrolysis of tetraketopiperazine at Wave II resulted in n-values close to 6 (Table 4). The average of these values is 5.5. Two different methods were used in obtaining the n-value for the Wave II process. In the first method the electrolysis potential was initially set to a value corresponding to the plateau of Wave I, and then upon the complete disappearance of Wave I, in-

TABLE 4

Coulometric n-Values for the Electrochemical Reduction of Tetraketopiperazine

pH	Electrode	Controlled Potential/V		Initial Concentration of Tetraketo-piperazine/mM	n-value[g]
0.5[a]	Hg[b]	-0.40		1.0	1.91
2.0[c]	Hg[b]	-0.48	Wave I	1.0	1.90
2.0[c]	PGE[d]	-0.50		1.0	2.1
2.0[c]	Hg[b]	-0.95		0.1	6.7[e]
2.0[c]	Hg	-0.95		0.2	6.5[e]
2.0[c]	Hg	-0.95		0.5	5.6[e]
2.0[c]	Hg	-0.95	Wave II	2.0	5.0[e]
2.0[c]	Hg	-0.95		5.0	5.5[e]
2.0[c]	Hg	-0.95		0.2	5.5[f]
0.5[a]	Hg	-0.80		0.2	5.4[f]
0.5[a]	Hg	-0.80		0.1	6.0[f]
0.5[a]	Hg	-0.95		1.0	8.0[h]
2.0[c]	Hg	-1.20	Wave III	1.0	7.8[h]

[a]Chloride supporting electrolyte (KCl + HCl).

[b]Stirred mercury pool electrode.

[c]McIlvaine buffer.

[d]Pyrolytic graphite electrode.

[e]Direct electrolysis of tetraketopiperazine at wave II potentials, n-value for wave I (2.0) subtracted.

[f]Electrolysis first at wave I then, when complete, further electrolysis at wave II. n-Value refers to value obtained only at wave II potentials.

[g]Average of at least two replicate values.

[h]Direct electrolysis of tetraketopiperazine on wave III.

creased to a more negative value corresponding to the plateau of Wave II. This procedure allows the n-value for the Wave I process and for the Wave II process to be determined individually. In the second method the potential was initially set on the plateau of Wave II without prior electrolysis of Wave I. The n-value determined upon completion of electrolysis represents that for the sum of the Wave I and Wave II processes. If the n-value for the Wave I process (2.0) is subtracted from this total, then the number of electrons involved in the Wave II process can be obtained. Completion of electrolysis was confirmed by d.c. polarography, cyclic voltammetry, and u.v. spectrophotometry.

The n-value of ca. 6 for Wave II can be supported polarographically. The limiting current of Wave II after electrolysis of Wave I was ca. 3 times that of Wave I (a 2e process) observed before electrolysis of tetraketopiperazine. From the Ilkovič equation:[34]

$$i_d = 607\ nD^{1/2}m^{2/3}t^{1/6}C \qquad (6)$$

assuming D and C to be equal for both the Wave I and Wave II processes, it can be seen that the current should triple for a three-fold increase in the value of n.

On occasions when the electrolysis on the plateau of Wave II was interrupted soon after the commencement of the electrolysis, a small u.v. peak at ca. 375 nm could

be observed. However, upon completion of the electrolysis, no u.v. absorption could be observed at the latter wavelength. This phenomenon will be discussed later.

The reduction of tetraketopiperazine at Wave III potentials resulted in a coulometric n-value of ca. 8 (Table 4). This was further supported by the potentiostatic current-time data (vide supra). As in the Wave II process described above at pH 2, the u.v. spectrum for an interrupted electrolysis at potentials corresponding to the plateau of Wave III also gave a small peak at ca. 375 nm. This suggested that perhaps the same intermediate species were involved in both Wave II and Wave III processes.

A d.c. polarographic stability study of the Wave I electroreduction product indicated that this material undergoes a moderately rapid decomposition or hydrolysis. Thus, the limiting current decreased ca. 23% in about 24 hours and the wave completely disappeared in 4-5 days. Inspection of previous electrolyses disclosed that the longer this product was allowed to stand in solution, i.e., longer electrolyses times, the smaller the value of the Wave II limiting current (Table 5). Since the Wave I product decomposes in solution this leaves less material which gives rise to the Wave II process. The longer it is in solution, e.g., longer electrolysis times, the lower the values of i_ℓ and the observed Wave II n-value. Thus, the experimental n-value for the Wave II

TABLE 5

Limiting Current Values (of Wave II) as a Function of Electrolysis Time for Reduction of Tetraketopiperazine[a] on Wave I

Experiment	Time of Electrolysis, hours	i_ℓ, μA
1	45	3.5
2	28	4.9
3	6	6.5

[a]All concentrations are 1 m*M*

process is dependent upon the electrolysis time, especially when the electrolysis is performed initially at Wave I (allowing this material to stand in solution longer causing more decomposition).

The rapid decomposition of tetraketopiperazine with increasing pH prevented controlled potential electrolysis above pH 3.

Macroscale Electrolyses, Product Isolation and Characterization

In order to obtain a sufficient amount of material for product characterization, 1 to 5 m*M* solutions of tetraketopiperazine were electrolyzed at a mercury pool electrode. Electrolyses were normally carried out in 1 *M* acetic acid (pH 2.3) because of its ease of removal by lyophilization. In addition, the behavior of tetra-

ketopiperazine in this medium was judged to be quite representative of its behavior at lower and higher pH.

The product of Wave I could not be unequivocally identified because of its relative instability. It slowly decomposed in aqueous solution to a mixture of oxamide and glyoxylic acid which were identified by mass spectrometry, d.c. polarography, and paper chromatography (see Experimental). The crude Wave I product gave a mass spectrum with an apparent molecular ion peak at m/e = 126 (see Experimental). A compound having this molecular weight and which could also decompose to glyoxylic acid and oxamide is triketopyrazine (VII, Fig. 9). Compound VII has not been previously reported in the literature.

The major product of the Wave II and Wave III processes was isolated by fractional sublimation and identified as 2,5-diketopiperazine (glycine anhydride) by comparison of its mass and i.r. spectra and chromatographic R_f value with those of authentic 2,5-diketopiperazine (see Experimental). The lack of a u.v. absorption spectrum is expected in view of the nature of 2,5-diketopiperazine (XIII, Fig. 9). According to Pratt[35] diketopiperazines exhibit only very weak, if any, absorption in the u.v. region.

However, if electrolyses at either Wave II or Wave III potentials are interrupted, a u.v. spectrum showing a small peak with λ_{max} ca. 375 nm is obtained.

It is reasonable to assume that since the Wave II and Wave III processes have the same final reduction product they would also have a common intermediate. Kland-English and Garrison[36] showed that certain pyrazines (V), especially the keto- and hydroxypyrazines, gave a u.v.

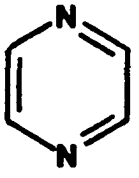

(V)

spectrum with λ_{max} values ranging from 300-400 nm, but principally at λ_{max} = 370 nm. This u.v. data strongly suggests that a pyrazine-type molecule could be the intermediate species in the Wave II and Wave III processes.

Reduction Scheme for Tetraketopiperazine

The proposed reduction scheme for tetraketopiperazine at both the mercury and pyrolytic graphite electrodes is shown in Figure 9. Polarographic and voltammetric data indicate that the electrochemical reduction of tetraketopiperazine (II, Fig. 9) at potentials corresponding to Wave I/Peak I_c proceeds by a quasi-reversible $2e/2H^+$ process. Potentiostatic experiments, polarography, and voltammetry suggest that while the electrode process is principally under diffusion control, there is also a minor contribution of kinetic control. The exact nature

of the process resulting in the partial kinetic control of the Wave I/Peak I_c process is not known. However, it seems reasonable to propose that some hydration-dehydration equilibrium of tetraketopiperazine occurs, imparting some kinetic control to the electrode process in much the same way as is observed for alloxan (vide supra).

In addition, constant potential electrolysis, mercury column height and temperature studies, and cyclic voltammetric voltage sweep rate studies (ratio of Peak I_a/Peak I_c increases with increasing sweep rate) clearly indicate that an EC type mechanism may be involved.

The product of the Wave I/Peak I_c process is proposed to be triketopyrazine (VII, Fig. 9) based on mass spectral data. Species VII is unstable and slowly decomposes to glyoxylic acid (VIII, Fig. 9) and oxamide (IX, Fig. 9) which have been positively identified.

Accordingly, the Wave I/Peak I_c process is proposed to be a $2e/2H^+$ reduction of tetraketopiperazine (II, Fig. 9) to 2-hydroxytriketopiperazine (VI, Fig. 9) which then undergoes a rapid dehydration to give triketopyrazine (VII, Fig. 9). This reaction is analogous to that proposed by Furlani[37] for the electrochemical reduction of 2,3-dihydroxyquinoxaline (X).

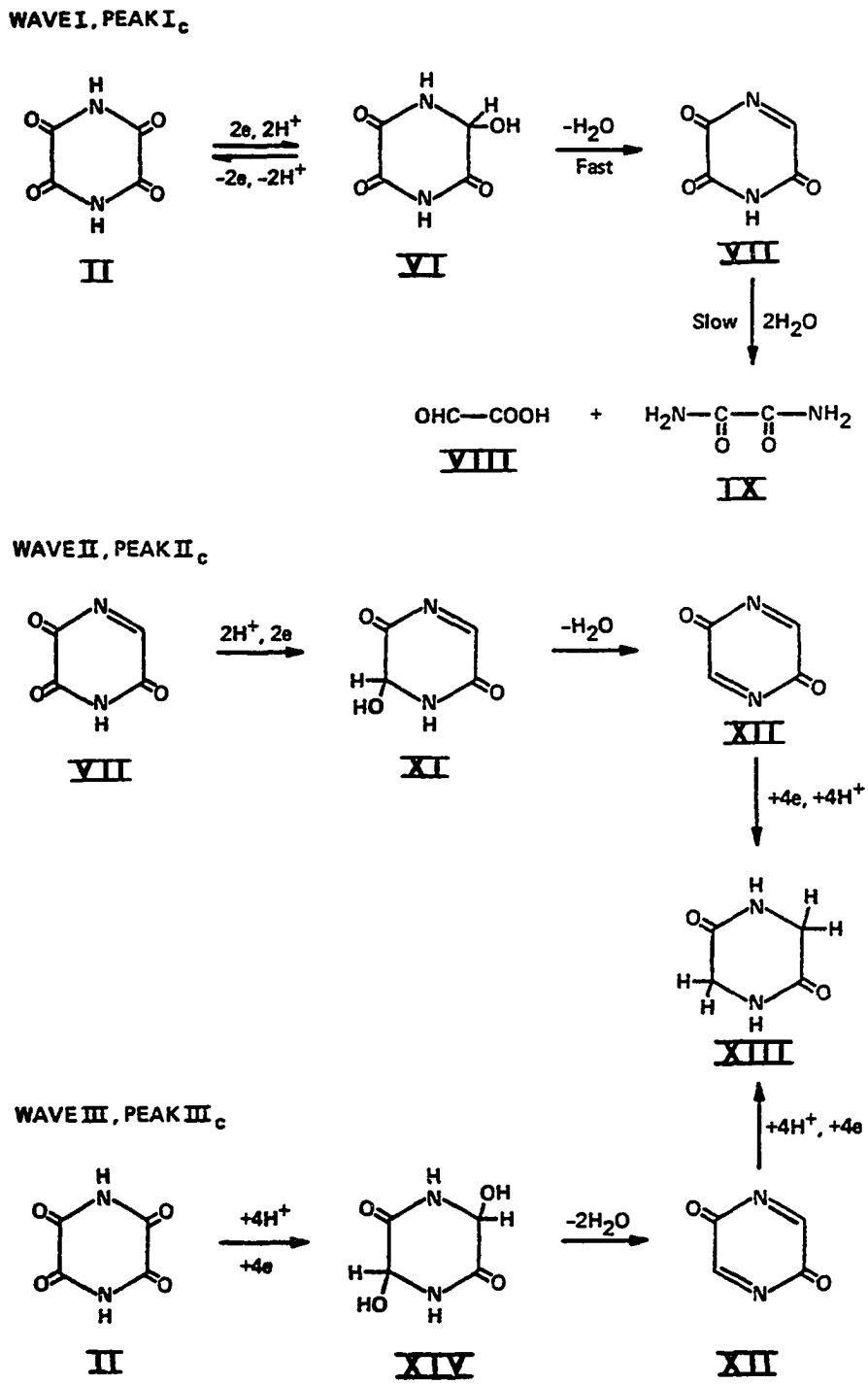

Figure 9. Proposed reaction scheme for the electrochemical reduction of tetraketopiperazine.

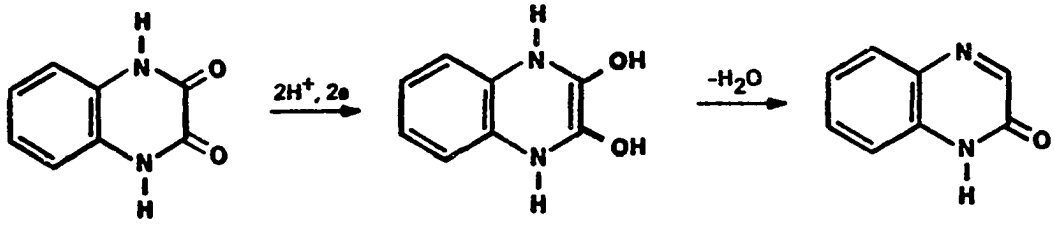

X

Voltammetric and coulometric evidence and product identification indicate that Wave II represents a further reduction of triketopyrazine (VII, Fig. 9). The kinetically controlled Wave II reduction proceeds initially via an irreversible $2\underline{e}/2H^+$ reduction of the 1,2-dione grouping to give 2,5-diketo-6-hydro-6-hydroxypyrazine (XI, Fig. 9), followed by dehydration to form 2,5-diketopyrazine (XII, Fig. 9). Species XII can then be further reduced in a $4\underline{e}/4H^+$ step to form 2,5-diketopiperazine (XIII, Fig. 9), the final and experimentally observed product.

After the elimination of Wave I by controlled potential electrolysis, only Wave II which is about three times the original height of Wave I remains. The height of Wave II and coulometry clearly indicate that it is a $6\underline{e}$ process, and that the entire Wave II process, (VII → XI → XII → XIII, Fig. 9) can occur within polaro-

graphic drop times (2-4 sec). This means that the dehydration step (XI → XII, Fig. 9) is very rapid. Because of this fact, and the tendency for VII to decompose to glyoxylic acid and oxamide, no attempt was made to measure the kinetics of the dehydration step.

Potentiostatic data indicates that the totally irreversible Wave III process involves an ECE type electrode mechanism. In the Wave III process, tetraketopiperazine (II, Fig. 9) initially undergoes a $4\underline{e}/4H^+$ reduction of two carbonyl groups to yield 2,5-dihydroxydiketopiperazine (XIV, Fig. 9). Loss of two molecules of water occurs in a chemical step yielding 2,5-diketopyrazine (XII, Fig. 9) which can then be reduced in a second $4\underline{e}/4H^+$ step to yield the final product, 2,5-diketopiperazine (XIII, Fig. 9). It is very probable that the dehydration of XIV to XII actually proceeds in two steps, each involving the loss of one molecule of water. Since the reaction XI → XII of Wave II is very fast, it seems reasonable to assume that the k_f value calculated from potentiostatic studies of the chemical reaction involved in Wave III refers to the loss of the first molecule of water to form XI. In addition, the dehydration is apparently an acid catalyzed process as the value of k_f decreased with increasing pH (vide supra).

Analytical Utility of D.C. Polarography

A linear limiting current vs. concentration relationship was obtained for Wave I of tetraketopiperazine in pH 2 buffer solution (Fig. 4). Concentration values ranged from 0.1 to 2 mM. A linear i_p vs. concentration relationship was also obtained in 1 M acetic acid (pH 2.3) for concentration values between 0.2 and 2.0 mM. In these two media tetraketopiperazine is reasonably stable and exhibits the best defined Wave I. Thus, from the viewpoint of quantitative analysis, tetraketopiperazine can be determined quite readily by preparation of a calibration curve in the desired solution and over the concentration range of interest. Much lower concentration levels may be determined by pulse or differential pulse polarography.

CHAPTER 3

EXPERIMENTAL

Chemicals

The disodium salt of tetraketopiperazine was synthesized by the method of de Mouilpied and Rule.[14] In order to obtain free tetraketopiperazine the salt was treated with 1 M HCl in the approximate ratio of 300 mg salt to 15 ml HCl, filtered, washed with water, and dried under vacuum. By an alternate but more time-consuming procedure, free tetraketopiperazine can be obtained by passing the disodium salt through a cation exchange column (Dowex 50W-X8). The purity of tetraketopiperazine was established by elemental analysis, flame emission spectroscopy (testing for Na^+), and potentiometric titration. The latter was accomplished by titrating an aqueous solution of tetraketopiperazine with 0.1 N sodium hydroxide using a Corning Model 10 pH meter. Two endpoints were obtained, one for each nitrogen in the ring. A universal indicator solution (Eastman 4953) can also be used for this titration with the endpoints characterized by first, a yellow to green color

change and second, a blue to violet color change. The purity, as determined by these methods, was usually 98 to 99%.

2,5-Diketopiperazine was purchased from Sigma. Oxamide was obtained from Matheson, Coleman, and Bell while glyoxylic acid was obtained from Aldrich.

Buffer solutions were prepared with an ionic strength of 1.0, giving a 0.5 ionic strength upon 1:1 dilution, and were constituted as follows: pH 0.5-1.0, HCl-KCl; pH 2.0-8.0, citric acid-Na_2HPO_4-KCl (McIlvaine); pH 8.0-11.0, $Na_2B_4O_7$-KCl; pH 11.0-13.0, NaOH-KCl. Acetic acid (1 M) and 1 M H_2SO_4 were also used. Argon and nitrogen used for deaeration of the test solutions were equilibrated with water in a bubbling chamber. Mercury used was triply distilled (Bethlehem Apparatus).

Thin-layer chromatography was carried out on Macherey-Nagel and Company MN-Polygram polyamide-6UV_{254}, Macherey-Nagel and Company Polygram CEL 300 UV_{254} (cellulose), and Eastman (6060) silica gel chromatography sheets impregnated with fluorescent indicator. Developing solvents were absolute methanol, n-propanol/H_2O (70:30), methanol/glacial acetic acid (90:10), n-butanol/pyridine/water (65:35:65), and n-butanol/glacial acetic acid/water (12:3:5). Visualization was accomplished with ultraviolet light.

Paper chromatograms (Whatman No. 1 filter paper)

for the detection of glyoxylic acid[38] were developed with ethyl acetate/glacial acetic acid/water (2:1:1), containing bromophenol blue (0.015% w:v) and sodium acetate (0.05% w:v). 2,5-Diketopiperazine was detected[39] using the cellulose thin-layer plates described above, developed with n-butanol/pyridine/water (65:35:65), and visualized by a spray of starch-iodide reagent (1% starch:1% potassium iodide in water).

Apparatus

Polarography, linear sweep voltammetry, and cyclic voltammetry were performed with an instrument of conventional operational amplifier design.[40,41] Polarograms and voltammograms were recorded on a Hewlett-Packard Model 7001A X-Y Recorder. Fast-sweep voltammograms were recorded on a Tektronix Model 5031 Dual Beam Storage Oscilloscope and photographed with a Tektronix Model C-70 camera. A.c. polarograms were obtained using a Princeton Applied Research Corporation Model 121 Lock-In Amplifier/Phase Detector both as the source of the alternating signal and as an a.c. voltmeter for detection of the alternating component of the current.[42] A sinusoidal signal having a frequency of 100 Hz or 40 Hz and 10 mV peak-to-peak amplitude was employed. A mechanical drop dislodger in conjunction with a dual-channel timing circuit described by Brown et al.[43] was

used to achieve a reproducible droptime, usually 2.00 seconds. The second channel of the timing circuit was connected to the remote pen input of the X-Y recorder and adjusted so that the current was recorded immediately before the drop was dislodged.

Single and double potential step chronoamperometry were performed with a Princeton Applied Research Corporation Model 175 Universal Programmer coupled with the electrochemistry system described above. The chronoamperograms were recorded on either the X-Y recorder or oscilloscope.

A water-jacketed three-compartment cell maintained at a known and constant temperature (usually 25° ± 0.1°C) with each compartment separated by a medium-porosity sintered glass disc was used for most electrochemical studies. Salt bridges placed on the counter and reference sides of the discs were prepared by dissolving 4 grams agar (Difco Laboratories) in 90 ml water and adding 30 grams KCl. A saturated calomel reference electrode (SCE) and a platinum foil counter electrode were utilized. All potentials are referred to the SCE at 25°C. The temperature of the three-compartment cell and water-jacketed bubbling chamber was maintained by circulating water from a bath heated by an incandescent bulb in circuit with 25°C or 40°C thermostats and a mercury relay (H-B Instrument Co.).

The pyrolytic graphite electrodes were machined from small rods of graphite (Super-Temp Company, Santa Fe Springs, California) to a diameter of 4 mm and length ca. 8 mm, and were sealed into lengths of 6 mm bore glass tubing with Hysol Epoxi-Patch (Hysol Corp., Olean, N.Y.). The electrodes were ground flush with the end of the glass tube, and were resurfaced prior to the running of each voltammogram with 600-grit silicon carbide paper (Buehler Ltd., Evanston, Ill.) mounted on a rotating disc. The electrode was then sprayed with a fine stream of deionized water to remove the graphite powder from the surface, and dried by gently touching the surface with an absorbent paper tissue. The hanging mercury drop electrode was a Metrohm A.G. Model BM 5-03 Microburet Electrode (area 2.22 mm^2).

Controlled potential electrolyses were carried out using Princeton Applied Research Corporation Models 173 or 373 Potentiostat/Galvanostats. Current integration during electrolysis was performed with a Koslow Scientific Model 541 coulometer or a Hewlett-Packard Model 2212A voltage-to-frequency converter and two Hewlett-Packard Model 5321A electronic counters connected in series. Controlled potential coulometry was performed at either the stirred mercury pool or the pyrolytic graphite electrode. Two different three-compartment cells were utilized for controlled potential coulometry, each compartment being

separated by a KCl-agar salt bridge. Both contained platinum gauze counter electrodes and SCE reference electrodes, but the working compartment of one had a volume of 120 ml and the other, 25 ml. The areas of the mercury pool working electrodes were ca. 16 cm^2 and ca. 3.8 cm^2, respectively, while the areas of the pyrolytic graphite electrodes were ca. 50 cm^2 and ca. 10.4 cm^2, respectively. The volume of the electrolysis solution was usually 80 ml or 10 ml. For macroscale electrolyses, a large three-compartment cell having a working electrode compartment volume of 300 ml was used. Each compartment was separated by an acetic acid-agar salt bridge. These salt bridges were prepared by dissolving 1.25 grams of agar in 20 ml of 1 M acetic acid. The working electrode was a stirred mercury pool (area ca. 38.5 cm^2). Platinum foil served as the counter electrode and a Fisher Porous Plug SCE was employed as the reference electrode. The volume of the electrolysis solution was typically 150 ml-200 ml. In all cells, argon or purified nitrogen was bubbled through the electrolysis solution via a gas dispersion tube. Solutions were stirred magnetically with a Teflon-covered bar during electrolysis.

A Corning Model 10 pH meter was used for pH measurements. Infrared spectra were recorded on a Beckman IR-8 Spectrophotometer. KBr pellets were made with a

Barnes Econo-Press. Ultraviolet spectra were obtained with a Perkin-Elmer Hitachi Model 124 Spectrophotometer using 1.00 cm quartz cells. A Hitachi RMU-7E Mass Spectrometer was employed for the recording of mass spectra. Lyophilization was accomplished using a Virtis 12-port manifold and a Vactorr 25 vacuum pump. Cooling traps contained isopropanol cooled by a CryoCool Mechanical Refrigeration System Model CC-60 (NESLAB Instruments, Inc.).

Polarographic and Voltammetric Procedure

Test solutions of tetraketopiperazine were prepared prior to each study. These solutions were made by dissolving the solid compound in a solution of 1:1 buffer:deionized water, yielding an ionic strength of 0.5. Deaeration was accomplished by bubbling nitrogen through the solution for approximately ten minutes before the experiment was run and then passed in a stream over the solution during the run.

Coulometric and Macroscale Electrolysis Procedure

For controlled potential coulometry, both at the mercury pool and pyrolytic graphite electrodes, 10 or 80 ml of a solution (concentration ranged from 0.1 mM to 5.0 mM but was usually 1.0 mM) of tetraketopiperazine in either pH 0.5 chloride or pH 2 McIlvaine buffer was

placed in the working electrode compartment of the electrolysis cell. The solution was deaerated while stirring with argon or purified nitrogen for approximately 30 minutes prior to the commencement of the electrolysis, and the gas flow was continued throughout the electrolysis. During the electrolysis, the current was monitored and when it had decreased to a low, constant value, the counts per unit time produced by the coulometer were noted, and the electrolysis stopped. In most cases, the background solution was reduced at the electrolysis potential until a constant current reading was attained prior to the addition of the test compound. The potential was turned off, the proper amount of tetraketopiperazine added and upon dissolution, the electrolysis was then continued. In some instances, dissolution was not complete before initiation of the electrolysis, but as the electrolysis proceeded, the undissolved tetraketopiperazine went into solution. D.c. polarography, u.v., and cyclic voltammetry were run before and after each electrolysis, and completion of the reduction was confirmed by the absence of the tetraketopiperazine polarographic wave and voltammetric reduction peak of interest. The procedure for macroscale electrolysis was essentially the same, except that ca. 7 mM solution (ca. 160 mg of tetraketopiperazine in 160 ml of solution) of tetraketopiperazine in 1 M acetic acid was used. Complete reduction required approximately

4-5 hours.

Isolation and Characterization of Electrolysis Products

After complete reduction of tetraketopiperazine on the plateau of Wave I (-0.5 V) in 1 M acetic acid, the solution was lyophilized, yielding a buff-colored solid. Thin-layer chromatography of this solid confirmed the absence of tetraketopiperazine. Attempts to further purify this lyophilized material were unsuccessful. However, a mass spectrum (12 eV, 195°C) of the impure solid showed a molecular ion peak at m/e = 126 (Fig. 10), which is the molecular weight of the proposed Wave I electroreduction product (VII, Fig. 9). Unfortunately, the authentic compound could not be obtained for comparison purposes.

Exhaustive reduction of tetraketopiperazine on both the plateau of Wave II (-0.95 V) and on the plateau of Wave III (-1.15 V) was carried out in 1 M acetic acid. The resulting product solutions were lyophilized and the off-white, fluffy solid obtained was shown by thin-layer chromatography to be free of tetraketopiperazine. This residue was then sublimed at approximately 110°C and 0.2 mm Hg pressure. The small amount of solid adhering to the cold finger was scraped off and identified as a mixture of oxamide and glyoxylic acid (see Determination of Oxamide and Glyoxylic Acid, below).

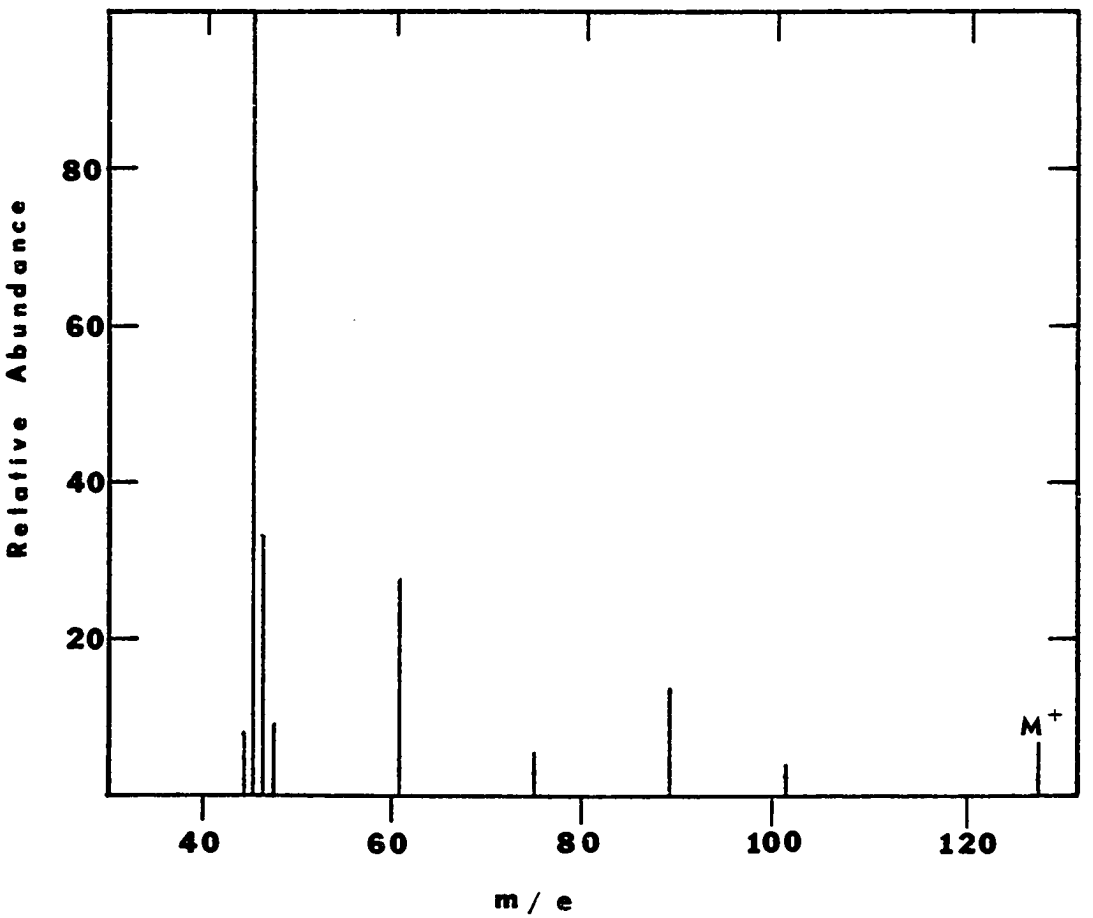

Figure 10. Mass spectrum of the tetraketopiperazine wave I reduction product. Mass spectrum obtained at 195°C with ionization voltage of 12 eV.

The remaining solid was further sublimed at ca. 170°C, 0.2 mm Hg pressure, and the white solid now adhering to the cold finger was collected and identified as 2,5-diketopiperazine (glycine anhydride) by comparison of its mass and i.r. spectra (Fig. 11) with that of authentic 2,5-diketopiperazine, and also by comparing the R_f value obtained from the paper chromatographic method of Rydon and Smith[39] with that of the authentic compound. The latter analysis gave a blue-black spot with an R_f of 0.58.

Quantitative removal of this material from the cold finger typically yielded 0.78 to 0.80 mole 2,5-diketopiperazine per mole tetraketopiperazine reduced. The product yield is slightly lower than that theoretically expected owing to the instability of the Wave I reduction product (VII).

Determination of Oxamide and Glyoxylic Acid

Oxamide and glyoxylic acid were detected by d.c. polarography in solutions above pH 6 and were confirmed by comparing the values of $E_{1/2}$ with those of the authentic compounds and also by "spiking" the unknown solution with a small amount of the authentic materials (added individually). In the latter case, the wave heights increased but the values of $E_{1/2}$ remained the same. For example, at pH 10, two polarographic waves were obtained, one at -1.25 V and the other at -1.60 V, corresponding to

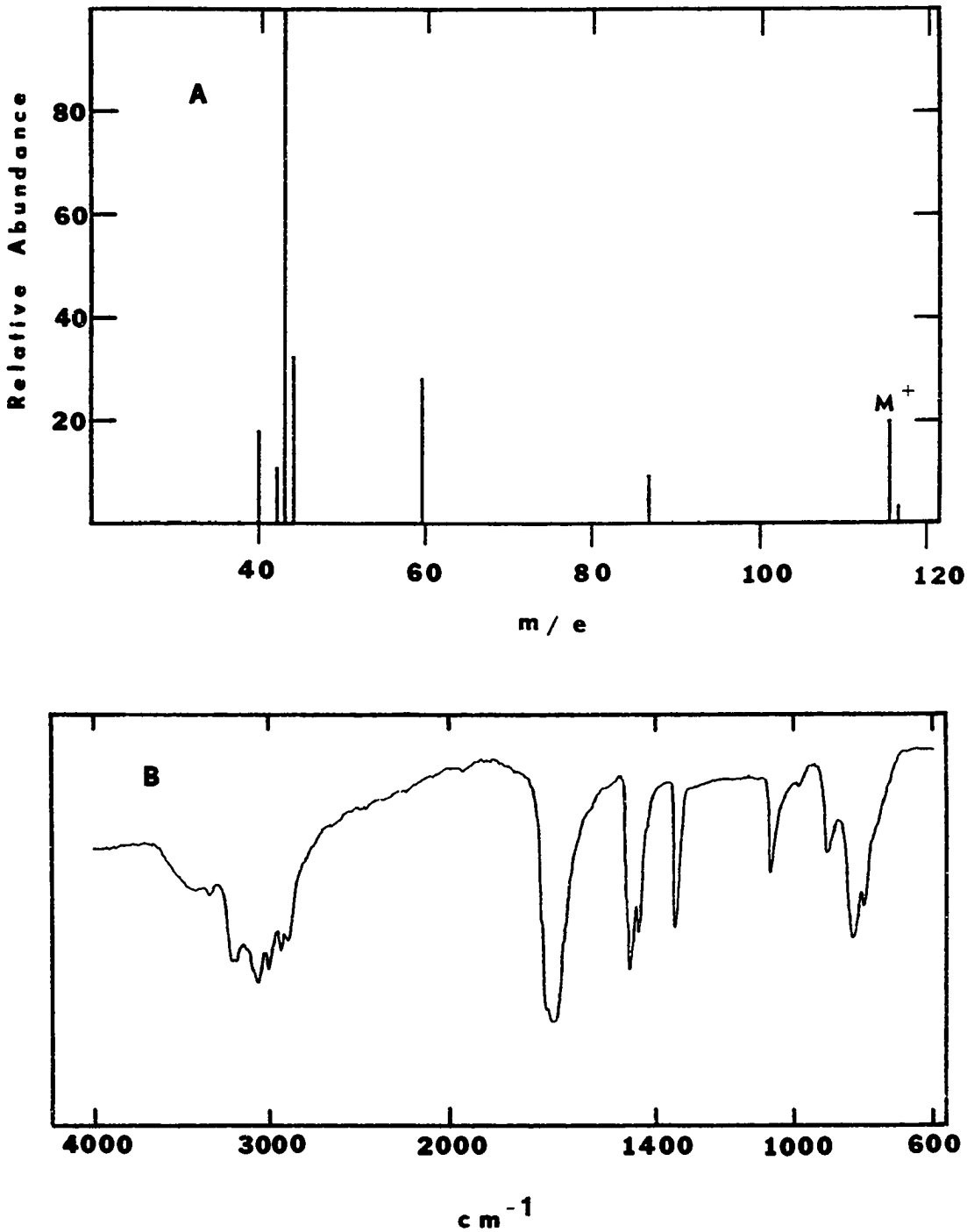

Figure 11. Mass (A) and i.r. (B) spectra of 2,5-diketopiperazine. Mass spectrum obtained at 130°C with ionization voltage of 10 eV. IR is KBr disc.

glyoxylic acid and oxamide, respectively. It should be noted that neither oxamide nor glyoxylic acid can be readily detected by d.c. polarography below pH 6 because the reduction wave for oxamide is obscured by background discharge[44] and due to the kinetic nature of the glyoxylic acid reduction wave.[45] Polarography at pH 8 of the unknown solution compared to a calibration curve for oxamide revealed almost complete quantitative decomposition to oxamide.

The paper chromatographic method of Hartley and Lawson[38] also revealed the presence of glyoxylic acid. Unknown samples were run simultaneously with authentic glyoxylic acid. Yellow spots against a blue background with an R_f value of 0.37 disclosed the presence of glyoxylic acid.

No attempts to further separate oxamide and glyoxylic acid were carried out. However, a mass spectrum of the mixture exhibited all of the peaks characteristic of each compound.

CHAPTER 4

SUMMARY

Between pH 0-2, tetraketopiperazine exhibits three d.c. polarographic reduction waves. Wave I is a quasi-reversible $2\underline{e}/2H^+$ reduction of tetraketopiperazine to 2-hydroxytriketopiperazine, which then undergoes dehydration to yield triketopyrazine, i.e., Wave I proceeds by an EC reaction. A possible structure for the product of the EC process has been proposed by analogy to a previously reported system. The mass spectrum of the product also supports this structure. A preceding chemical process affecting the Wave I charge transfer reaction was evidenced by voltammetric and potentiostatic studies but no possible structures were proposed. Wave II is due to further electrochemical reduction of triketopyrazine in an overall $6\underline{e}$ process to 2,5-diketopiperazine. Initially, triketopyrazine undergoes an irreversible $2\underline{e}/2H^+$ electroreduction followed by a relatively rapid dehydration reaction to form 2,5-diketopyrazine which is then further reduced in a $4\underline{e}/4H^+$ step to the observed product, 2,5-diketopiperazine (glycine anhydride). Since Wave II

depends upon formation of triketopyrazine by a chemical reaction of 2-hydroxytriketopiperazine, it is under kinetic control. Wave III has been shown by potentiostatic experiments to proceed by an ECE mechanism. The first step in this process is a $4\underline{e}/4H^+$ reduction of tetraketopiperazine to 2,5-dihydroxydiketopiperazine which then loses two molecules of water to give 2,5-diketopyrazine. This is then reduced in a second $4\underline{e}/4H^+$ reaction to yield 2,5-diketopiperazine. The homogeneous rate constant for the interposed chemical step was calculated from current-time data at pH 0.5 and at pH 2. The electrochemical products of the Wave I, II, and III processes were examined by u.v., i.r., mass spectrometry, d.c. polarography, and voltammetry at both the HMDE and PGE.

CHAPTER 5

References

1. Y. T. Pratt, Heterocyclic Compounds, Vol. 6, 1957, p. 440, R. C. Elderfield, ed., Wiley, New York.
2. The Merck Index, Merck and Co., Inc., New York, 1952, pp. 361, 762.
3. J. H. Gardner and J. H. Schneider, J. Amer. Chem. Soc., 55, 3823 (1933).
4. F. L. Pyman, J. Chem. Soc., 93, 1795 (1908).
5. H. W. Stewart, R. J. Turner, J. J. Denton, S. Kushner, L. M. Brancone, W. L. McEwen, R. I. Hewitt, and Y. Subbarow, J. Org. Chem., 13, 134 (1948).
6. S. Kushner, L. M. Brancone, R. I. Hewitt, W. L. McEwen, Y. Subbarow, H. W. Stewart, R. J. Turner, and J. J. Denton, J. Org. Chem., 13, 144 (1948).
7. R. I. Hewitt, D. E. White, S. Kusher, W. S. Wallace, H. W. Stewart, and Y. Subbarow, Ann. N.Y. Acad. Sci., 50, 128 (1948).
8. E. Cerkovnikov, N. Škarica, P. Štern, and N. Marijan, Arkiv Kemi, 18, 12, 37, 96 (1946).

9. K. E. Hamlin, A. W. Weston, F. E. Fischer, and R. J. Michaels, Jr., J. Amer. Chem. Soc., 71, 2731 (1949).

10. S. H. Jaros, J. C. Castillo, and E. J. DeBeer, Ann. Allergy, 7, 458, 466, 489 (1949).

11. Y. T. Pratt, Heterocyclic Compounds, Vol. 6, 1957, p. 435, R. C. Elderfield, ed., Wiley, New York.

12. Y. T. Pratt, Heterocyclic Compounds, Vol. 6, 1957, p. 436, R. C. Elderfield, ed., Wiley, New York.

13. D. L. McAllister and G. Dryhurst, J. Electroanal. Chem., 55, 69 (1974).

14. A. T. de Mouilpied and A. Rule, J. Chem. Soc., 91, 176 (1907).

15. Y. T. Pratt, Heterocyclic Compounds, Vol. 6, 1957, p. 454, R. C. Elderfield, ed., Wiley, New York.

16. B. M. Visinski and G. Dryhurst, J. Electroanal. Chem., 70, 199 (1976).

17. L. Meites, Polarographic Techniques, 2nd ed., Wiley, New York, 1965, p. 132.

18. L. Meites, Polarographic Techniques, 2nd ed., Wiley, New York, 1965, p. 139.

19. L. Meites, Polarographic Techniques, 2nd ed., Wiley, New York, 1965, p. 126.

20. L. Meites, Polarographic Techniques, 2nd ed., Wiley, New York, 1965, p. 177.

21. L. Meites, Polarographic Techniques, 2nd ed., Wiley, New York, 1965, p. 229.

22. L. Meites, Polarographic Techniques, 2nd ed., Wiley, New York, 1965, p. 218.

23. L. Meites, Polarographic Techniques, 2nd ed., Wiley, New York, 1965, p. 197.

24. B. Breyer and H. H. Bauer, Alternating Current Polarography and Tensammetry, Interscience Publishers, New York, 1963, pp. 267-269.

25. R. N. Adams, Electrochemistry at Solid Electrodes, Marcel Dekker, Inc., New York, 1969, p. 145.

26. R. S. Nicholson and I. Shain, Anal. Chem., 36, 706 (1964).

27. R. S. Nicholson, Anal. Chem., 37, 1351 (1965).

28. R. N. Adams, Electrochemistry at Solid Electrodes, Marcel Dekker, Inc., New York, 1969, p. 124.

29. P. Delahay, New Instrumental Methods in Electrochemistry, Interscience Publishers, Inc., New York, 1954, p. 51.

30. R. N. Adams, Electrochemistry at Solid Electrodes, Marcel Dekker, Inc., New York, 1969, pp. 62-63.

31. B. H. Hansen and G. Dryhurst, J. Electrochem. Soc., 118, 1747 (1971).

32. W. V. Childs, J. T. Maloy, C. P. Keszthelyi, and A. J. Bard, J. Electrochem. Soc., 118, 874 (1971).

33. G. S. Alberts and I. Shain, Anal. Chem., 35, 1859 (1963).

34. L. Meites, Polarographic Techniques, 2nd ed., Wiley, New York, 1965, p. 114.

35. Y. T. Pratt, Heterocyclic Compounds, Vol. 6, 1957, p. 440, R. C. Elderfield, ed., Wiley, New York.

36. M. Kland-English and W. M. Garrison, Nature, 197, 895 (1963).

37. C. Furlani, Gazz. Chim. Ital., 85, 1646 (1955).

38. R. D. Hartley and G. J. Lawson, J. Chromatography, 4, 410 (1960).

39. H. N. Rydon and P. W. G. Smith, Nature, 169, 922 (1952).

40. G. Dryhurst, M. Rosen, and P. J. Elving, Anal. Chim. Acta, 42, 143 (1968).

41. D. L. McAllister and G. Dryhurst, Anal. Chim. Acta, 64, 121 (1973).

42. D. L. McAllister and G. Dryhurst, Anal. Chim. Acta, 58, 273 (1972).

43. E. R. Brown, T. E. McCord, D. E. Smith, and D. D. DeFord, Anal. Chem., 38, 1119 (1966).

44. D. L. McAllister, J. Pinson, and G. Dryhurst, Anal. Chim. Acta, 67, 415 (1973).

45. M. Takagi, S. Ono, and T. Wasa, Rev. Polarogr., 11, 210 (1963).

PART II

SPECTROELECTROCHEMICAL INVESTIGATIONS OF SOME BIOLOGICALLY IMPORTANT PURINES

CHAPTER 1

INTRODUCTION

Purines occur widely in nature. Several derivatives of purine are found in every living cell. They are usually associated with large macromolecules but in certain biological systems they can sometimes be found in their free state.

Purine (I) is a combination of fused pyrimidine and imidazole rings. Emil Fischer named the compound[1]

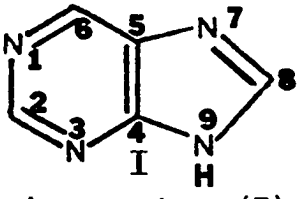

I

and devised the numbering system (I) most widely employed today.[2] The purine nomenclature found in the literature can be somewhat confusing because trivial names are very often assigned to many purine derivatives in addition to the typical chemical names. An excellent and detailed guide to purine nomenclature has been prepared by Robins.[3]

In addition, a very helpful and brief description of the nomenclature for some of the more common purines has been summarized by Dryhurst.[4]

The purines are generally very stable, but they also have quite low solubilities.[5-7] Infrared spectral studies[8] indicate that most hydroxypurines exist in the keto form.[5,9]

Purines are quite widely distributed in nature, and as mentioned earlier, are vital components in all living cells. Uric acid was probably the first purine to be discovered (by Scheele in 1776[10]). It is found in human urine, human and animal milk, blood, cerebral spinal fluid, bird excrement, and other sources.[3] Xanthine (discovered by Marcet[11]) is also found in milk, human urine, bladder stones and other miscellaneous biological sources.[3,12] Hypoxanthine (6-oxypurine) is also present in various animal tissues and fluids. Several N-methylated derivatives are found in a diversity of natural products and human urine,[13-16] and possess some rather significant pharmacological properties.[17-19]

Purines (especially adenine and guanine) are commonly found as constituents of high molecular weight nucleic acids. The carbohydrate derivative in which the purine is linked through its N-9 position via a β-N-glycosidic bond is called a nucleoside. Depending on

whether the sugar moiety is D-ribose or 2-deoxy-D-ribose determines whether the nucleoside is a ribonucleoside or deoxyribonucleoside. Purine nucleotides are phosphate esters (usually through the C-5' or C-3' hydroxyl group of the sugar) of the nucleosides. These purine nucleotides, in conjunction with pyrimidine nucleotides, can form highly polymerized structures called nucleic acids. The many and varied sequences of these nucleotide polymers are intimately involved in protein synthesis, and in the storage and transfer of genetic information. The tri-phosphate purine nucleotides of adenine (ATP) and to a lesser extent guanine, can hydrolyze with removal of a single molecule of phosphoric acid resulting in a fairly large decrease in free energy. This makes these energy-rich compounds extremely important in intermediary metabolism.[20]

Purines belong to a large class of compounds called N-heterocycles (N for nitrogen in the ring). Many of the fundamental reactions of living organisms are performed by nitrogen heterocycles containing delocalized or mobile (π) electrons. Most of these compounds are both theoretically and experimentally good electron donors/acceptors. This fact makes these compounds (purines, for example) good candidates for the electrochemical examination of their electron transfer reactions.

Electrochemical studies of molecules can provide very useful information on the nature of electron transfer processes.[21] It is possible to determine precisely how many electrons are involved in the electron transfer reaction at a selected potential, as well as the number of protons, if any, associated with this transfer of electrons. It is also possible, under suitable conditions, to detect intermediates or products formed after the electron transfer, whether they be fairly stable or relatively unstable. Very detailed and useful mechanistic data can also be obtained.[22] In addition, a large number of experimental conditions (pH, temperature, buffer systems, etc.) can be employed for electrochemical studies of biologically important electron transfer reactions which are usually difficult to control in in vivo studies.

The application of electrochemical investigations to biological systems is quite justifiable in that there are many similarities between biological (enzymatic) and electrochemical reactions. Among these are:

1. Both may involve heterogeneous electron transfer processes; one at an enzyme-solution interface, the other at an electrode-solution interface.
2. Both may occur at very similar temperatures.
3. Both can take place at similar pH.

4. Both can occur in similar ionic strengths of an inert electrolyte.
5. The orientation of the molecule in some sort of specific fashion for both processes is apparently very important before electron transfer can take place.

Studies of the electrochemical reduction of purines are quite recent.[23-25] It was not until 1962 that a detailed study of the electrochemical reduction of some purines was reported by Smith and Elving.[26] A comprehensive review has been presented by Dryhurst.[27]

The more important reactions of purines from a biological viewpoint are their oxidation processes. The importance of the catabolic degradation of purines is a particular example. In recent years, more information has been accumulating on the reaction pathways of biological (or enzymatic) oxidations of purines. Moreover, a large amount of work on the electrochemical, photochemical, and radiochemical oxidation of purines and the correlation of their mechanisms to the biological oxidative pathways has been reported.[28]

Investigations of the electrochemical oxidation of biologically important molecules have probably been hindered for a variety of reasons. Among these is the fact that electrochemical oxidation of organic compounds

is not as simple or straightforward as is usually the case for the electrochemical reduction of the same compounds, especially in aqueous media.[29] The lack of suitable electrodes for observing electrochemical electron transfer reactions at very positive potentials (vs. SCE) is probably another important reason for the slow growth of electrooxidation studies. Metal electrodes usually suffer from limited positive or negative potential ranges. This renders them poor for cyclic voltammetric studies. Some, like platinum electrodes, are plagued with hydrogen sorption. Adams has prepared a very useful description of several solid electrode materials.[30] Those based on carbon, including glassy carbon, spectroscopic graphite (usually wax-impregnated), carbon paste, and pyrolytic graphite, are probably the best electrodes for use at both very negative and very positive potentials. Pyrolytic graphite electrodes (PGE)[31,32] have excellent potential limits (positive and negative)[30,33] and are easily constructed.[34,35] In this study the PGE will be the usual electrode utilized unless otherwise stated.

The importance of electrochemical studies can be illustrated by briefly looking at some examples of various oxidative processes (enzymatic, photochemical, etc.) and comparing the results of these studies. The work in the present study is concerned mostly with two biologically

significant purines: uric acid and xanthine. Accordingly, the following review will focus on these compounds.

Several workers, including Keilin and Hartree[36] and Bentley and Neuberger,[37] have studied the biochemical oxidation of uric acid in the presence of the enzyme uricase. On the basis of their experiments they showed that uricase catalyzes the transfer of two electrons from uric acid to oxygen and that this attack probably occurs at the C4=C5 position giving a short-lived intermediate (they propose a carbonium ion). This intermediate then reacts further, ultimately giving allantoin. Furthermore, they proposed that the electron transfer step was the only one in which the enzyme was involved and that further changes were purely chemical reactions arising from the reactivity of the intermediates.

The results of studies by several investigators[38-41] on the oxidation of uric acid by various peroxidase enzymes showed that the products obtained were dependent upon the buffer system and solution pH utilized. At low pH the primary product was alloxan; at intermediate pH allantoin was the principal product. Moreover, they proposed that some reactive intermediate was formed upon the initial oxidation by the enzyme, and that this species reacted further resulting ultimately in the observed products. Paul and Avi-Dor[40] suggested that this intermediate could be uric acid diimine (II) or uric

acid-4,5-diol (III). Additional studies of the enzymatic

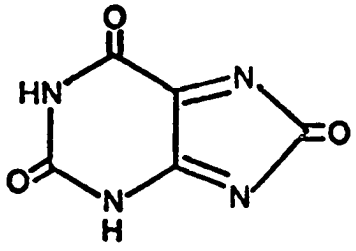

II

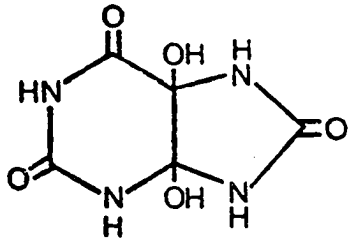

III

oxidation of uric acid[42,43] have resulted in proposed mechanisms and observed products similar to those just described.

Relatively little work has been carried out on the photochemical and radiochemical oxidations of uric acid. However, the studies that have been done generally propose that preferential attack is at the C4=C5 double bond with the formation of various forms of C-4 or C-5 hydroxy or hydroperoxide intermediates.[44-50] Similar results were obtained for the photo- and radiochemical oxidations of xanthine.[44,45,49]

Although there were some early investigations on the electrochemical oxidation of uric acid,[51,52] it was not until Struck and Elving's report[53] that the electrooxidation process was studied in some detail. On the basis of their work and the products observed,

a reaction scheme was proposed whereby uric acid was oxidized in a primary 2e process to a short-lived dicarbonium ion (IV) which then reacts further to yield

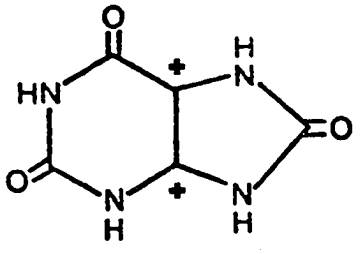

IV

the ultimate products. However, Dryhurst has outlined several objections to this scheme which should be considered.[54,55] First, the oxidation peak for uric acid is pH dependent (protons must be associated with the electron transfer) and the Struck-Elving reaction scheme does not indicate this. Second, it would be much more likely, if a positively charged species is formed, that the positive charge would be localized on surrounding nitrogen atoms instead of at C-4 and C-5 (IV). Finally, the Struck-Elving reaction scheme proposed[53] that IV was further oxidized (at the same potential at which uric acid is electrooxidized) to parabanic acid. However, the probability of a doubly positively charged ion losing two more electrons is very remote.

In view of these facts, Dryhurst carried out a further investigation of the electrochemical oxidation of uric acid at the PGE.[54] A cyclic voltammogram of uric acid at pH 7 is illustrated in Figure 6, Chapter 3. Equation 1 outlines the proposed reaction scheme.[54,56]

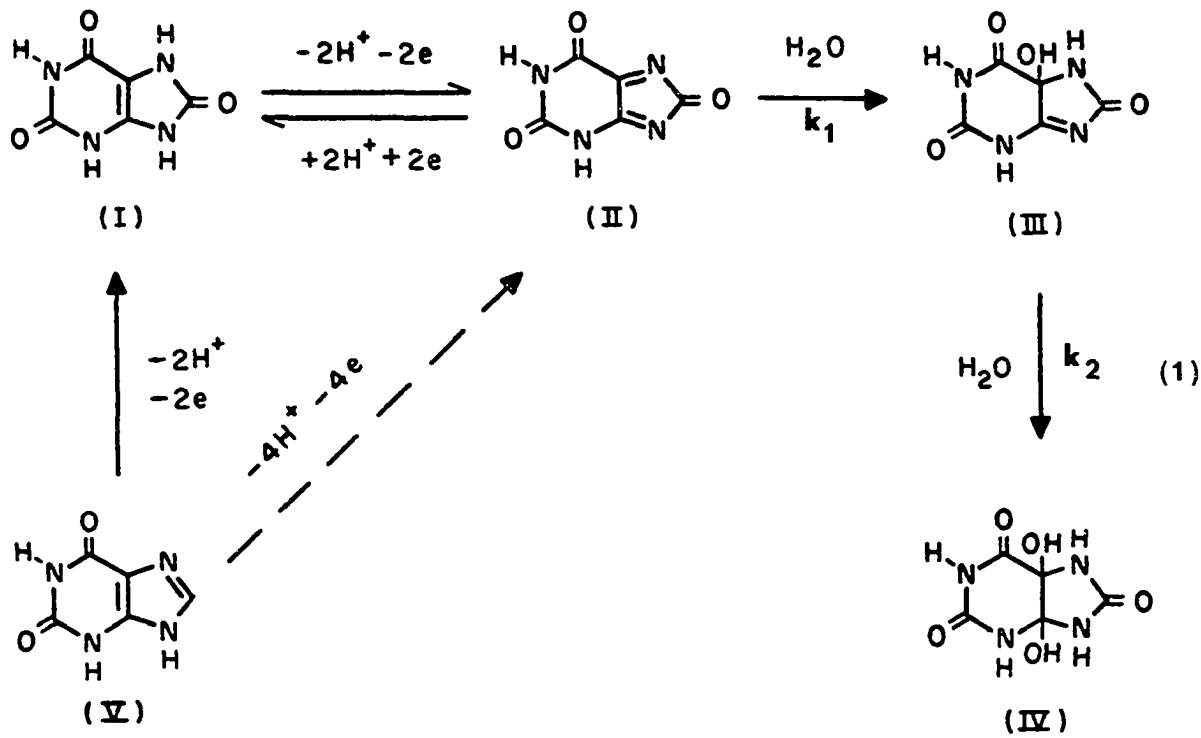

The oxidation peak I_a (Fig. 6) has been proposed to correspond to the $2\underline{e}/2H^+$ electrooxidation of uric acid (I, equation 1) to uric acid diimine (II, equation 1). Cyclic voltammetry indicates that II is very unstable but easily reducible,[54,57,58] giving rise to peak I_c (Fig. 6). As the voltage sweep rate is decreased, the

height of peak I_c decreases relative to that of peak I_a and eventually disappears, i.e., the species responsible for peak II is unstable. This proposed diimine intermediate (II, equation 1) can exist in two tautomeric forms, having a system of conjugated double bonds which would be expected to be very electroreducible. (Indeed, molecules with similar diimine structure are readily electroreducible.[59-66]) The diimine is then postulated to undergo a two step hydration, first to an imine-alcohol (III, equation 1) and then to uric acid-4,5-diol (IV, equation 1). One reason that Dryhurst postulates a two-stage hydration is the fact that reduction peak II_c is generally always present even at very slow sweep rates, and is apparently not due to reduction of one of the final products.[54,56] Accordingly, it is proposed that the first hydration step is a relatively fast process and the second hydration is much slower. The diol species, IV, then fragments to final observed products (e.g., primarily allantoin at pH 7, while alloxan and urea are the major products at low pH).

The electrochemical oxidation of xanthine (V, equation 1) at the PGE is a $4e/4H^+$ process which occurs at a more positive potential than that required to electrooxidize uric acid.[54,56] Actually, it has been proposed that the oxidation of xanthine proceeds via two $2e/2H^+$ steps. The first of these steps has been

proposed to be the potential controlling reaction involving oxidation of the N7=C8 (or C8=N9) bond to give uric acid. Since uric acid is more easily oxidized than is xanthine[54] the former is immediately oxidized further in the second $2\underline{e}/2H^+$ step to give uric acid diimine (II). This species then undergoes the same secondary reactions as described above (equation 1) giving the same products in about the same yields.[54,58]

This discussion of various uric acid oxidations has pointed out a number of similarities between the *in vivo* and *in vitro* processes. First, the preponderance of evidence favors some sort of attack at the C4=C5 double bond. Second, it seems that most reaction schemes propose some type of unstable hydroxy or hydroperoxide product or intermediate. Third, comparison of the final products from the various oxidative processes, particularly those from the electrochemical and enzymatic (especially peroxidases) oxidations, reveals that they are essentially identical with respect to their nature, yields, and pH effects on them. A more comprehensive comparison is given in reference 28. In view of these findings it can be seen that electrochemical oxidation studies of biologically important compounds (namely, purines) and the reaction schemes or mechanisms developed as a consequence of these studies can serve as a guide

to interpreting enzymatic reactions.

The present study described in the following chapters was undertaken to more clearly confirm the formation of the diimine intermediate species (and any other intermediates, if possible) as part of the proposed mechanism for the electrochemical oxidation of certain biologically important purines. The development of an alternate method of studying short-lived intermediate species in addition to the more conventional electrochemical techniques was an important aspect of this work. Another goal of the investigation was to initiate preliminary studies on the electrochemical oxidation of purine nucleosides.

CHAPTER 2

THIN-LAYER SPECTROELECTROCHEMICAL OXIDATION OF 5,6-DIAMINOURACIL

INTRODUCTION

It was pointed out in Chapter 1 that the formation of intermediate diimine species has been proposed in both the electrochemical and enzymatic oxidation reaction schemes of some biologically important purines. The electrochemical reaction schemes proposed for uric acid and other related purines are based primarily on evidence obtained by linear and cyclic sweep voltammetry, coulometry, mass electrolysis, and product isolation, identification, and quantitation. Detailed mechanistic and kinetic studies were not possible with most purines previously studied due to the large number of complex chemical and electrochemical reactions following the initial electron transfer step. In addition, the very extensive adsorption of simple purines at the PGE effectively precludes the meaningful application of techniques such as double potential step chrono-amperometry and fast sweep cyclic voltammetry in any

sort of quantitative fashion.

Because of the interest in establishing the relationship between biological and electrochemical oxidations, alternate methods for confirming the existence of diimine species as important intermediates in the overall electro-oxidation behavior of purines were sought. The first step in this process was the apparent correlation between the electrode reaction of 5,6-diaminouracil (I, equation 2) and uric acid.[67] 5,6-Diaminouracil serves as a quite good model for uric acid and related purines since its structure is clearly very similar to that of uric acid.

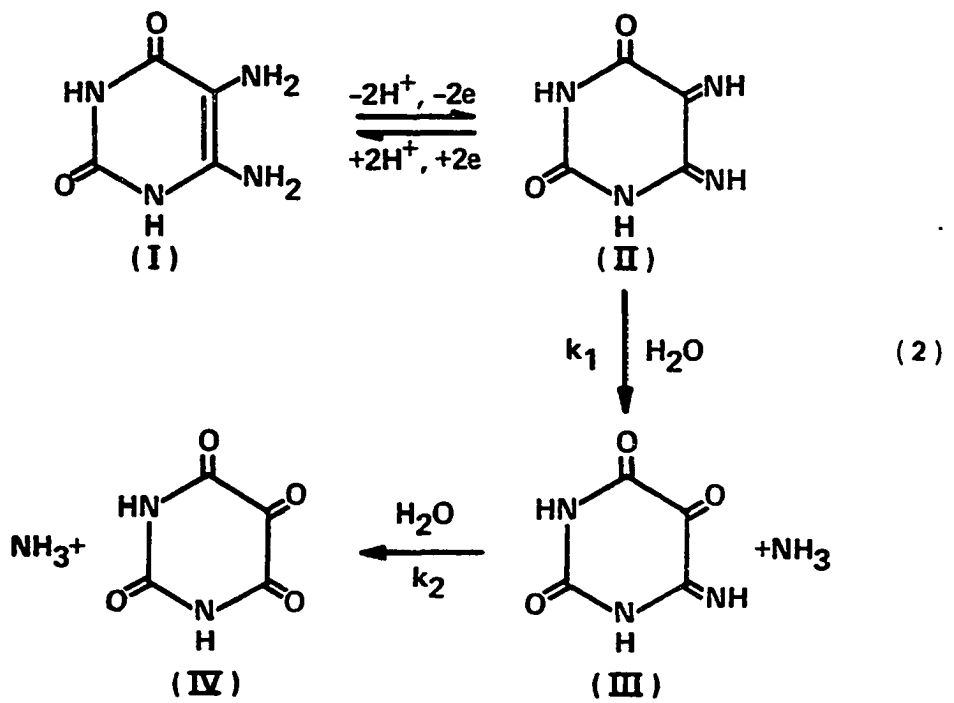

This compound has been shown to be electrochemically oxidized at the pyrolytic graphite electrode in a quasi-reversible $2e/2H^+$ reaction to an intermediate species proposed to be a diimine (II, equation 2). This diimine is then hydrolyzed in a stepwise process first to a quinoneimine (III, equation 2) and ammonia, then to alloxan (IV, equation 2) and ammonia. The nature of the electrode reaction, i.e., an e.c. process, and numerical values for the rate constant k_1 were determined by means of double potential step chronoamperometry using the methods of Childs et al.[68] The reaction scheme outlined for 5,6-diaminouracil (equation 2) is very similar to that proposed for uric acid (Chapter 1) and has been employed to support the uric acid reaction scheme.

The second step in developing alternate methods for confirming the formation of diimine intermediates has been to investigate the electrooxidation of 5,6-diaminouracil using the recently developed technique of thin-layer spectroelectrochemistry. Since the diimine species has been proposed to have a quinoid-like structure, its u.v. absorption spectrum was expected to be in a different region than that of the parent compound. By using the thin-layer spectroelectrochemical methodology first proposed by Murray et al.[69] coupled with a rapid scan spectrometer, RSS (see Experimental),

it was hoped that by monitoring the u.v.-visible spectrum of an electrolyzing solution of 5,6-diaminouracil any transient but absorbing intermediates could be detected. It was anticipated that this method would allow a more detailed study of any absorbing intermediates and would permit a more useful characterization of such species to be carried out. If the kinetics of intermediate formation could be measured, this data could then be compared to that obtained from electrochemical studies already reported.[67] After having developed the spectro-electrochemical methodology on 5,6-diaminouracil, a purine model compound, such studies could be extended to investigate the electrooxidation behavior of certain biologically important purines.

RESULTS

Voltammetry at the gold electrode

Since the thin-layer spectroelectrochemical cells were fabricated from gold minigrids (see Experimental) and previous studies of the electrochemical oxidation of 5,6-diaminouracil were carried out at the PGE,[67] it was necessary to briefly investigate the voltammetry of 5,6-diaminouracil at a gold electrode. In order to do this a 9 mm^2 gold foil electrode was fabricated as described by Adams.[70] Cyclic voltammograms were obtained

for solutions of 5,6-diaminouracil at pH 2 (Fig. 1A & C) and pH 4 (Fig. 1B & D) at both the PGE and gold foil electrode. At pH 2 the initial electrooxidation peak at each electrode surface is considerably larger than the reverse electroreduction peak. The oxidation to reduction current ratios for the PGE and gold foil electrode are 3.8 and 4.0, respectively. The smaller value of the reduction current at slow sweep rates has been attributed to a relatively rapid chemical follow-up reaction of the primary electrooxidation product at low pH.[67]

Cyclic voltammograms of 5,6-diaminouracil at pH 4 at the PGE and the gold foil electrode are shown in Figure 1B and D. The reverse, reduction peak is now considerably larger and was shown at the PGE to be due to a slower chemical follow-up reaction of the primary electrooxidation product thus allowing more product of the initial oxidation to be available for reduction back to the starting material.[67] The corresponding ratios of anodic to cathodic peak currents are 1.3 and 1.6.

The peak potentials for the oxidation peaks occurred at slightly more positive potentials at the gold foil electrode than at the PGE and, correspondingly the peak potentials for the reverse reduction peaks

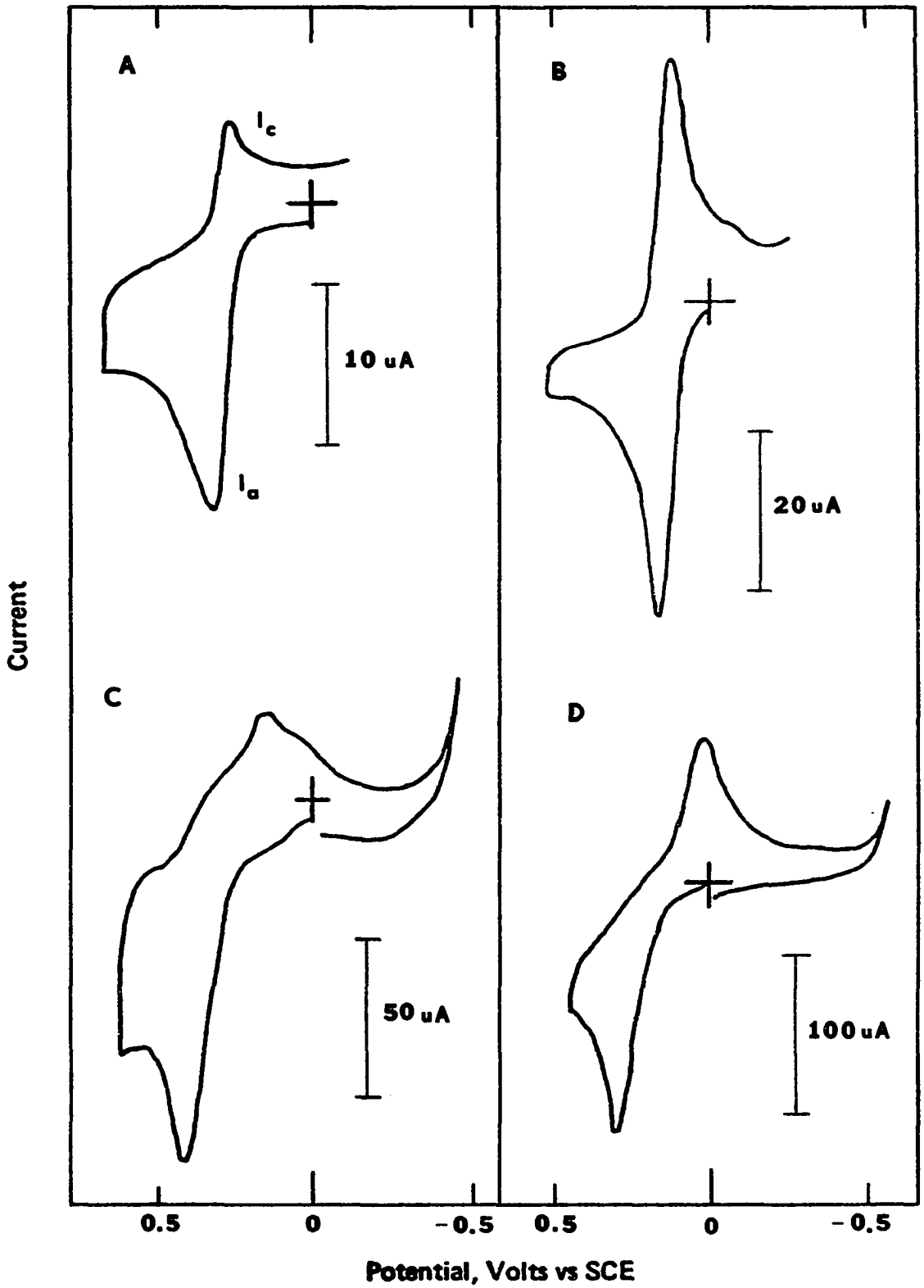

Figure 1. Effect of pH and nature of electrode on cyclic voltammograms of 1 mM 5,6-diaminouracil at the PGE (A & B) and at the gold foil electrode (C & D). Voltammograms (A & C) pH 2.0 McIlvaine buffer, and (B & D) pH 4.0 McIlvaine buffer. Starting potential indicated by (+); initial sweep towards positive potentials. Scan rate 100 mV sec^{-1}.

occurred at slightly more negative potentials at gold foil than at the PGE. These small differences in peak potentials are no doubt attributable to the different type of electrode material.[71]

Coulometric n-values for the electrochemical oxidation of 5,6-diaminouracil at a gold electrode were obtained by controlled potential electrolysis in a thin-layer electrolysis cell using a gold minigrid electrode. Among the advantages of electrolyses in a thin-layer cell are speed, simplicity, and elimination of possible complicating secondary reactions between electrode reaction products and initial reactants.[72] Typical results of thin-layer coulometry are shown in Table 1, where it is clear that an n-value close to 2 is observed. This is in agreement with the n-value obtained from conventional, large-scale controlled potential coulometry of 5,6-diaminouracil at the PGE.[67]

Based on such cyclic voltammetric and coulometric studies, it was concluded that the basic electrode reaction scheme of 5,6-diaminouracil at a gold electrode is the same as at the PGE.

Spectroelectrochemistry

Prior to spectroelectrochemical experiments the stability of 5,6-diaminouracil at various values of pH was studied by observing its u.v. spectrum and voltammetric

TABLE 1

Experimental n-Values Observed for Electrochemical Oxidation of 5,6-Diaminouracil in a Thin-Layer Cell at a Gold Minigrid Electrode

pH	Initial concentration of 5,6-diaminouracil, mM	Controlled potential V vs. SCE	n-Value
2	0.7	0.6	1.8[a]
2	3.0	0.6	1.8[a]
2	3.0	0.6	1.9[a]
4	5.0	0.5	2.1[a]
4	5.0	0.5	1.7[b]
4	5.0	0.5	1.6[b]

[a]By graphical integration of current-time curve.

[b]By electronic integration of electrolysis current.

response at the PGE as a function of time. In solutions of pH $\leq$ 4, 5,6-diaminouracil exhibited no change either in its u.v. spectrum or its voltammetric peak current over one to two hours, well within the time necessary to conduct spectroelectrochemical experiments (typically 30 minutes). At pH 5 a slight decomposition (1-3% decrease in the u.v. absorbance and peak current) occurred over one to two hours but was not sufficient to affect the results of the experiment. Only at pH $\geq$ 6 was there significant decomposition of 5,6-diaminouracil. Decomposition was also characterized by the appearance of a pale yellow color within 30-45 minutes. However, if the spectroelectrochemical study was performed within

30 minutes the decomposition of 5,6-diaminouracil did not affect the experimental results (see Experimental).

Electrolysis potentials were chosen from linear sweep voltammograms (2 mV sec^{-1}) run in the thin-layer cell and also at the gold foil electrode. Because of the rapid decomposition of 5,6-diaminouracil at pH 6, separate solutions were used for voltammetry and the spectroelectrochemical experiments.

A typical u.v. spectrum obtained throughout the initial stages of an electrolysis of 5,6-diaminouracil at a gold minigrid electrode in a thin-layer cell is shown in Figure 2A. This electrolysis was carried out at pH 5 which is very illustrative of the behavior of 5,6-diaminouracil. Before electrolysis, 5,6-diaminouracil exhibits two u.v. absorption peaks at pH 5. The monocation of 5,6-diaminouracil absorbs at λ_{max} = 255 nm, while the neutral molecule absorbs at λ_{max} = 275 nm. Since the pK_a of 5,6-diaminouracil is 4.56,[73] then at lower pH only the peak at λ_{max} = 255 nm is observed, while at higher pH only the peak at λ_{max} = 275 nm is observed. At pH 5, upon application of a potential of 0.35 V, the u.v. spectral peaks of 5,6-diaminouracil decrease (Fig. 2B). The spectrum was scanned at a rate of 0.2 Hz so that each trace in the spectrum corresponds to 5 seconds. As these peaks at 255 nm and 275 nm de-

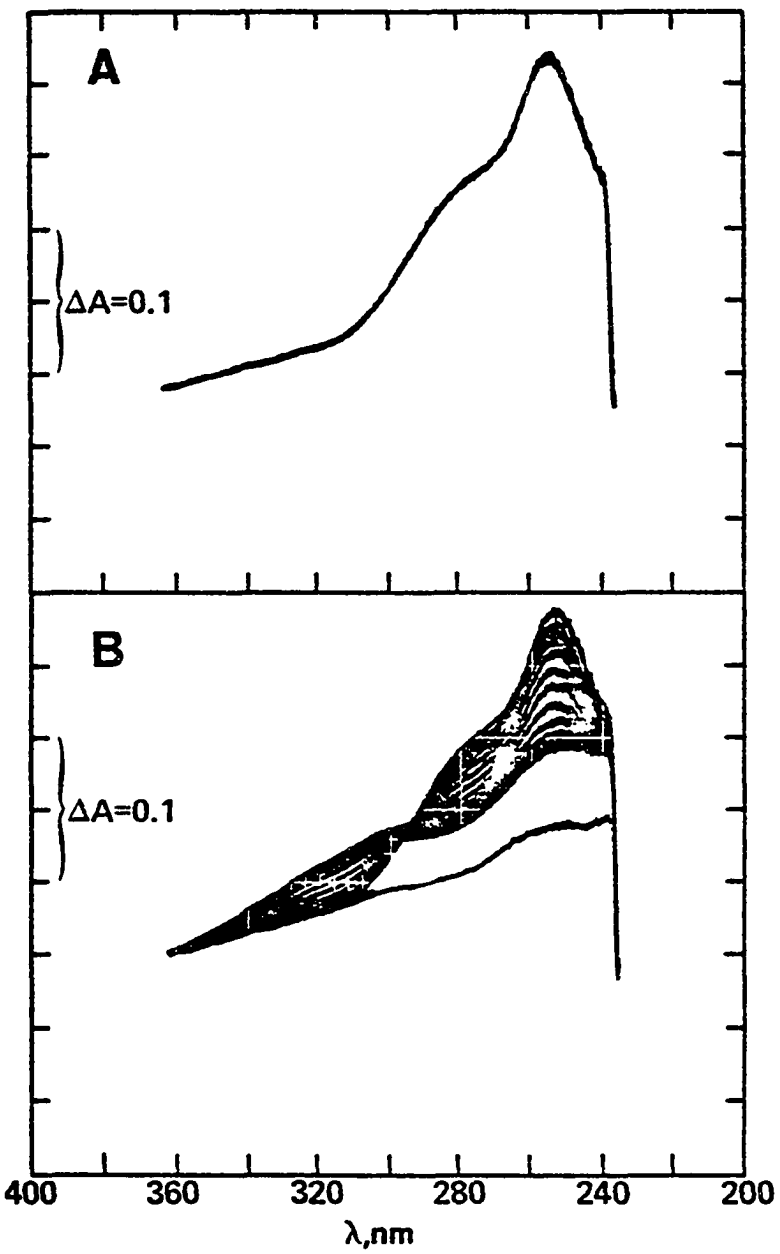

Figure 2. Spectra of 5 mM 5,6-diaminouracil in pH 5.0 McIlvaine buffer (A) before electrolysis, (B) during electrolysis at 0.35 V at gold minigrid electrode in thin-layer cell. Repetitive scans are 5 seconds.

crease, a rather broad peak centered at ca. 310-331 nm appears and increases. The electrolysis shown in Fig. 2B was stopped at the point when the latter broad peak had reached its approximate maximal value. With continued electrolysis the 5,6-diaminouracil peaks at 255 nm and 275 nm further decreased and disappeared. The broad peak at ca. 320 nm, after reaching its maximal value, decreased and ultimately disappeared after about five minutes. The clear space in the spectrum in Figure 2B was caused by decreasing the intensity of the oscilloscope when the intermediate reached its maximum absorbance (ca. two minutes) and then increasing it once again to obtain the lowest trace after about 10 minutes.

Solutions of 5,6-diaminouracil at pH 2 and 3 yielded no apparent increase in absorbance in the 310-330 nm region upon application of the potential. The peak due to the monocation of 5,6-diaminouracil (λ_{max} = 255 nm) did, however, decrease as expected upon application of the potential. The presence of an absorbing intermediate was not indicated even after the sweep rate was increased to as fast as 400 Hz (0.0025 seconds per sweep) or the spectrum width increased far into the visible region. The apparent non-absorption of the proposed intermediate at low pH will be discussed later.

The spectroelectrochemical behavior of 5,6-

diaminouracil at pH 4 was similar to that at pH 5 except that the absorption peak for the monocation of 5,6-diaminouracil (λ_{max} = 255 nm) was the most prevalent and the lifetime of the intermediate (characterized by the broad peak between 310-330 nm) was shorter. The increase and subsequent decrease in absorbance of the intermediate was completed in about two minutes for a 5 m*M* solution, implying that the chemical rate of decomposition of the intermediate is significantly faster at pH 4 than at pH 5.

Likewise, the behavior at pH 6 was similar to the process at pH 5 except that the neutral form of 5,6-diaminouracil (λ_{max} = 275 nm) was predominant.

By very careful subtraction of background absorbance, it was found that between pH 4 and 6 the broad absorption band associated with an intermediate formed on electrooxidation of 5,6-diaminouracil was composed of two overlapping peaks with λ_{max} = 332 and 312 nm. Because of the very low absorbance values generally observed, these two low, rounded peaks are not well defined in Fig. 2B.

The broad absorption peak centered around *ca*. 260 nm observed at the end of a complete electrolysis of 5,6-diaminouracil (Fig. 2B) corresponds to that observed under identical conditions for a 5 m*M* solution

of alloxan, the ultimate product of the reaction.

Kinetic measurements

The highest pH value at which the kinetics of hydrolysis of the intermediate species in the electro-oxidatin of 5,6-diaminouracil was measured by double potential step chronoamperometry was pH 4.[67] At pH 4 the first-order solution rate constant, corresponding to k_1 in equation (2), was 0.04 sec^{-1}. At higher pH the rate of the hydrolysis reaction became too slow to be measured by chronoamperometric methods. The thin-layer spectroelectrochemical experiments were carried out between pH 4 and 6. At lower pH the rate of the follow-up reaction was too fast for accurate spectral measurements; at higher pH 5,6-diaminouracil was too unstable. Basically, the absorbance at λ_{max} of the absorbing intermediate species or at a wavelength where there is no absorbance interference from 5,6-diaminouracil was monitored while 5,6-diaminouracil was electrolyzed at constant potential at a gold minigrid electrode. This is illustrated in Figure 3 where the variation in the absorbance of the intermediate species is monitored as a function of time for 5,6-diaminouracil at pH 5.

The absorbance due to the intermediate reaches its maximal value at or close to the time when 5,6-diaminouracil is completely electrolyzed. The decrease

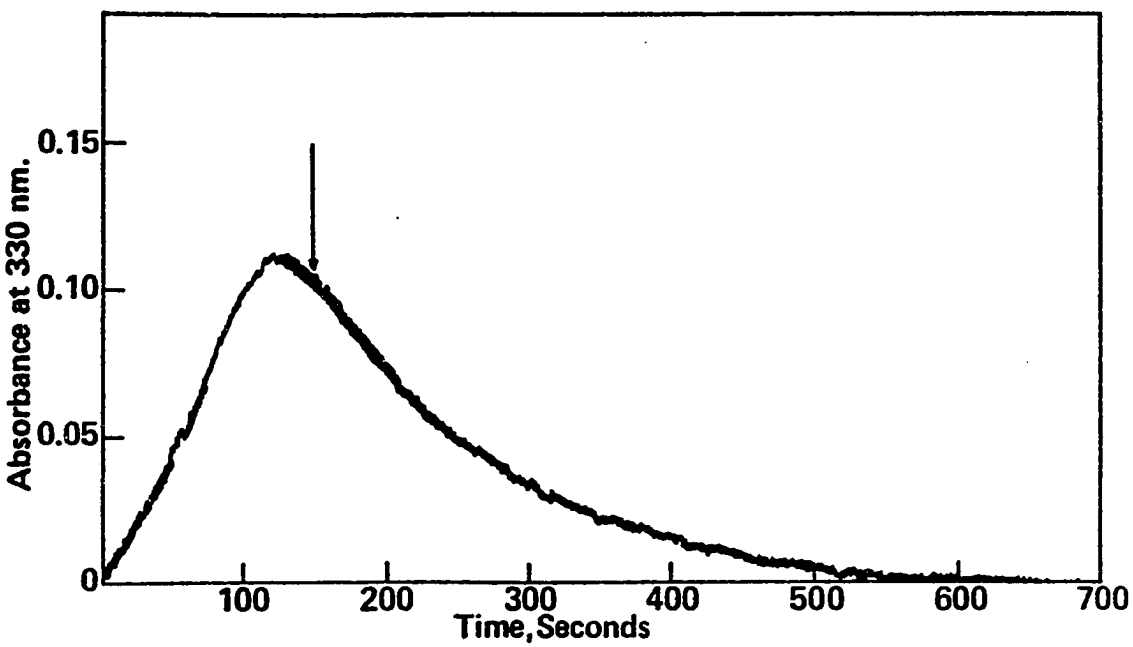

Figure 3. Variation of the absorbance of the intermediate species ($A_{320\ nm}$) with time during electrooxidation of 10 mM 5,6-diaminouracil in pH 5.0 McIlvaine buffer at 0.35 V in a thin-layer cell at a gold minigrid electrode. Arrow indicates time at which all 5,6-diaminouracil has been electrolyzed.

in absorbance of the intermediate species with time was used to elucidate the kinetics of the hydrolysis process. A typical rate plot obtained from the data at pH 5 is shown in Figure 4. The hydrolysis reaction is clearly a first-order (or pseudo first-order) process. Entirely analogous results were obtained at pH 4 and pH 6 with the hydrolysis reaction following first-order kinetics. Typical rate constant data are presented in Table 2, which further confirms the fact that with increasing pH the rate of the follow-up hydrolysis reaction decreases.[67]

TABLE 2

First-Order Rate Constants for Hydrolysis of the Intermediate Formed on Electrochemical Oxidation of 5,6-Diaminouracil at a Gold Minigrid Electrode

pH[a]	Initial concentration of 5,6-diaminouracil, mM	k, sec^{-1}, thin-layer spectroelectrochemistry	k, sec^{-1}, double potential step chronoamperometry
4	5	0.04	0.04[b]
5	5	0.01	-
	10	0.008	
	20	0.01	
6	5	0.003	-

[a]McIlvaine buffers containing K_2SO_4, ionic strength 0.5.

[b]From reference 67.

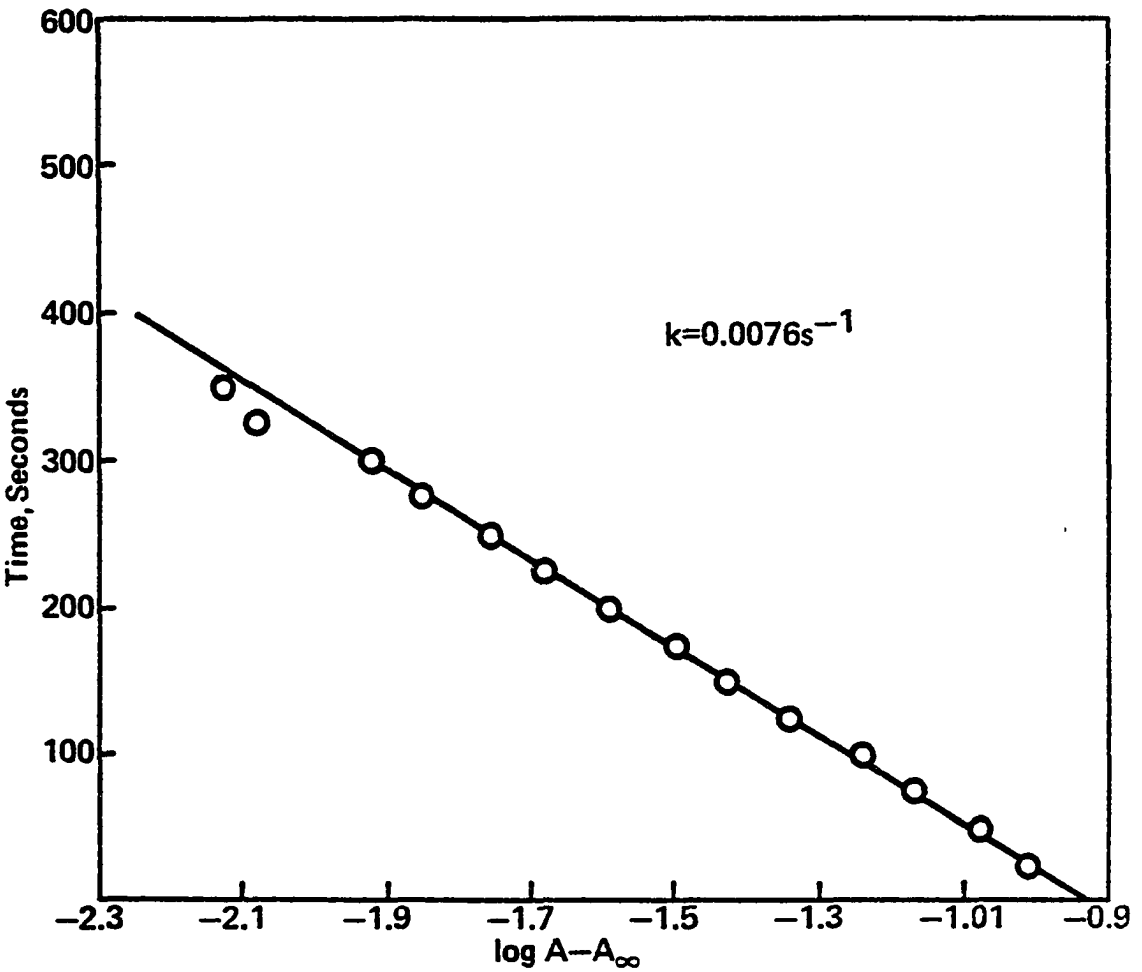

Figure 4. Kinetic plot of time versus absorbance at 330 nm of the intermediate species formed on electrooxidation of 5,6-diaminouracil. Absorbance data taken from Fig. 3 setting time=0 at the point where the concentration of 5,6-diaminouracil was zero, i.e., at the arrow in Fig. 3.

The effect of concentration on the observed kinetics was studied at pH 5 (Table 2). The usable range of concentrations is limited to the region of ca. 5-20 mM 5,6-diaminouracil because the maximum solubility of this compound is ca. 20 mM between pH 4-6. Below 5 mM the absorbance due to the intermediate species becomes very small and difficult to measure. Nevertheless, over the concentration range 5-20 mM and the pH range 4-6 the hydrolysis reaction of the intermediate exhibits first-order kinetics with no change in the rate constant with concentration.

The large variation in k_{obs} with pH clearly suggests an acid catalyzed process. This was confirmed by a typical kinetic analysis method.[74] For a chemical reaction that is both acid and base catalyzed the total reaction rate is given by:

$$k_{obs} = k_1[H^+]^n + k_2 + k_3[OH^-]^m \qquad (3)$$

where k_{obs} = experimentally determined first-order rate constant

k_1 = catalytic rate constant for $[H^+]$

k_3 = catalytic rate constant for $[OH^-]$

k_2 = non-catalyzed rate constant

n = order with respect to $[H^+]$

m = order with respect to $[OH^-]$

In regions of high acidity (large $[H^+]$, low pH) and k_2 is negligible relative to the other terms, then equation (3) reduces to

$$k_{obs} = k_1[H^+]^n \tag{4}$$

Taking logarithms,

$$\log k_{obs} = \log k_1 - n(pH) \tag{5}$$

Thus, a plot of log k_{obs} vs. pH should give a straight line, the slope being equal to -n.

Likewise, in the very basic region, a plot of log k_{obs} vs. pH will be linear with the slope = +m. Typically, then, in a log k_{obs} vs. pH plot a positive constant slope indicates dependence upon hydroxide ion, and a negative constant slope shows dependence on hydronium ion. Of course, it is not necessary that a reaction be catalyzed by both acid and base.

The analysis described above was applied to 5,6-diaminouracil. The values of the rate constant were obtained from both the electrochemical method[67] and the present study. Figure 5 is a plot of log k_{obs} vs. pH. As can be seen, a negative, constant slope with a value of n = -0.7 was obtained which, in view of the fact that two different methods were utilized to obtain k_{obs} data, may be considered equal to unity.[74] This further

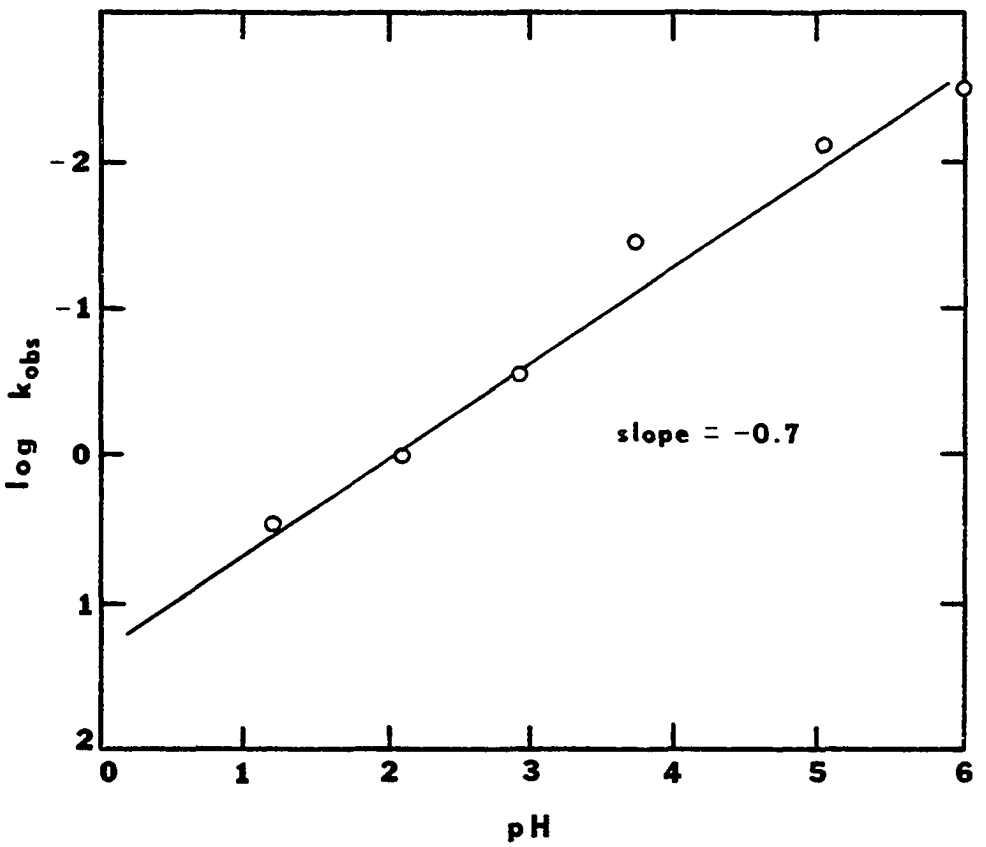

Figure 5. Log of the rate constant k_{obs} versus pH for the follow-up hydrolysis reaction of 5,6-diaminouracil.

confirms the fact that the follow-up hydrolysis reaction (k_1, equation 2) is overall a first-order, acid catalyzed process.

Over the pH range examined in this study, kinetic data (absorbance vs. time) were not taken until all of the 5,6-diaminouracil had been electrolyzed, i.e., the absorbance at 255 nm and 275 nm had been reduced to background levels. With the relatively slow reaction rates involved in this study this procedure was the most straightforward. However, for more rapid follow-up reactions it is not necessary that the reactant be completely removed. Simply stopping the electrolysis at a point where sufficient absorbing product has been produced and monitoring the product decay will yield the desired kinetic information.

DISCUSSION

This thin-layer spectroelectrochemical study clearly reveals that when 5,6-diaminouracil is electrochemically oxidized it produces an intermediate product which decomposes in a first-order, acid catalyzed reaction. The ultimate reaction products are alloxan and ammonia.[67] The order and the solution rate constants for hydrolysis of the intermediate are in excellent agreement with the kinetics of hydrolysis of the diimine (II, equation 2) to the quinoneimine (III, equation 2) measured by double

potential step chronoamperometry.[67] It would seem quite reasonable, then, to propose that the intermediate species absorbing at ca. 320 nm is the diimine electrooxidation product of 5,6-diaminouracil.

However, the previously reported cyclic voltammetric study of 5,6-diaminouracil[67] suggested that the hydrolysis of the quinoneimine to alloxan (characterized by k_2 in equation 2) is a somewhat slower process than hydrolysis of the diimine to the quinoneimine (characterized by k_1 in equation 2). Indeed, certain compounds such as phenylenediamine are electrooxidized to diimines that hydrolyze in a stepwise fashion, first to quinoneimines and then further to quinones with the quinoneimine-to-quinone step being the slower process.[75] Moreover, results in Chapter 3 for the electrooxidation of uric acid will show that the proposed hydrolysis step imine-alcohol to 4,5-diol species (characterized by k_2, equation 1, Chapter 1), which is analogous to the slow k_2 step above, is a relatively slow process.

Thus, the possibility that these spectroelectrochemical studies of 5,6-diaminouracil are measuring the quinoneimine-to-alloxan step (k_2, equation 2) cannot be ruled out. However, since the values of k_{obs} determined by chronoamperometry[67] and spectroelectrochemistry of 5,6-diaminouracil at pH 4 agree so well, it may be likely

that in the case of 5,6-diaminouracil the two hydrolysis steps (k_1 and k_2, equation 2) have essentially the same value for the rate constant.

A possible reason why an intermediate was not observed in the spectroelectrochemical oxidation of 5,6-diaminouracil at pH values <4 is that the rate constant is so large that only a very low concentration of the u.v.-absorbing intermediate is present. Inspection of Figure 5 shows that a pH 2 the observed rate constant is ca. 1 ($\log k_{obs} = 0$). This corresponds to a half-life, $t_{1/2}$, of ca. 0.7 seconds. Since this would result in a very small amount of material in a short time period, and since the cell thickness (ca. 0.01 cm) is already very small, the total absorbance observed would be quite small indeed and very difficult to detect.

These studies support the idea that the diimine species proposed as important intermediates in the electrochemical and biological oxidation of certain purines should be detectable and hence amenable to kinetic investigations using thin-layer spectroelectrochemical techniques.

EXPERIMENTAL

5,6-Diaminouracil, which was recrystallized from 2 N H_2SO_4 prior to use, was obtained from Pfaltz and Bauer. Alloxan was purchased from Nutritional Biochemicals

Corporation. Buffer solutions were prepared with reagent grade chemicals with an ionic strength of 1.0, giving a 0.5 ionic strength upon 1:1 dilution with deionized water. These buffers (pH 2.0-6.0) were constituted as follows: citric acid/$Na_2HPO_4 \cdot 7H_2O/K_2SO_4$ (McIlvaine). Chloride-containing media could not be used because the oxidation of gold to complex chlorides severely limits the positive potential range.[76]

Apparatus

The optically transparent thin-layer electrochemical cells were designed and constructed after those described by Murray et al.[69] and Heineman et al.[77] Gold minigrids purchased from Buckbee Mears Company, St. Paul, Minnesota were used for the optically transparent electrodes. The gold minigrid employed had 1000 wires per inch and had a transmittance of approximately 50% relative to air. A strip of the minigrid cut to about 1x4 cm was placed between two 25x50x1 mm quartz plates (Esco Optics Products, Oak Ridge, New Jersey). For spacing the two slides, four layers of one-inch wide, 3/4-mil Flurofilm Type C Teflon tape (Dilectix Corporation, Farmingdale, New York) were used. This tape was placed on the quartz slides and a section of the tape was cut away, leaving strips of about 3 mm on the two vertical edges and all but 5 mm on the top edge. The gold minigrid

was positioned such that about 1.5 cm extended past the vertical edge of the slides (for electrical contact) and the lower edge was positioned about 5 mm from the bottom of the quartz slides (to minimize the IR drop). With the gold minigrid firmly sandwiched between the quartz plates and Teflon spacers, the edges were painted with Tygon paint (Carboline K-63 white, Carboline Company, St. Louis, Missouri) in order to seal the cell and hold it firmly together. The bottom edge and the 5 mm space on the top edge were left unpainted. This open bottom allowed contact with the test solution and the opening at the top was used to draw test solutions (or water for washing and rinsing purposes) into the cell. The thickness of the thin-layer cell was determined spectrophotometrically at 283 nm using a solution of o-tolidine in ethanol ($\varepsilon = 2.39 \times 10^4$ $\underline{M}^{-1}$ cm^{-1}).[78] The thickness of the cells used in these studies ranged from 101 to 104 μm.

The solution to be studied was placed in a 6 ml glass cap and the open end of the thin-layer cell was dipped into this solution. A saturated calomel reference electrode (SCE) fitted with a Luggin capillary was positioned in the test solution beneath the open base of the thin-layer cell. A piece of platinum foil, shaped to line the inside of the glass reservoir cup, was

utilized for the auxiliary (counter) electrode.

An instrument of conventional operational amplifier design patterned after that of Dryhurst et al.[79] was employed for voltammetry and, on occasion, as a constant potential source. Generally, potentials were applied and maintained with a Wenking Model LT 73 potentiostat. Voltammograms and absorbance-time data were recorded on a Hewlett-Packard Model 7001A X-Y Recorder. Absorption spectra were usually recorded on a Tektronix Model 5031 Dual Beam Storage Oscilloscope equipped with a Tektronix Model C-70 camera. At times, the spectra were recorded on the X-Y recorder.

Optical measurements utilized a Harrick Rapid Scan Spectrometer (RSS) with a Signal Processing Module (Harrick Scientific Company, Ossining, New York). This is an oscillating mirror spectrometer originally developed by Kuwana.[80] The optical layout and description for this instrument is described elsewhere.[81] Spectral scanning from several minutes per spectrum to less than a millisecond per spectrum is possible with the RSS. The RSS offers a high degree of flexibillty since frequency of scan, scan width, and wavelength region (u.v.-near i.r.) can all be varied simultaneously. The RSS incorporates double beam signal processing (two photomultiplier tubes) for absorbance readout. The sample

compartment is large enough to accommodate the thin-layer cell, sample cup, reference electrode, and the necessary electrical connections. A second, essentially identical thin-layer cell arrangement containing the appropriate background buffer solution only was placed in the reference beam of the RSS.

Procedure

The solution of interest was placed in the sample cup and the thin-layer cell was carefully lowered until its open end was immersed to a depth of 3-5 mm. The solution was drawn up into the cell and held by capillary action. Occasionally, it was necessary to apply vacuum to the top of the cell. The light beam (ca. 1 mm^2) was positioned approximately in the center of the gold minigrid electrode for both the sample and reference cells. Normally, a slow sweep rate voltammogram (2-10 mV sec^{-1}) was run in the thin-layer cell to determine the potential for controlled potential electrolysis. Once the latter potential was decided, controlled potential electrolysis experiments were carried out during which the u.v. spectrum was continuously scanned. The wavelength range scanned normally extended from 240-380 nm, although much broader spectral regions were scanned in preliminary experiments. At the short wavelength end of the spectral region the spectra obtained were somewhat noisy. It

was also impossible to establish a flat baseline even with sample and reference cells filled with only non-absorbing supporting electrolyte. These base line and noise problems often necessitated manual subtraction of background from test solution traces. It was necessary to replenish the solution in the sample cell after each experimental run. At the end of each experiment at a particular pH a background was run (buffer solution _vs._ buffer solution).

Owing to the relative instability of 5,6-diaminouracil at pH 6,[67] solutions at this pH were prepared immediately prior to their investigation.

Absorbance-time curves were obtained by using the X-Y recorder in the time sweep mode and connecting the vertical output (absorbance) of the RSS to the Y-axis of the recorder. Thin-layer coulometry, for obtaining _n_-values, was achieved by monitoring the current as a function of time with an X-Y recorder. The current-time curve was then integrated graphically (area) to calculate the number of coulombs.

The RSS, thin-layer cells, and associated accessories were tested together initially with a solution of o-tolidine in 1 _M_ $HClO_4$-0.5 _M_ acetic acid and the results compared to those of Murray _et al._[69] Essentially identical curves were obtained for the current-potential,

absorbance-potential, and absorbance-time data. Moreover, utilizing the RSS system enabled the absorbance to be monitored over a wavelength range from 230 nm to 460 nm as the potential was stepped from 0.4 V to 0.85 V (vs. SCE). This allowed the u.v. peak of o-tolidine (λ_{max} = 250 nm) and the visible peak (λ_{max} = 438 nm) of the oxidation product to be monitored simultaneously instead of monitoring each λ_{max} individually as in reference 69. As expected, the peak at 250 nm decreased in absorbance while the peak at 438 nm gradually increased when the potential was applied.

SUMMARY

The electrochemical oxidation of 5,6-diaminouracil has been studied by thin-layer spectroelectrochemistry at a gold minigrid electrode. Electrooxidation of 5,6-diaminouracil yields an intermediate species which can be detected by means of its u.v. absorption spectrum. The kinetics of the apparent hydrolysis of this species has been measured and is first-order. The solution rate constant over the range of pH 4 to 6 has been measured. It is very possible that the observed intermediate is the diimine species since the observed rate constant determined by thin-layer spectroelectrochemistry correlates quite well with that obtained by purely electrochemical methods for the hydrolysis of the diimine to the quinone-

imine. However, it is also possible that the intermediate is the quinoneimine and that its rate of hydrolysis (to alloxan) is essentially the same as the rate of hydrolysis of the diimine. This study also indicates the potential utility of thin-layer spectroelectrochemical methods for the investigation of the electrooxidation reactions of biologically important purines.

CHAPTER 3

SPECTROELECTROCHEMICAL OXIDATION OF URIC ACID AND XANTHINE

INTRODUCTION

The study in Chapter 2 was undertaken to investigate the spectroelectrochemical behavior of 5,6-diaminouracil in order to develop the methodology needed to study the electrooxidation of purines such as uric acid and xanthine. Both the electrochemical oxidation[67] and the spectroelectrochemical oxidation[82] (Chapter 2) of 5,6-diaminouracil were investigated. The results of these studies will be compared to the behavior of uric acid and xanthine in order to support their previously proposed reaction schemes (equation 1, Chapter 1).

The present study was undertaken to investigate electrooxidation of uric acid and xanthine using thin-layer spectroelectrochemistry. Some additional experiments using cyclic voltammetry and double potential step chronoamperometry will also be described. In particular, it was hoped to confirm the formation of the diimine (II,

equation 1, Chapter 1) and imine-alcohol (III, equation 1, Chapter 1) species in the overall electrooxidation of these purines and to obtain some detailed kinetic measurements on the diimine to imine-alcohol and imine-alcohol to uric acid-4,5-diol (IV, equation 1, Chapter 1) hydrolysis reactions.

RESULTS

pK_a's of uric acid and xanthine

According to Johnson[86] uric acid has pK_a values of 5.4 and 10.3. These correspond to the neutral molecule to mono-anion and the mono-anion to di-anion transitions, respectively. The same transitions occur for xanthine, with pK_a values of 7.53 and 11.63, respectively.[87] These pK_a values for both uric acid and xanthine were obtained by u.v. spectrophotometry.

Voltammetry of uric acid and xanthine at carbon and gold electrodes

The voltammetry of uric acid and xanthine at the pyrolytic graphite electrode (PGE) has been studied previously.[54] Uric acid gives a single, 2e voltammetric oxidation peak, the peak potential (E_p) for which, between pH 1-12, is described by the equation $E_p = 0.76 - 0.069$ pH at a sweep rate of 5 mV sec^{-1}. A typical cyclic voltammogram of uric acid at a rough PGE (RPGE, see

Experimental) at a sweep rate of 200 mV sec^{-1} in phosphate buffer pH 7.0 is shown in Figure 6A. Earlier studies[54] suggested that electrooxidation peak I_a is due to the primary 2e oxidation of uric acid (I, equation 1, Chapter 1) to its diimine, peak I_c to the quasi-reversible reduction of the diimine back to uric acid, and peak II_c to the reduction of the imine-alcohol (III, equation 1, Chapter 1).

If, instead of the RPGE, a smooth PGE (SPGE, see Experimental) is employed, peak I_c completely disappears at relatively slow sweep rates (Figure 6B). Indeed, peak I_c could not be observed to any significant extent at the SPGE at pH 7.0 until sweep rates $\geq$ 1 V sec^{-1} were employed. At the gold foil electrode, peak I_a of uric acid was well defined, yet at a sweep rate of 200 mV sec^{-1} peak I_c was also absent (Figure 6C) and again could not be observed except at higher sweep rates (> 20 V sec^{-1}).

These observations seemed to imply that the roughness of the electrode surface is responsible for the appearance of the diimine reduction peak I_c. Earlier reports have shown that uric acid is quite strongly adsorbed at the RPGE.[83] The fact that the peak current for uric acid at the RPGE (Fig. 6A) is considerably larger than that at a SPGE (Fig. 6B) having the same geometric area under otherwise identical conditions supports the latter

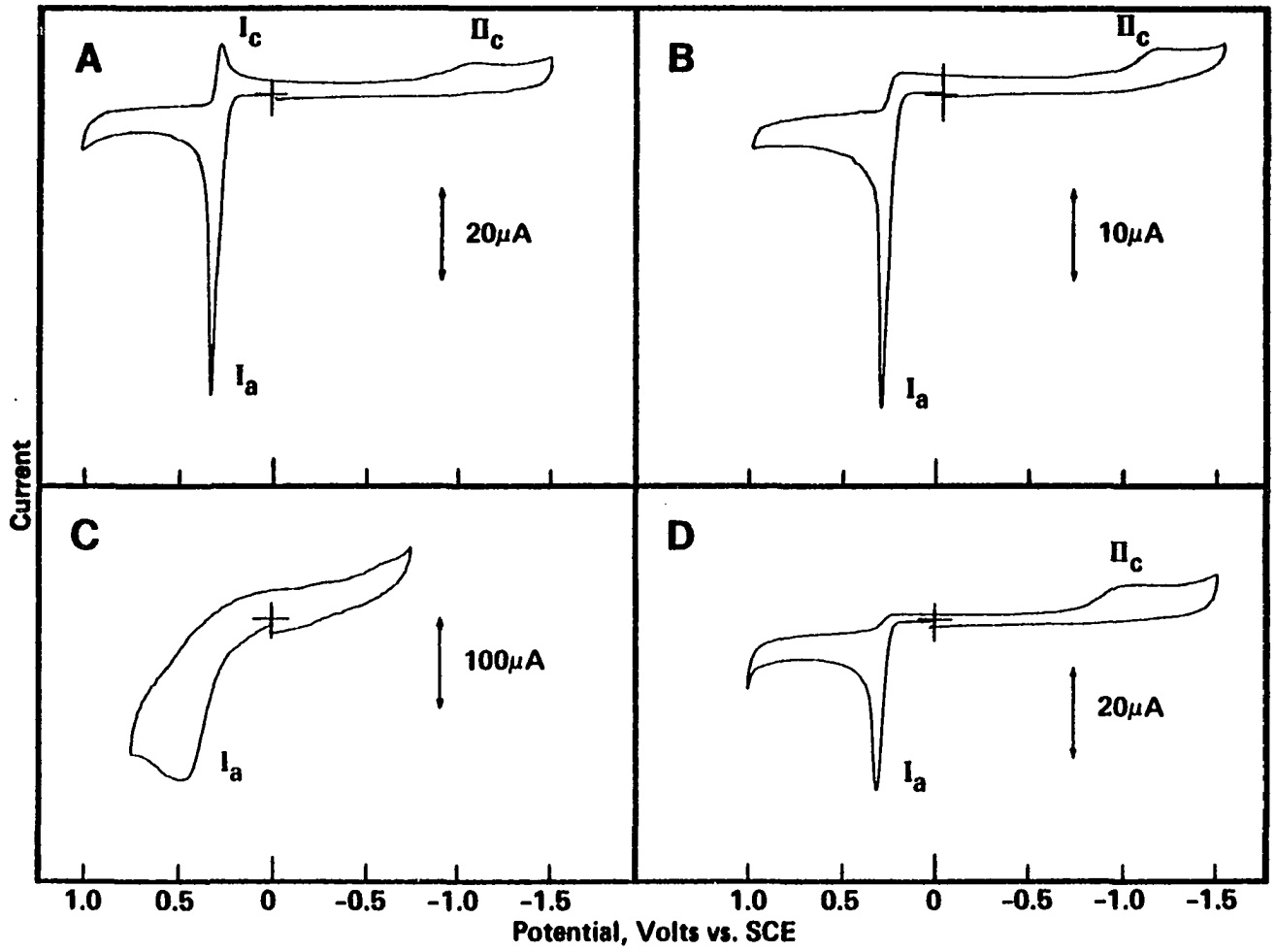

Figure 6. Cyclic voltammograms of 1 mM uric acid in pH 7.0 phosphate buffer at (A) RPGE, (B) SPGE, (C) gold foil electrode, and (D) RPGE, solution saturated with allopurinol. The starting potential is indicated by (+). Initial scan towards (+) potentials. Scan rate 200 mV sec^{-1}. Geometric area for PGE's 0.03 cm^2; for gold electrode 0.28 cm^2.

finding. However, the appearance of peak I_c at only the RPGE at slow sweep rates suggests that the diimine intermediate on oxidation of uric acid is adsorbed at the RPGE and is stabilized to some extent in the adsorbed state. The latter suggestion is further supported by the fact that saturation of a solution of uric acid with allopurinol (1H-pyrazolo[3,4-d]pyrimidin-4-ol, I)

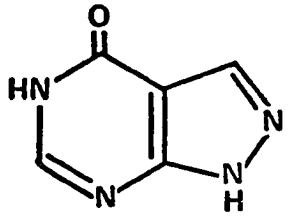

I

also causes peak I_c to disappear even at the RPGE (Figure 6D). Allopurinol has been reported to be strongly adsorbed at the RPGE such that the adsorption of uric acid is significantly decreased.[83] It seems quite logical, therefore, that the presence of a large excess of allopurinol would also decrease the extent of adsorption of the diimine electrooxidation product of uric acid. Hence, the reduction peak I_c should decrease or even be eliminated. Under the conditions shown in Figure 6D, the reduction peak I_c could not be observed to any significant extent until sweep rates of ca. 10 V sec^{-1} were employed.

The second reduction peak (II_c) observed on

cyclic voltammetry of uric acid at the PGE (Fig. 6A,B,D) is observed at slow and fast sweep rates. This peak has been proposed[54,56] to be due to reduction of the imine-alcohol (III, equation 1, Chapter 1) formed on partial hydration of the diimine electrooxidation product of uric acid. There is no reason, on the basis of the work reported here, to believe that the latter explanation of peak II_c is not correct. Indeed, evidence will be presented below to support this explanation. Failure to observe peak II_c upon cyclic voltammetry of uric acid at the gold electrode is simply due to the fact that the negative potential range at the latter electrode does not extend to potentials where peak II_c may be observed. Peak II_c was not well defined under any of the conditions reported in this study even at graphite electrodes. It usually had the appearance of a low, drawn-out or rounded peak.

Cyclic voltammetry of uric acid at a rough spectroscopic graphite electrode (see Experimental) gave rise to a very large peak I_c even at slow sweep rates (Figure 7A). On the other hand the rough wax-impregnated spectroscopic graphite electrode (WISGE, see Experimental) gave a significant peak I_c only at sweep rates $\geq$ 1 V sec^{-1} (Figure 7B). A smooth WISGE gave no evidence for peak I_c at a sweep rate of 1 V sec^{-1} (Figure 7C). Indeed, peak I_c could be observed at the smooth WISGE only at sweep

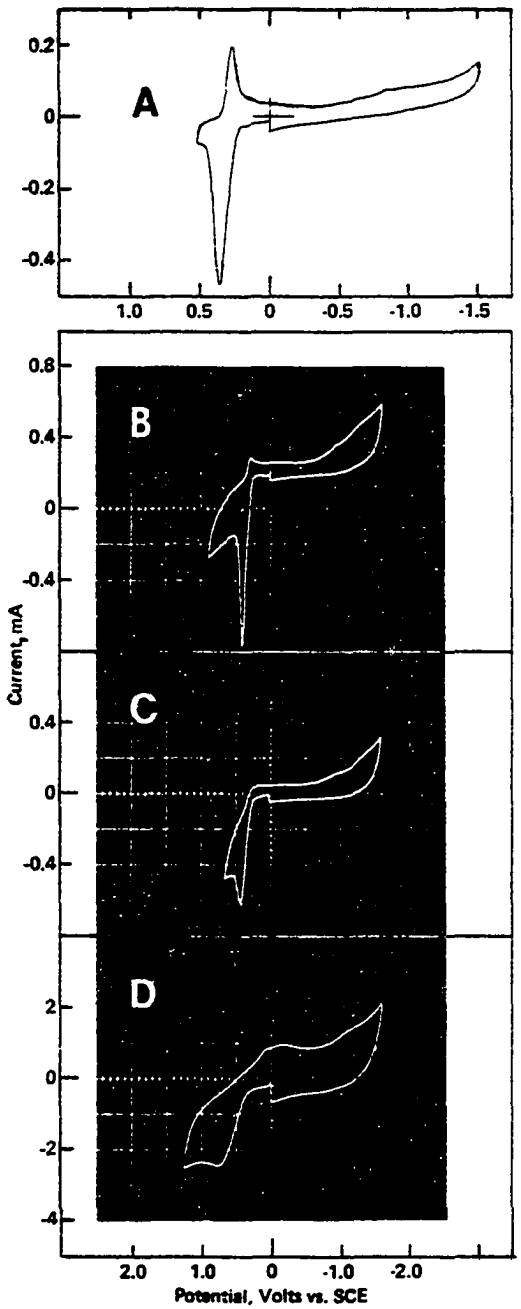

Figure 7. Cyclic voltammograms of 1 mM uric acid in pH 7.0 phosphate buffer at (A) rough spectroscopic graphite electrode at 200 mV sec^{-1}, (B) rough WISGE at 1 V sec^{-1}, (C) smooth WISGE at 1 V sec^{-1}, and (D) smooth WISGE at 50 V sec^{-1}. Initial sweep towards positive potentials. Geometric area of spectroscopic graphite electrode 0.16 cm^2, WISGE 0.28 cm^2.

rates of ca. 50 V sec^{-1} at pH 7 (Figure 7D). The cyclic voltammetric behavior of uric acid at the latter spectroscopic graphite electrodes may also be explained in terms of adsorption of the diimine intermediate at the electrode surface. Thus, at the rough spectroscopic graphite electrode the open, porous graphite structure provides a very large surface area for adsorption and stabilization of the intermediate, hence a large peak I_c is observed. Because the WISGE has all internal pores filled with wax the surface area of the rough electrode would be less than at the nonimpregnated spectroscopic graphite, hence peak I_c is correspondingly smaller. The highly polished smooth WISGE would have even fewer adsorption sites so that peak I_c could be observed only at very fast sweep rates. The shape of peak I_c at fast sweep rates at the smooth WISGE is more typical of an electrode process which is not complicated by adsorption effects. On the other hand the spiky appearance of peak I_c at both the rough spectroscopic graphite and rough WISGE are characteristic of adsorption processes.

The voltammetry of xanthine at the RPGE has been studied extensively[54,56] with E_p = 1.07-0.060 pH between pH 1-12 at a sweep rate of 5 mV sec^{-1}. Cyclic voltammetry of xanthine over a range of pH values at the RPGE shows a primary 4e electrooxidation peak II_a (Figure 8A) which

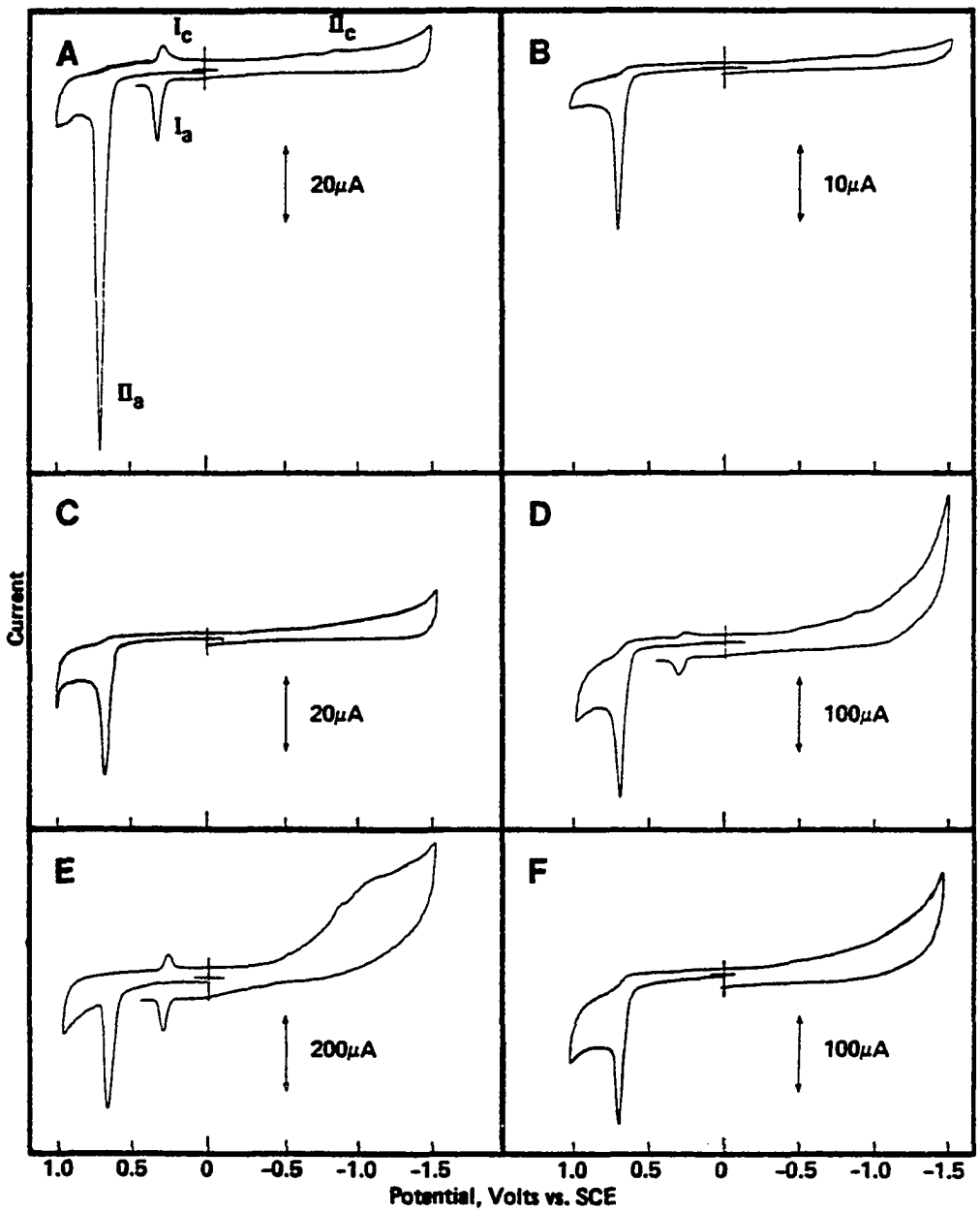

Figure 8. Cyclic voltammograms of 1 mM xanthine in pH 7.0 phosphate buffer at (A) RPGE, (B) SPGE, (C) RPGE, solution saturated with allopurinol, (D) rough WISGE, (E) rough spectroscopic graphite electrode and (F) smooth WISGE. Initial scan towards positive potentials. Geometric area of PGE's 0.03 cm^2, WISGE's 0.28 cm^2, spectroscopic graphite electrode 0.16 cm^2. Scan rate 200 mV sec^{-1}.

has been proposed to be due to oxidation of xanthine to the same diimine species formed on electrooxidation of uric acid. Peak I_c has been proposed to be due to reduction of this species to uric acid and peak II_c to reduction of the partially hydrated diimine, i.e., the imine-alcohol. On the second sweep towards positive potentials peak I_a appears which is due to electrooxidation of the uric acid formed in the peak I_c process. The effect of decreasing the electrode roughness on cyclic voltammetry of xanthine parallels that observed with uric acid at the PGE, WISGE, and the spectroscopic graphite electrode (Figure 8). Thus, at a smooth electrode surface the proposed diimine reduction peak I_c and the corresponding uric acid oxidation peak I_a do not appear at slow sweep rates. They can, however, be observed at much faster sweep rates. Similarly, addition of excess allopurinol to a solution of xanthine results in elimination of cyclic voltammetric peaks I_c and I_a (Figure 8C).

The information obtained from these cyclic voltammetric studies of uric acid and xanthine at graphite and gold electrodes suggests that the appearance and magnitude of peak I_c is directly related to the electrode surface roughness and hence to the availability of adsorption sites. It would appear that the diimine species formed upon electrooxidation of uric acid and xanthine is stabilized to some extent by adsorption at the electrode

surface and that the rate of hydration of this diimine in solution is very rapid.

The effect of pH on the cyclic voltammetry of uric acid at slow sweep rates is shown in Figure 9A and B. These voltammograms clearly show that reduction peak I_c is observed only at the RPGE at slow sweep rates and is most pronounced around neutral pH. This suggests that the species responsible for reduction peak I_c has maximal stability at pH 7-8 (vide infra). Xanthine gives very similar cyclic voltammetric results.

Double potential step chronoamperometry

In view of the fact that peak I_c observed by cyclic voltammetry of uric acid is always smaller than peak I_a except at very high sweep rates it may be concluded that the diimine primary electrooxidation product (II, equation 1, Chapter 1) undergoes a rapid follow-up chemical reaction presumably forming an imine-alcohol. An attempt was made to study the kinetics of this process using double potential step chronoamperometry[84] after the method of Bard.[68] Initial experiments utilizing both the RPGE and SPGE were unsuccessful owing to the irreproducibility of the chronoamperometric curves which appeared to be associated with the rather significant adsorption of the diimine intermediate at the PGE's. Somewhat more reproducible data could be obtained using a smooth WISGE

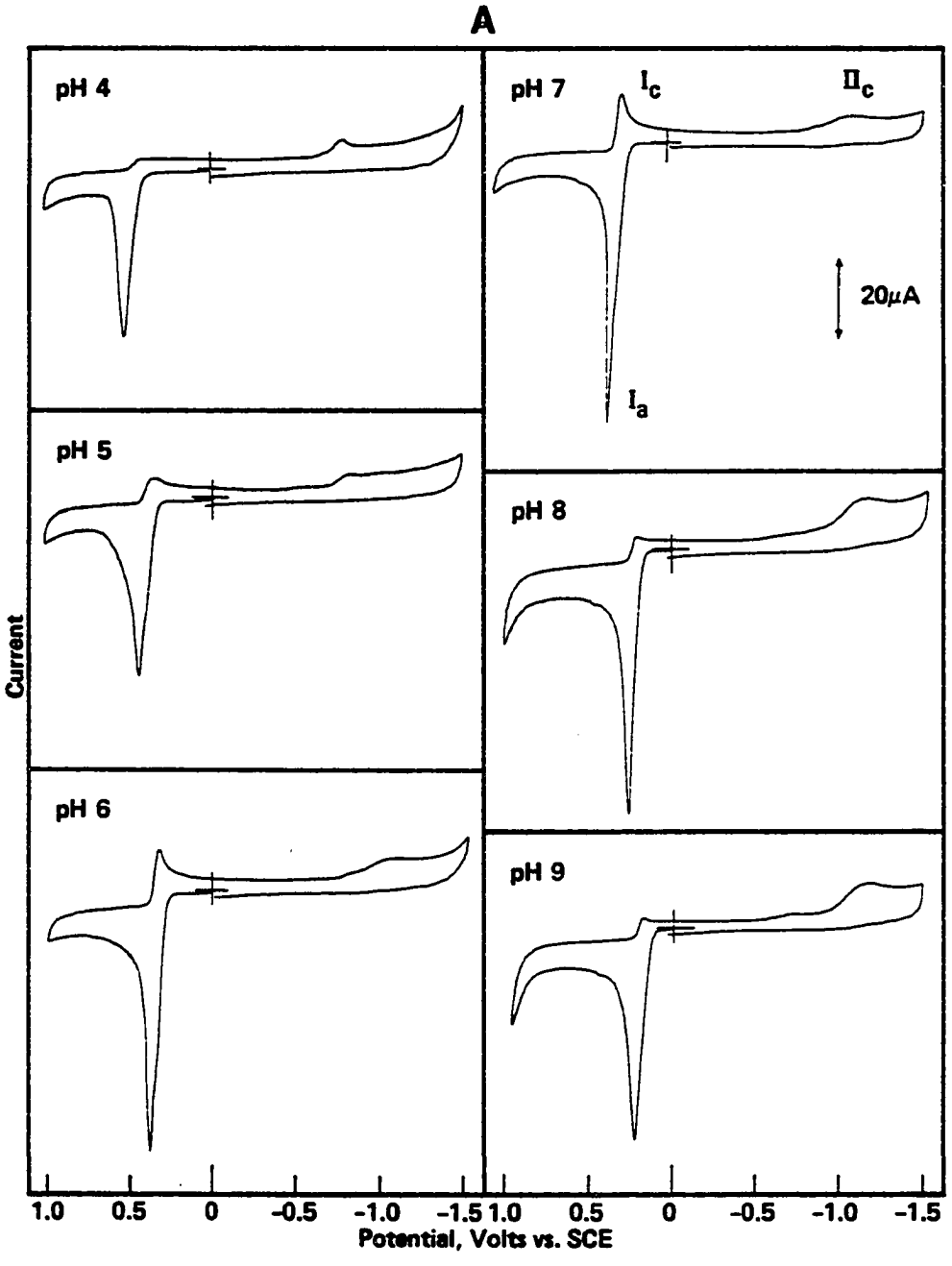

Figure 9A. Cyclic voltammograms of 1 mM uric acid at RPGE in phosphate buffer between pH 4 and 9. Initial scan towards positive potentials. Scan rate 200 mV sec^{-1}.

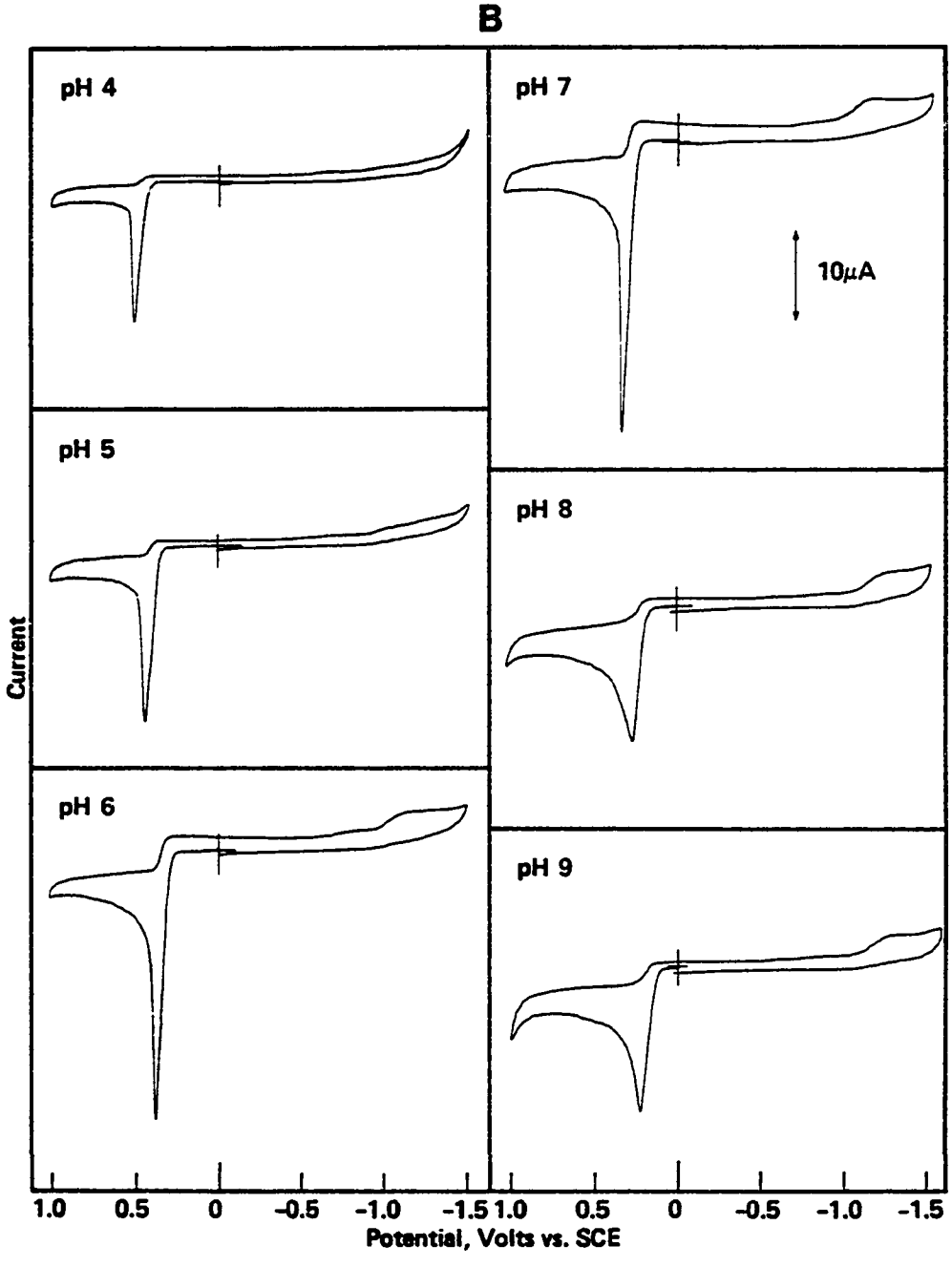

Figure 9B. Cyclic voltammograms of 1 mM uric acid at SPGE in phosphate buffer between pH 4 and 9. Initial scan towards positive potentials. Scan rate 200 mV sec^{-1}.

where adsorption effects were far less pronounced. The most reliable chronoamperometric results were obtained at pH 8.0, giving an apparent first-order solution rate constant of 32.5 sec^{-1}. At pH values lower or greater than 8 the solution rate constants appeared to increase, again suggesting the diimine intermediate has a maximal stability at pH 8. However, because of the greater uncertainty regarding both the order of the follow-up reaction and the observed rate constants, the results will not be presented here. The double potential step experiments do support, however, the general conclusion that the hydration reaction of the diimine of uric acid is very rapid in solution (> 30 sec^{-1}).

Thin-layer spectroelectrochemical studies

Thin-layer spectroelectrochemical studies of uric acid and xanthine using a rapid scan spectrophotometer (RSS) employed a gold minigrid working electrode similar to that described by Heineman and coworkers.[69,77] Since previous studies of the electrochemical oxidation of uric acid and xanthine were carried out at graphite electrodes, the electrochemical behavior of these compounds were briefly investigated at a gold electrode. The peak potential for oxidation of uric acid at the gold electrode follows the relationship E_p = 1.03-0.086 pH between pH 4-9 at 5 mV sec^{-1}, while in the case of xanthine the

relationship E_p = 1.15-0.06 pH is observed over the same pH range under identical conditions. Thus, the peak potentials for electrooxidation of uric acid and xanthine at the gold electrode occur at somewhat more positive potentials than the values observed at the PGE (vide supra). Cyclic voltammetry of uric acid at the gold electrode is similar in many respects to that observed at a SPGE, i.e., a single voltammetric oxidation peak (peak I_a) is observed. At slow sweep rates no reduction peak I_c is noted (Figure 6C) although at sweep rates > 20 V sec^{-1} the latter peak may be observed. It was not possible to carry out very meaningful cyclic voltammograms of xanthine at the gold electrode. At potentials of 1.0 V or more positive in phosphate and sulfate buffers (only slightly more positive than E_p for xanthine at pH 7) the positive potential window of the gold electrode is limited by gold oxide formation.[76] On the subsequent sweep towards negative potentials a large reduction peak due to reduction of the gold oxide is formed.[85] The latter peak would obscure peak I_c of xanthine.

Coulometric n-values for electrochemical oxidation of uric acid and xanthine were obtained by controlled potential electrolysis in a thin-layer electrolysis cell using a gold minigrid electrode. Some typical results of such thin-layer coulometry are presented in Table 3 where it is clear that uric acid is electrooxidized in a

2e reaction and xanthine in a 4e reaction in agreement with previous results obtained in traditional macroscale coulometric experiments at the PGE. Based on such voltammetric and coulometric studies, it was concluded that the basic electrode reaction schemes for uric acid and xanthine at the gold and graphite electrodes are the same.

TABLE 3

Experimental n-Values Observed for Electrochemical Oxidation of Uric Acid and Xanthine in a Thin-Layer Cell at a Gold Minigrid Electrode

Compound	pH	Initial Concentration, mM	Controlled potential, V vs. SCE	n-Value[a]
Uric acid	7	5	0.9	1.8
Uric acid	8	5	0.8	1.9
Uric acid	9	1	0.8	1.6
Xanthine	8	1.5	1.2	3.7

[a]By graphical integration of current-time curve.

A typical u.v. spectrum obtained prior to electrolysis of uric acid at pH 7.0 at the gold minigrid electrode in a thin-layer cell is shown in curve 1 of Figure 10 where it may be observed that uric acid exhibits an absorption peak with λ_{max} of 287 nm. Upon application of a potential of 0.9 V the u.v. peak of uric acid decreases

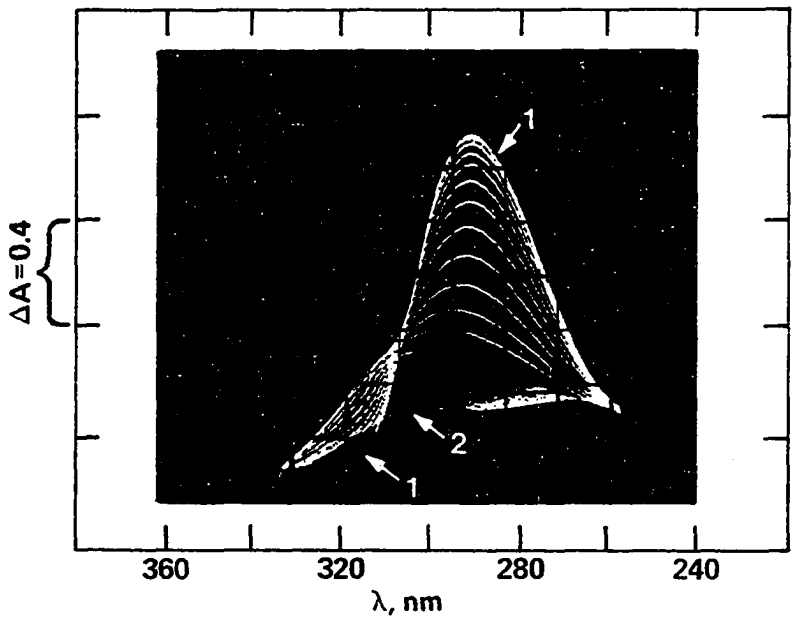

Figure 10. Spectrum of 10 mM uric acid solution electrolyzing at 0.9 V in pH 7.0 phosphate buffer at a gold minigrid electrode in a thin-layer cell. Curve (1) is uric acid spectrum before electrolysis. Trace (2) is the spectrum of the exhaustively electrolyzed solution. Repetitive scans are 9.5 seconds.

with time and, correspondingly, a rather broad peak (λ_{max} = 304 nm between pH 6 and 9) appears and grows. The latter peak reaches a maximum value and then it also decreases. This strongly supports the view that upon electrochemical oxidation of uric acid an unstable intermediate absorbing at longer wavelengths than uric acid is formed.

Curve 2 in Figure 10 is the spectrum of an exhaustively electrolyzed uric acid solution at a time when all of the absorbing intermediate species has disappeared. This spectrum is identical to that of a ca. 10 mM solution of allantoin, the ultimate product of electrooxidation of uric acid at pH 7,[54,56] under the same conditions. Thin-layer spectroelectrochemical studies of uric acid over a range of concentrations (1-10 mM) at pH 7 at different potentials (0.4 V to 1.0 V) gave results similar to those shown in Figure 10. However, at applied potentials more negative than E_p the rate of electrooxidation was significantly slower. The thin-layer spectroelectrochemical behavior of uric acid at pH 8 and 9 was essentially identical to that reported above for pH 7. However, below pH 7 it became increasingly more difficult to observe the spectrum of the intermediate species and at pH 5, for example, it was not possible to observe any absorption due to any species other than uric acid even using very fast spectral sweep rates. This implies that the stability of the intermediate observed at pH 7-9 is significantly

lower below pH 7 or that its absorption behavior is quite different. With decreasing pH below pH 7 the solubility of uric acid decreases ($\leq$ 1 m$\underline{M}$) such that thin-layer spectroelectrochemical studies became very difficult.

Thin-layer spectroelectrochemical studies of the electrooxidation of xanthine between pH 7-9 indicated that the same unstable intermediate (λ_{max} = 304 nm) formed upon electrooxidation of uric acid was produced. However, the low solubility of xanthine resulted in the formation of much poorer quality spectra than those observed for uric acid. It was not possible to carry out thin-layer spectroelectrochemical studies of the electrooxidation of xanthine below pH 7 because of the very low solubility of this compound (< 0.5 m$\underline{M}$). Between pH 7 and 9 formation of the unstable, absorbing intermediate upon electrochemical oxidation of xanthine was not dependent upon the applied potential employed. Following complete electrooxidation of xanthine and decomposition of the intermediate species (λ_{max} = 304 nm) the spectrum of the solution remaining in the thin-layer cell was identical to that of allantoin under similar conditions.

Kinetic measurements

The kinetics of the decomposition reaction of the u.v.-absorbing intermediate species formed on electrooxidation of uric acid and xanthine were studied by thin-

layer spectroelectrochemistry. The absorbance of the intermediate species was monitored at a wavelength at which there was minimal interference from the absorption of uric acid or xanthine (ca. 320 nm). The absorbance at this wavelength was measured while uric acid or xanthine was electrooxidized at a constant potential at the gold minigrid electrode. A typical plot of absorbance versus time throughout the course of such an experiment with uric acid is shown in Figure 11A. The absorbance due to the intermediate species reached its maximal value at, or close to, the time when uric acid (or xanthine) was completely electrolyzed. The decrease of the absorbance of the intermediate species with time was used to study the kinetics of its decomposition reaction.

A typical rate plot obtained for the intermediate formed on electrooxidation of uric acid at pH 7 is presented in Figure 11B. Clearly, the plot of log $A-A_{\infty}$ vs. time is linear indicating that the reaction of the absorbing intermediate species follows first-order kinetics. The value of the observed first-order solution rate constant for reaction of the u.v.-absorbing intermediate formed on electrochemical oxidation of uric acid at pH values between 7 and 9 are presented in Table 4. Thus, the value of the observed rate constant is essentially independent of concentration and of pH. The small decrease of the rate constant between pH 7 and 9 is probably

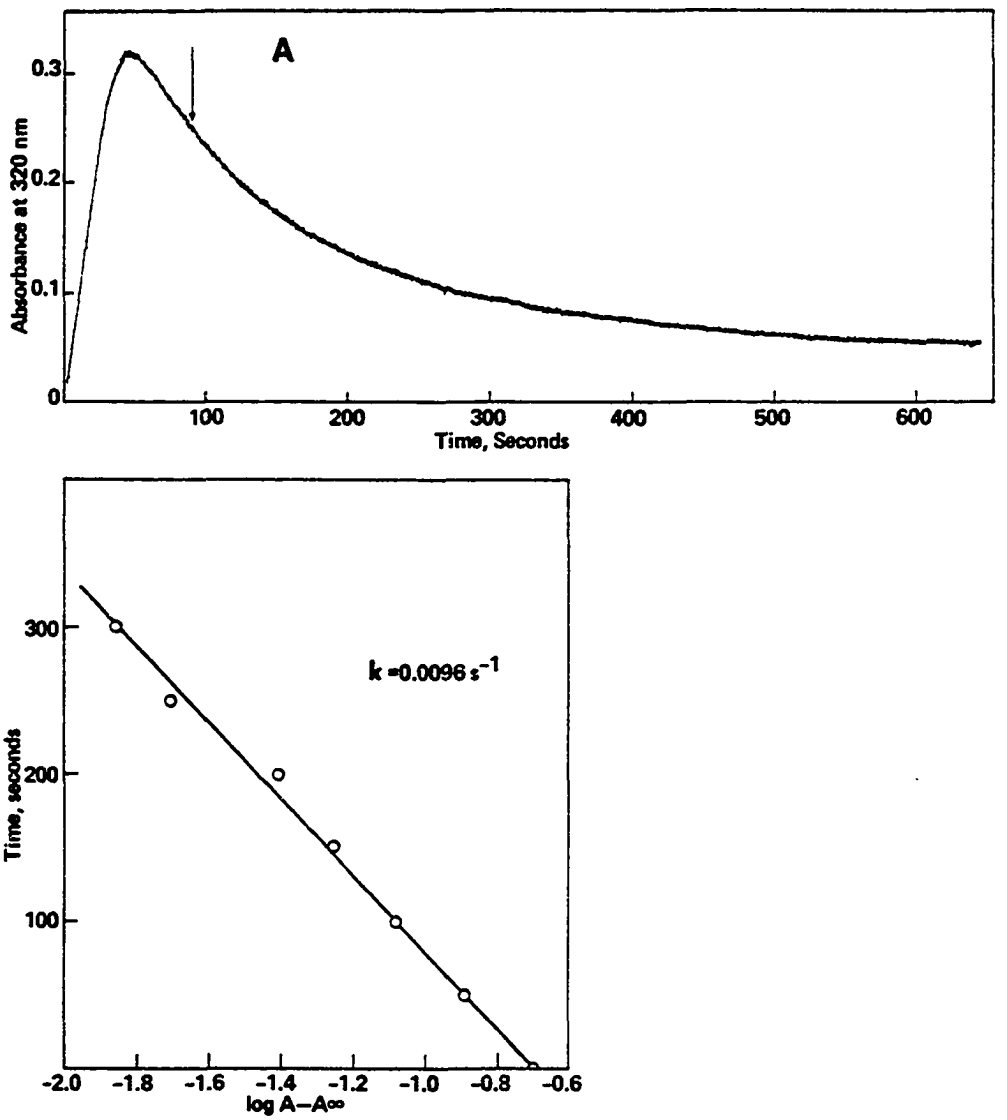

Figure 11. (A) Variation of the absorbance with time observed on electrochemical oxidation of 5 mM uric acid in pH 7.0 phosphate buffer at a gold minigrid electrode (0.9 V) in a thin-layer cell. (B) Kinetic plot of time versus log absorbance at 320 nm. Absorbance data were taken from curve (A) setting t=0 at the point where the concentration of uric acid was at or very near to zero, i.e., at arrow in (A).

related to changes in buffer composition and is much too small to suggest that the reaction is acid catalyzed.

TABLE 4

Observed First-Order Rate Constants for Reaction of the U.v.-absorbing Intermediate Formed on Electrochemical Oxidation of Uric Acid at Gold Minigrid Electrode

Initial Concentration of uric acid, mM	pH[a]	k_{obs}, sec^{-1}
1.0	7	0.010
5.0		0.009
10.0		0.008
1.0	8	0.009
5.0		0.006
10.0		0.007
1.0	9	0.007
5.0		0.004
10.0		0.006

[a]Phosphate buffers containing K_2SO_4, all having an ionic strength of 0.5.

Accordingly, it was concluded that the observed rate constant for the reaction of the u.v.-absorbing intermediate is 0.008 ± 0.002 sec^{-1}.

The u.v.-absorbing intermediate observed on thin-layer spectroelectrochemistry of xanthine gave an average observed first order rate constant of 0.006 ± 0.003 sec^{-1} over the pH range 7-9. In view of the

similarity of these first-order rate constants for disappearance of the u.v.-absorbing intermediates formed on electrooxidation of uric acid and xanthine, it seems reasonable to conclude that they are identical species. This conclusion is further supported by the identical u.v. spectra (λ_{max} = 304 nm, pH 7-9) of the intermediates formed from both purines and the fact that the product observed upon reaction of the intermediate formed from both uric acid and xanthine is allantoin (vide supra).

DISCUSSION

The experiments reported above indicate that at graphite and gold electrodes uric acid and xanthine are electrochemically oxidized to a very short-lived ($\leq$ 23 m sec) primary product. This primary product is rather readily reducible as evidenced by peak I_c observed on cyclic voltammetry of uric acid and xanthine. Earlier reports and the work reported here support the view that the primary electrooxidation product of uric acid and xanthine is the diimine (II, equation 1, Chapter 1). However, it is possible to observe electrochemical reduction of this diimine via peak I_c on cyclic voltammetry of uric acid or xanthine at relatively slow sweep rates (ca. 200 mV sec^{-1}) only at graphite electrodes which have a rough surface. At a gold electrode or graphite electrodes

resurfaced in such a fashion that their surface is highly polished and smooth, the diimine reduction peak I_c can only be observed at fast sweep rates ($\geq$ 50 V sec^{-1}). The only rational explanation of this effect is that the primary diimine product of electrooxidation of uric acid and xanthine is very unstable in homogeneous solution but when adsorbed at graphite electrodes it is attacked more slowly. The rough graphite surfaces appear to provide an increased number of adsorption sites for the diimine compared to the highly polished, smooth electrodes. The diimine primary electrooxidation product is attacked by water to give the imine-alcohol (III, equation 1, Chapter 1). Attempts to study the kinetics of this hydration reaction by double potential step chronoamperometry indicate that it is a first-order process characterized by an apparent rate constant at pH 8.0 of 32.5 sec^{-1}. At both higher and lower pH values the rate of the hydration reaction appears to increase.

Thin-layer spectroelectrochemical experiments reveal that electrooxidation of uric acid or xanthine gives rise to a further intermediate that exhibits a well-defined absorption spectrum having λ_{max} = 304 nm between pH 7-9. This species also undergoes a first-order hydration reaction with an apparent rate constant of about 8 x 10^{-3} sec^{-1} which corresponds to a half-life of more than 1 minute. It is therefore quite impossible

for this intermediate to be the same species responsible for peak I_c, i.e., the diimine. Accordingly, it is concluded that the u.v.-absorbing intermediate observed in thin-layer spectroelectrochemical studies of uric acid and xanthine is the imine-alcohol and the first-order reaction of this species corresponds to hydration of the imine-like C(4)=N(9) (or C(5)=N(7)) double bond to give uric acid-4,5-diol (IV, equation 1, Chapter 1). Between pH 7-9 the latter reaction is not significantly influenced by the solution pH.

In addition, in the cyclic voltammetry of uric acid and xanthine, peak II_c is usually always present at both fast and slow voltage sweep rates (vide supra). This indicates that the hydration reaction of the diimine to the imine-alcohol is very fast, but that the hydration of the imine-alcohol to uric acid-4,5-diol is rather slow.

These investigations provide considerably more insight into the mechanism of electrochemical oxidation of uric acid and xanthine. Thin-layer spectroelectrochemical studies, in conjunction with cyclic voltammetry and double potential step chronoamperometry (when appropriate), should be quite helpful in the investigations of the electrochemical oxidation of other biologically important purines.

EXPERIMENTAL

Chemicals

Xanthine was obtained from Nutritional Biochemicals, uric acid from Eastman, and allopurinol from Calbiochem.

Buffer solutions were prepared from reagent grade chemicals with an ionic strength of 1.0 (0.5 upon 1:1 dilution with deionized water). These buffers were constituted as follows: $NaOH/KH_2PO_4/K_2SO_4$.

Apparatus

Linear sweep voltammetry and cyclic voltammetry were carried out with the instrument described previously. The potential pulses for the double potential step chronoamperometric studies were obtained from a Princeton Applied Research Corporation Model 175 Universal Programmer. The three-compartment cell utilized for all voltammetric experiments has been described in Part I.

The rapid scan spectrometer for optical measurements, the optically transparent thin-layer electrochemical cells, the potentiostat for controlling the applied potential, and the apparatus for recording all voltammograms, chronoamperograms, absorbance *vs.* time curves, and RSS spectra were all described in Chapter 2.

The gold foil electrode employed for voltammetric studies was constructed by attaching a *ca.* 1 cm^2 piece

of gold foil across the end of a 6 mm o.d. glass tube. This was accomplished with Duro Super Glue 3 (Woodhill Chemical Sales Corporation, Cleveland, Ohio). The gold foil was fitted tightly around the body of the glass tube with epoxy resin (Epoxi-Patch, Dexter Corporation, Olean, New York) so that only the gold stretched across the end of the glass tube was exposed. In order to protect the epoxy coating from the strong cleaning solutions used on the gold electrode the lower 6-7 cm of the tube was painted with three coats of Tygon paint (Carboline K-63 white paint, Carboline Company, St. Louis, Missouri). Finally, the glass tube was packed firmly with carbon paste (3g Ultra Carbon UCP-1-M, Ultra Carbon Corporation, Bay City, Michigan, in 2 ml Nujol) and a copper wire inserted for electrical contact. The gold electrode was pretreated before each run[88] by immersing first in chromic acid solution for 2 minutes, followed by a thorough water wash. The electrode was then placed in the test solution and maintained at a potential of -0.5 V for two minutes. The electrode was then gently tapped to remove gas bubbles and a voltammogram was run immediately.

The construction of the rough pyrolytic graphite electrode (RPGE) has been described in Part I, Chapter 3). The construction of the smooth pyrolytic graphite electrode (SPGE) was similar to that described above except that the graphite rod was sealed into the glass tube with about

4-5 mm protruding from the bottom. The protruding graphite was coated with epoxy resin. This electrode was resurfaced by cleaving a small slice off the tip of the graphite with a sharp knife or razor blade. The freshly exposed tip was then polished on an alumina (< 0.1 micron, Grade B Gamma Alumina, Fisher Scientific) impregnated felt cloth. The surface of this electrode had the appearance of a metallic mirror and was considerably less rough than the RPGE.

Two spectroscopic graphite electrodes were utilized. The first was a rod of pure spectroscopic graphite (Ultra Carbon, Bay City, Michigan). This was resurfaced by grinding on a 600 grit silicon carbide paper. Because test solutions impregnated this porous electrode material, it was usual to grind off at least 0.25 inch of this electrode. A wax-impregnated spectroscopic graphite electrode (WISGE, Princeton Applied Research Corporation type 9319) was also utilized. A rough WISGE was prepared by resurfacing the electrode on a 600 grit silicon carbide polishing disc. A smooth WISGE was prepared by polishing the electrode on the alumina-impregnated felt cloth described above.

Procedures

Test solutions for voltammetric studies were generally 1 mM in uric acid or xanthine. Double potential

step chronoamperometric and RSS studies utilized concentration ranges of 0.3 m*M* to 10 m*M* depending upon the solubility at a particular pH and the nature of the study.

The procedure employed for the spectroelectrochemical studies was essentially the same as that outlined in Chapter 2, except that the wavelength range scanned was normally 260-340 nm. However, much broader regions were scanned, including the visible region, in preliminary experiments.

Since the oxidation of xanthine occurs at potentials more positive than *ca.* 1 V at pH 5-9, it was necessary to precathodize the thin-layer electrode at -0.5 V for three minutes prior to each run to reduce the heavily oxidized gold film formed on the surface of the electrode.[88]

In all spectroelectrochemical experiments at least three replicate runs were recorded. Background runs were also carried out in exactly the same way except that no uric acid or xanthine was included.

SUMMARY

The electrochemical oxidation of uric acid and xanthine has been studied at various graphite electrodes and at a gold electrode by a variety of techniques including cyclic voltammetry, double potential step chronoamperometry, and thin-layer spectroelectrochemistry. It

has been confirmed that the primary electrooxidation product formed from uric acid or xanthine is a diimine species. This diimine is very unstable in solution and is rapidly hydrated to an imine-alcohol in a first-order reaction. Although this diimine is very unstable in solution, its voltammetric reduction peak may be observed at rough graphite electrode surfaces at quite slow sweep rates. This is so because the diimine is strongly adsorbed at the rough electrode surface and is appreciably more stable than in solution. The imine-alcohol, formed by partial hydration of the diimine, may be observed as a further intermediate by thin-layer spectroelectrochemical studies. The kinetics of the hydration of this species to uric acid-4,5-diol was determined by spectroelectrochemistry.

CHAPTER 4

EFFECT OF 9-METHYL SUBSTITUTION ON THE ELECTROCHEMICAL OXIDATION OF URIC ACID AND XANTHINE

INTRODUCTION

Chapter 3 described the use of cyclic voltammetry, double potential step chronoamperometry, and thin-layer spectroelectrochemistry to investigate the electrochemical oxidation of uric acid and xanthine. The present study was undertaken to determine the effect of 9-methyl substitution on the electrochemical oxidation of uric acid and xanthine. It was hoped that these studies would provide a useful guide to the behavior of the more complex purine nucleosides, nucleotides, oligonucleotides, and nucleic acids which are or contain 9-substituted purines.

Accordingly, the electrochemical oxidations of 9-methyluric acid (VI) and 9-methylxanthine (VII) were studied by cyclic voltammetry, controlled potential coulometry, and thin-layer spectroelectrochemistry. No previous investigations of the electrochemical oxidation

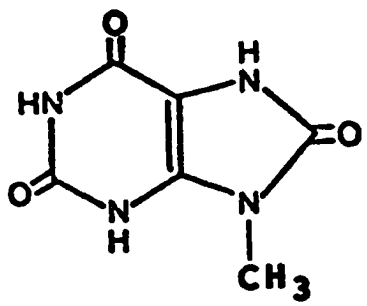

VI

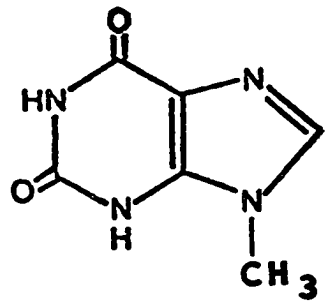

VII

of these compounds have been reported. The results of these studies were compared to the results of the electrochemical oxidation of uric acid and xanthine described in Chapter 3.

RESULTS AND DISCUSSION

pK_a Values for 9-methyluric acid and 9-methylxanthine

The pK_a values for 9-methyluric acid and 9-methylxanthine are a little lower than for the parent compounds as shown in Table 5. The values for uric acid[86] and xanthine[87] were presented in Chapter 3. Jordan reported the pK_a for 9-methylxanthine as 6.3.[89] The pK_a for 9-methyluric acid could not be located in the literature. The value reported in Table 5 was obtained from plots like those shown in Figure 12. Figure 12A shows the variation of λ_{max} with pH for the two u.v.-absorbing

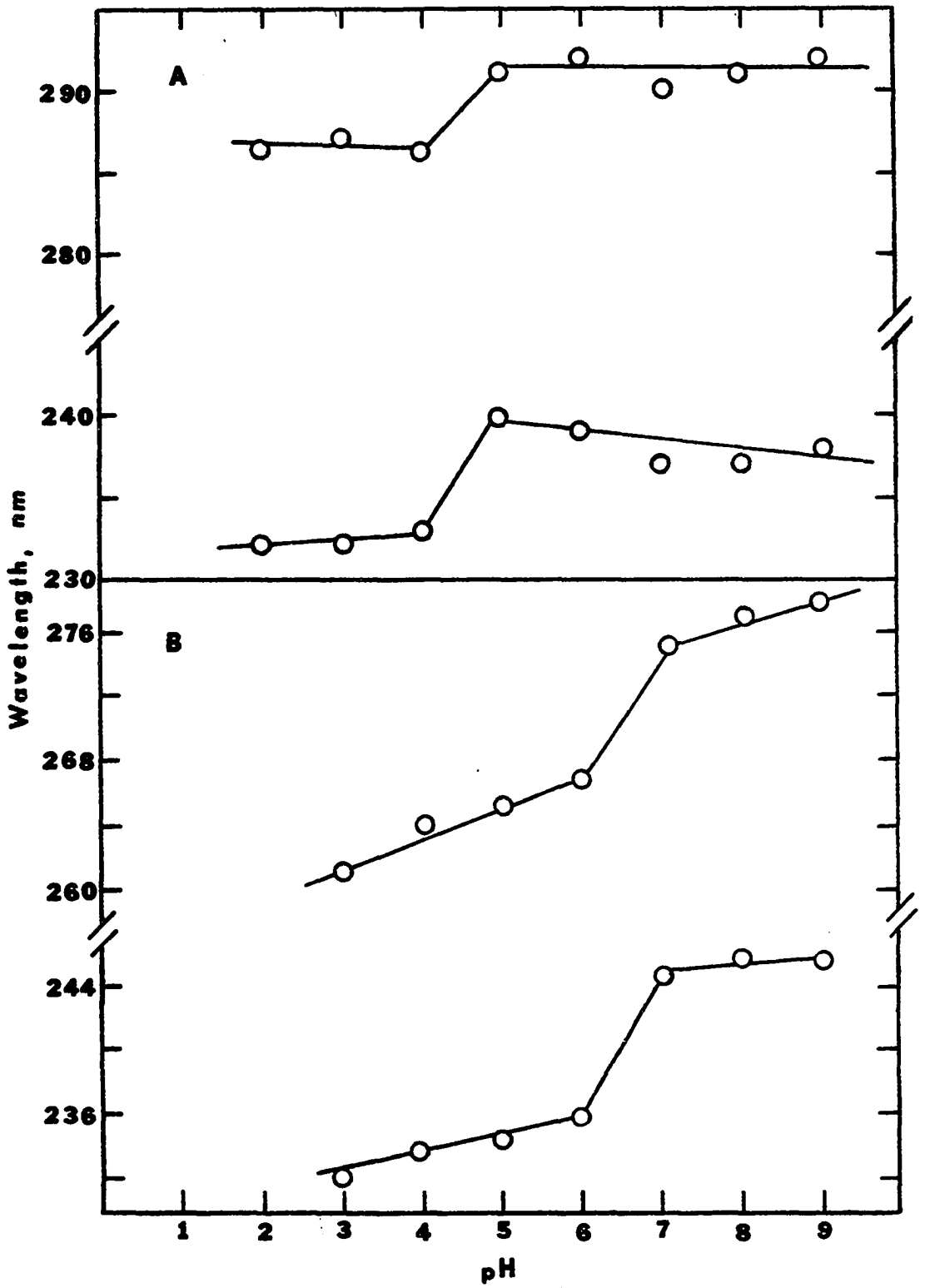

Figure 12. Wavelengths versus pH for the two u.v.-absorbing peaks of (A) 1m$\underline{M}$ 9-methyluric acid and (B) 1m$\underline{M}$ 9-methylxanthine.

TABLE 5

Comparison of pK_a Values for Uric Acid, Xanthine, and Their 9-Methyl Derivatives

Compound	pK_a
Uric Acid	5.4
9-Methyluric Acid	4.5[a]
Xanthine	7.53
9-Methylxanthine	6.3

[a]Based on u.v. shift in λ_{max}, others are literature values.

peaks of 9-methyluric acid. For both peaks λ_{max} remains essentially constant below pH 4 and above pH 5. In the region pH 4-5 a drastic shift occurs for both u.v. peaks. Figure 12B illustrates the same type of behavior for 9-methylxanthine, the major shift for the two λ_{max}'s occurring at ca. pH 6.3. This correlates well with the reported value for the pK_a of 6.3 in reference 89. It is quite reasonable, then, to assume that the pK_a for 9-methyluric acid is 4.5.

Voltammetry at carbon and gold electrodes

9-Methyluric acid gives a single, 2e voltammetric oxidation peak, the peak potential (E_p) for which, between pH 1-10, is described by the equation $E_p = 0.61 - 0.046$ pH at a sweep rate of 5 mV sec^{-1}. A typical cyclic voltammogram of 9-methyluric acid at the rough PGE (RPGE,

see Chapter 3) at 200 mV sec^{-1} sweep rate in pH 7.0 phosphate buffer is shown in Figure 13A. The voltammetry of 9-methyluric acid is nearly identical to that of uric acid. In Chapter 3, it was established that electro-oxidation peak I_a for uric acid is due to the primary 2e oxidation of uric acid to its diimine (see equation 1, Chapter 1); peak I_c to the quasi-reversible reduction of the diimine back to uric acid, and peak II_c to the reduction of the imine-alcohol. It would therefore be quite reasonable to assume that the peak assignments for 9-methyluric acid would be similar to that for uric acid, with its corresponding diimine and imine-alcohol.

If, instead of the RPGE, a smooth PGE (SPGE) is employed, peak I_c completely disappears at relatively slow sweep rates (Figure 13B). Indeed, peak I_c could not be observed to any significant extent at the SPGE at pH 7.0 until sweep rates $\geq$ 5 V sec^{-1} were employed. Likewise, at the gold foil electrode peak I_a of 9-methyl-uric acid was well-defined yet at sweep rates of ca. 200 mV sec^{-1} peak I_c was also absent and could not be observed except at sweep rates > 20 V sec^{-1}.

The appearance of peak I_c at only rough electrode surfaces at slow sweep rates suggests that the diimine intermediate of oxidation of 9-methyluric acid is adsorbed and is stabilized to some extent in the adsorbed

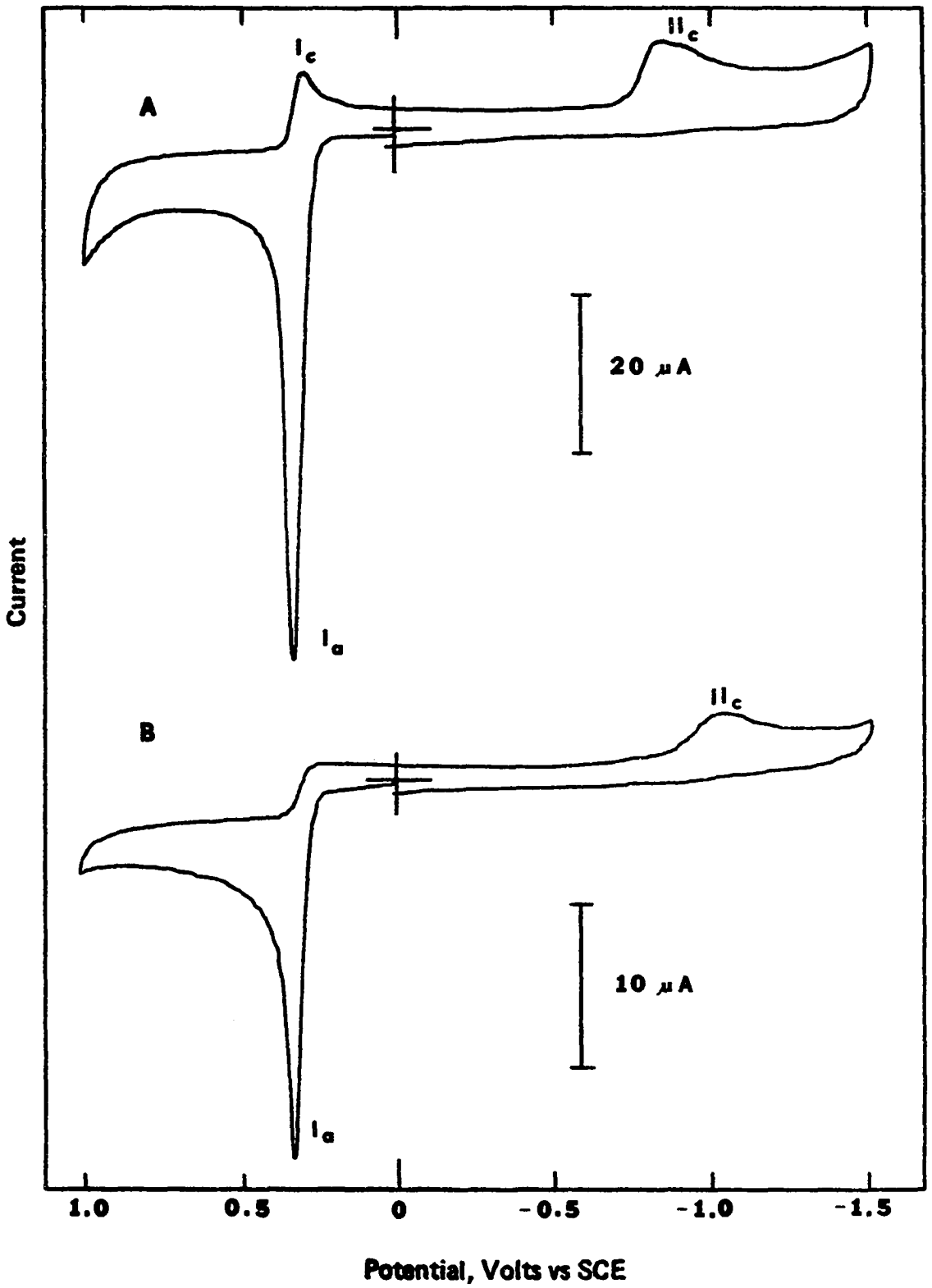

Figure 13. Cyclic voltammograms of 1mM 9-methyluric acid at pH 7 at (A) RPGE and (B) SPGE. Initial scan towards (+) potentials. Scan rate 200 mV sec^{-1}.

state. Uric acid shows identical behavior (see Chapter 3).

The peak potential for oxidation of 9-methyluric acid at the gold electrode follows the relationship E_p = 0.85-0.058 pH between pH 1-10 at a sweep rate of 5 mV sec^{-1}. Thus, the peak potentials for electrooxidation of 9-methyluric acid at the gold electrode occur at somewhat more positive potentials than the values observed at the PGE. Cyclic voltammetry of 9-methyluric acid at the gold electrode is similar in many respects to that observed at a SPGE, and is described in more detail above.

The effect of pH on the cyclic voltammetry of 9-methyluric acid at slow sweep rates again parallels that of uric acid (Figure 9, Chapter 3). That is, the ratio of peaks I_c/I_a increases with increasing pH until pH 7-8 and then decreases with higher pH. This suggests that the species responsible for reduction peak I_c has maximal stability at pH 7-8.

The voltammetry of 9-methylxanthine at the RPGE has been studied extensively with E_p = 1.05-0.055 pH between pH 1-7 at a sweep rate of 5 mV sec^{-1} for electrooxidation peak II_a. At pH > 7 the peak potential becomes independent of pH with E_p = 0.65±0.03 between pH 7-10. Electrooxidation peak III_a follows the relationship E_p = 1.16-0.057 pH between pH 1-7 and E_p = 0.77±0.02 between pH 7-10. Owing to the closeness to background discharge potentials, peaks IV_a and V_a became increasingly more

difficult to distinguish at lower values of pH. Accordingly, the following relationships are given with less reliability:

peak IV_a (pH 1-7); E_p = 1.17-0.04 pH

peak V_a (pH 1-7); E_p = 1.39-0.05 pH

Between pH 7-10, both peaks are independent of pH with (peak IV_a) E_p = 0.89±0.02 and (peak V_a) E_p = 1.02±0.01.

Cyclic voltammetry of 9-methylxanthine, shown in Figure 14A, is significantly different than that for xanthine shown in Chapter 3. One of the most obvious differences is the presence of the four oxidation peaks on the initial positive-going sweep of 9-methylxanthine. This is in contrast to only one electrooxidation peak for xanthine on the initial positive-going sweep. Another difference noted from switching potential (E_λ) studies (i.e., reversing the sweep from positive to negative-going at different potentials) was the fact that the I_c-I_a couple and peak II_c were observed to any significant degree only after sweeping into the peak IV_a or peak V_a region. The I_c-I_a couple and peak II_c were absent even when the sweep was stopped and held at a potential in the vicinity of peak II_a equal to the time required to sweep to peaks IV_a-V_a and back again. The peak potentials of the I_c-I_a system and peak II_c observed in the voltammetry of 9-methylxanthine are similar to those observed in the voltammetry of uric acid, xanthine, and 9-methyluric acid.

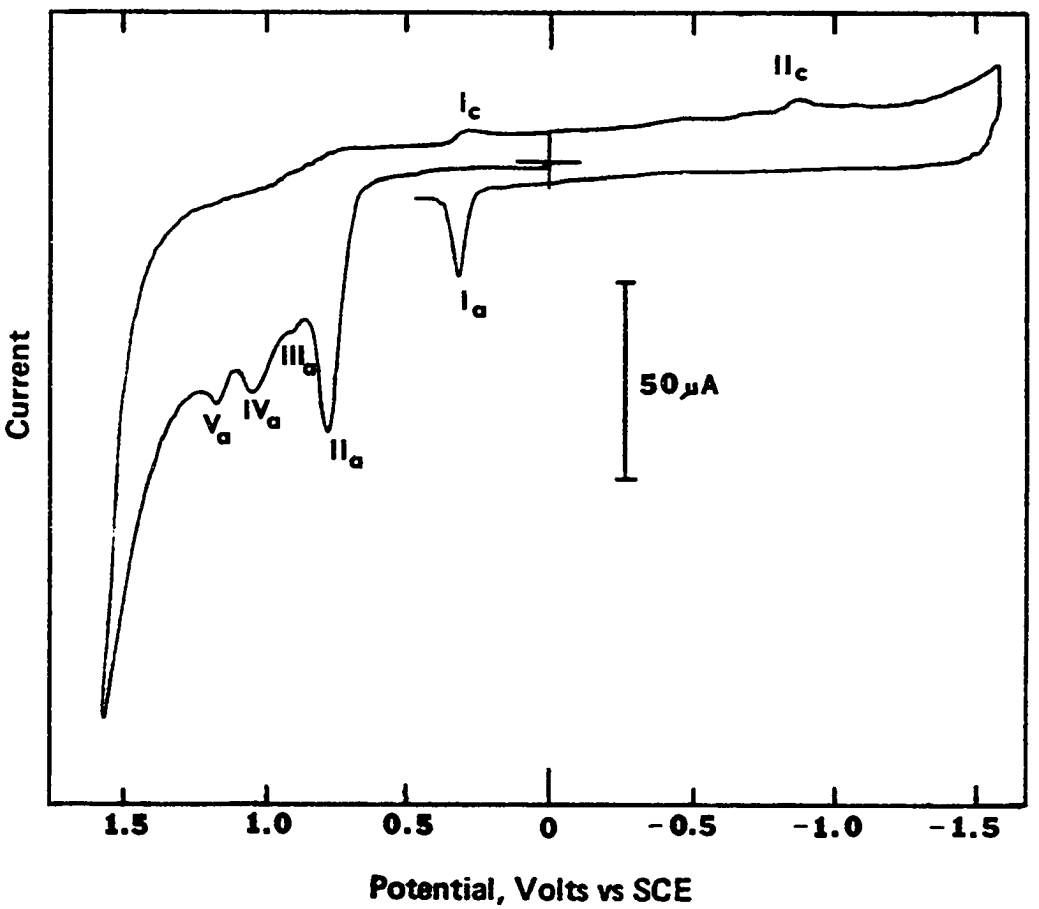

Figure 14A. Cyclic voltammogram of 1mM 9-methylxanthine at pH 8 at the RPGE. Initial scan towards (+) potentials. Scan rate 500 mV sec^{-1}.

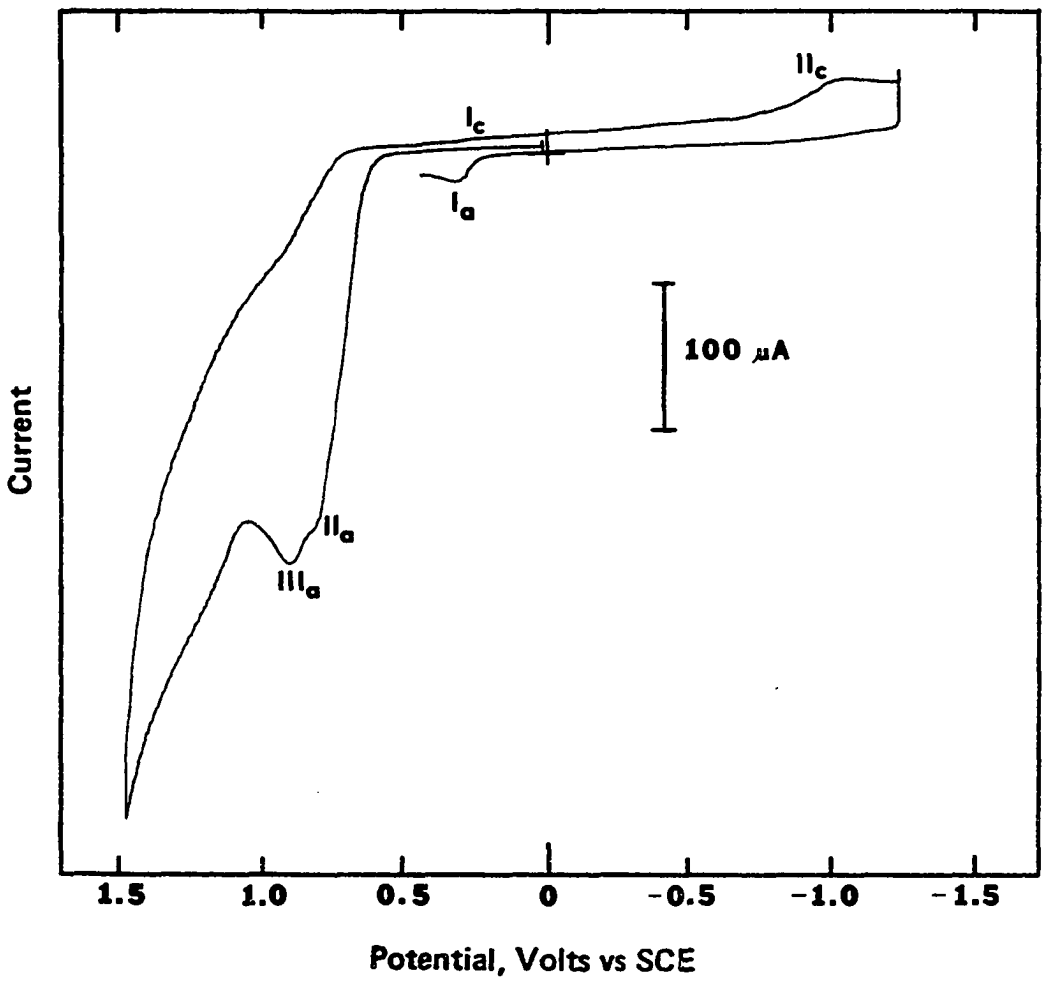

Figure 14B. Cyclic voltammogram of 20m<u>M</u> 9-methylxanthine at pH 8 at the RPGE. Initial scan towards (+) potentials. Scan rate 500 mV sec^{-1}.

A further discussion on the nature of these voltammetric peaks will be presented later.

The effect of decreasing electrode roughness on the cyclic voltammetry of 9-methylxanthine parallels that observed with uric acid and xanthine (Chapter 3), and with 9-methyluric acid (vide supra). Thus, at a smooth electrode surface peak I_c does not appear at slow sweep rates (ca. 200 mV sec^{-1}). It can, however, be observed at much faster sweep rates ($\geq$ 5 V sec^{-1}).

Cyclic voltammetry at varying concentrations (0.5 mM - 20 mM) of 9-methylxanthine was performed at the PGE. It was observed that at low concentrations (for example, 1 mM, Figure 14A) peak III_a was quite small in relation to peak II_a, while at higher concentrations (20 mM, Figure 14B) peak III_a became very large with respect to the other peaks. In fact, peak III_a was so large that the other peaks were barely detectable at the current sensitivity used. A possible explanation for this behavior is summarized in Conclusions.

The peak potential for oxidation of 9-methylxanthine at the gold foil electrode for peak II_a follows the relationship E_p = 1.24-0.055 pH from pH 1-7 at a sweep rate of 5 mV sec^{-1}, and between pH 7-10 E_p = 0.86±0.02. Peak III_a follows the relationship E_p = 1.40-0.056 pH between pH 1-7 and E_p = 1.06±0.01 between pH 7-10. As

with xanthine, it was not possible to carry out meaningful cyclic voltammograms of 9-methylxanthine at the gold electrode owing to the formation of gold oxide(s) at very positive potentials (Chapter 3). Consequently, peaks IV_a and V_a were not discernible and peak potential relationships could not be obtained.

The effect of pH on the cyclic voltammetry of 9-methylxanthine at the PGE follows the behavior for uric acid, xanthine, and 9-methyluric acid, i.e., the species responsible for peak I_c is most stable at pH 7-8.

Controlled potential coulometry

Over the pH range 4-8 at 1-10 mM concentration levels a faradaic n-value of about 2 (1.85-1.97) was obtained for the electrochemical oxidation of 9-methyluric acid at the PGE. Coulometry of 9-methylxanthine (1 mM) yielded a faradaic n-value of about 4 (4.03-4.2) at potentials positive of peaks IV_a or V_a (see Figure 14A). When the applied potential was less positive, e.g., in the vicinity of peak II_a for 9-methylxanthine, the observed faradaic n-value ranged from ca. 3.1-3.4, and gradually increased toward 4 as the potential was set more positive.

In addition, the coulometric n-value for 9-methylxanthine at the PGE decreased with increasing concentration of this material. For example, a 1 mM solution of 9-methyl-

xanthine at pH 8 electrolyzed at 1.0 V (near peaks IV_a and V_a) yielded a faradaic n-value of 4.05, while a 20 mM solution (same pH and applied potential) resulted in an n-value of 3.4.

Coulometric n-values for electrochemical oxidation of 9-methyluric acid and 9-methylxanthine were also obtained by controlled potential electrolysis in a thin-layer electrolysis cell using a gold minigrid electrode (Chapters 2 and 3). Some typical results are presented in Table 6 where it is clear that 9-methyluric acid is electrooxidized in a 2e reaction and 9-methylxanthine in a 4e reaction in agreement with the above results at the PGE.

It was noted during conventional, large-scale controlled potential electrolyses of 9-methylxanthine at pH 7 at the PGE at potentials of ca. 1.0-1.2 V that a yellow color appeared in the solution within approximately 10 minutes. The intensity of the yellow solution reached its maximum in about one hour and then gradually faded and completely disappeared within 2-3 hours. Ultraviolet spectra were taken during the course of some of these electrolyses and it was observed that a peak with λ_{max} = 340-350 was associated with the appearance of the yellow solution, i.e., as the yellow color became more intense, the absorbance, A, at 340-350 nm increased and decreased as the color faded and finally was absent when

TABLE 6

Experimental n-Values Observed for Electrochemical Oxidation of 9-Methyluric Acid and 9-Methylxanthine in a Thin-layer Cell at a Gold Minigrid Electrode

Compound	pH	Initial Concentration, mM	Controlled Potential, V vs. SCE	n-Value
9-Methyl-uric Acid	5[a]	1	0.8	1.89
9-Methyl-uric Acid	7[a]	5	0.8	1.82
9-Methyl-xanthine	4[a]	2	1.2[b]	3.91
9-Methyl-xanthine	8[a]	5	1.2[b]	3.80

[a]Phosphate buffer containing K_2SO_4. Ionic strength 0.5.

[b]Precathodized first at -0.5 V for ca. 3 minutes. Applied potential at or near peaks IV_a-V_a.

all of the yellow color had disappeared.

It was also learned that the yellow color (and A_{340}) appeared when the applied potential corresponded to peak II_a of 9-methylxanthine (0.70-0.80 V). The stability of the material causing the color was studied by stopping the electrolysis when the intensity of the yellow solution and A_{340} had seemingly reached their maxima. The color and u.v. spectrum were monitored periodically to check for any decay. Indeed, over a

period of 36 hours the yellow intensity did not change and the u.v. absorbance at ca. 340 nm only decayed a very slight amount.

The appearance of the yellow material was also found to be pH dependent. No color change or u.v. peak at ca. 340 nm was noted in electrolyses of solutions at various applied potentials at pH 2 and 3. With increasing pH, however, there is a gradual increase in the intensity and duration of the yellow color as well as A_{340}.

Cyclic voltammetry was also run periodically on these solutions during the course of some of the latter electrolysis experiments. For example, when 9-methylxanthine was electrolyzed at a potential corresponding to peak II_a (ca. 0.75 V) at pH 7, peak III_a began to grow significantly (refer to Figure 15) in relation to the other peaks. As the electrolysis progressed, peak III_a continued to grow while peaks II_a, IV_a, V_a, I_c, and I_a all began to diminish. Finally, as shown in Figure 15D, only peak III_a is present. In addition, it was discovered that the growth of peak III_a was related to the increases in yellow color intensity and the u.v. absorbance at λ_{max} = 340 nm. Thus, it is evident that the material which gives rise to peak III_a is electrochemically oxidizable, yellow, and has a λ_{max} = 340 nm.

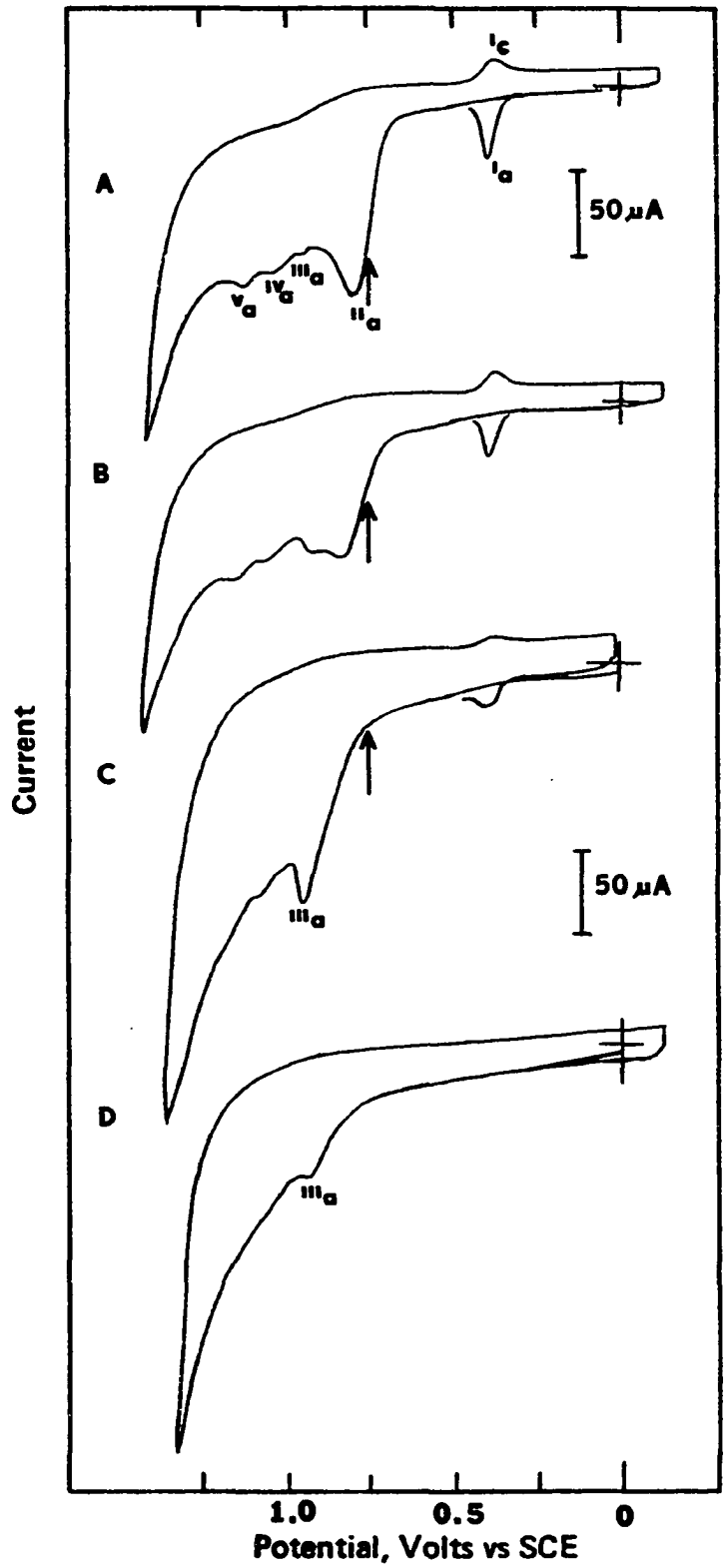

Figure 15. Cyclic voltammograms at various stages during electrolysis of 1mM 9-methylxanthine at pH 7 at PGE. (A) before electrolysis, (D) after electrolysis. Arrow at applied potential (0.75V). Scan rate 200 mV sec^{-1}.

The effect of pH on the appearance of peak III_a parallels the behavior observed with the appearance of the yellow color and the u.v. peak. That is, at low pH, peak III_a is also absent (vide supra).

It seems quite apparent then, that peaks IV_a and V_a represent further oxidation(s) of the initially present 9-methylxanthine. Thus, as the initial 9-methylxanthine is consumed in the peak II_a process (giving rise to a larger peak III_a) peaks IV_a and V_a correspondingly disappear. Finally, when no starting material remains, that is peak II_a is absent, peaks IV_a and V_a have also disappeared. As was noted in earlier discussions, the peak I_c-I_a couple and peak II_c are related to peaks IV_a and V_a, and hence peaks I_c, and I_a, and II_c disappear as does peak II_a (Figure 15).

Thin-layer spectroelectrochemical studies

Thin-layer spectroelectrochemical studies of 9-methyluric acid and 9-methylxanthine were conducted utilizing the rapid scan spectrophotometer (RSS) and the gold minigrid working electrode described earlier in Chapters 2 and 3. Comparison of the voltammetric and coulometric studies conducted at gold and graphite electrodes indicated the electrooxidation processes for 9-methyluric acid and 9-methylxanthine to be essentially the same at both electrode materials.

A typical u.v. spectrum obtained prior to electrolysis of 9-methyluric acid at pH 7.0 at the gold minigrid electrode in a thin-layer cell is shown in curve 1 of Figure 16 where it can be observed that 9-methyluric acid exhibits an absorption peak with λ_{max} = 292 nm. Upon application of a potential of 0.8 V (positive of peak I_a) the u.v. peak of 9-methyluric acid decreases with time. However, in contrast to the behavior of uric acid, a second peak at longer wavelengths does not appear. Rather, it was noticed that as the electrolysis proceeded and the u.v. peak of 9-methyluric acid decreased the λ_{max} of the observed peak shifted to shorter wavelengths and finally centered around λ_{max} = 284 nm. This behavior is illustrated in Figure 16. Presumably, the absorption and shift to shorter wavelength is due, to a large extent, to some electrooxidation product or intermediate.

In order to test this hypothesis a solution of 9-methyluric acid was electrolyzed at 0.8 V for 30 seconds. At the point when approximately 75% of the initial 9-methyluric acid was oxidized, the potential was turned off (Curve 2, Figure 16) and the u.v. spectrum was monitored as a function of time. Under these conditions a decay in the absorbance of the solution was noted at 284 nm. A stable intermediate or product would not exhibit such a decay in absorbance but rather, the absorbance

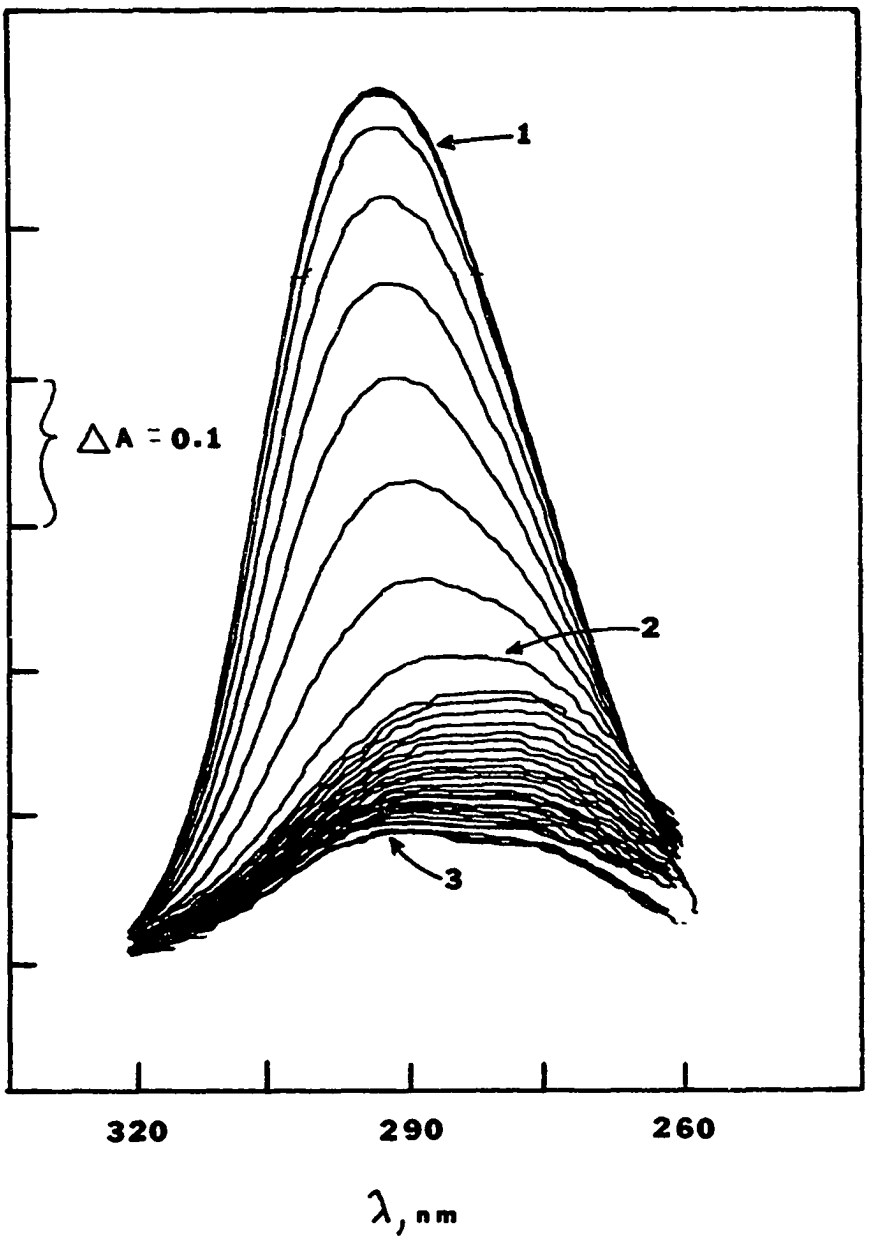

Figure 16. Spectrum of 5mM 9-methyluric acid solution electrolyzing at 0.8V in pH 7.0 phosphate buffer at gold minigrid electrode in a thin-layer cell. Curve (1) is spectrum before electrolysis. Electrolysis stopped at Curve (2). Curve (3) is the spectrum after decay of intermediate. Repetitive scans are 4.7 seconds.

would remain constant. Curve 3 in Figure 16 is the minimum absorbance of the decayed intermediate. This behavior strongly supports the view that upon electrochemical oxidation of 9-methyluric acid an unstable intermediate is formed which absorbs at slightly shorter wavelengths than 9-methyluric acid.

Thin-layer spectroelectrochemical studies of 9-methyluric acid over the concentration range (1-10 m$\underline{M}$) at pH 7 gave results similar to those shown in Figure 16. In addition, studies at varying potentials (0.4 V to 1.0 V in 0.1 V intervals) also gave similar results; however, at applied potentials more negative than E_p the rate of electrooxidation was, as expected, significantly slower.

The thin-layer spectroelectrochemical behavior of 9-methyluric acid at pH 6, 8, and 9 was essentially identical to that reported at pH 7. Below pH 6 it became increasingly difficult to observe the spectrum of the intermediate species, even at fast spectral sweep times. This implies that the stability of the intermediate observed at pH 6-9 is significantly lower below pH 6 or that its absorption behavior is quite different. In addition, with decreasing pH the solubility of 9-methyluric acid decreases (< 1 m$\underline{M}$) such that thin-layer spectroelectrochemical studies became extremely difficult.

Thin-layer spectroelectrochemical studies of the

electrooxidation of 9-methylxanthine yielded quite different results than those of 9-methyluric acid. A typical u.v. spectrum obtained prior to electrolysis of 9-methylxanthine at pH 8.0 in the thin-layer cell is shown in curve 1 of Figure 17 where it can be observed that there are two absorption peaks with λ^1_{max} = 245 nm and λ^2_{max} = 277 nm. Upon application of a potential of 1.2 V, i.e., corresponding to peaks IV_a and V_a, the u.v. peaks of 9-methylxanthine decrease with time and, correspondingly, a broad peak (λ_{max} ca. 340-350 nm) appears and grows. This peak corresponds to that observed in the controlled potential coulometry experiments (vide supra).

Curve 2 in Figure 17 represents the maximum absorbance the peak at 340 nm reaches and is the point at which the electrolysis is discontinued. An absorbance decay was then observed in the region 330-360 nm (curve 3).

Thin-layer spectroelectrochemical studies of 9-methylxanthine over the concentration range 2-20 mM at pH 8 gave somewhat similar results to those shown in Figure 17. However, one important phenomenon was noted. For example, at 2 mM the maximum absorbance, A, at 340 nm was about one-third the initial absorbance of 9-methylxanthine at 277 nm; whereas at 20 mM $(A_{max})_{340}$ was almost as large as $(A_{init})_{277}$. For concentrations between 2 and 20 mM the ratio $(A_{max})_{340}/(A_{init})_{277}$ increased with

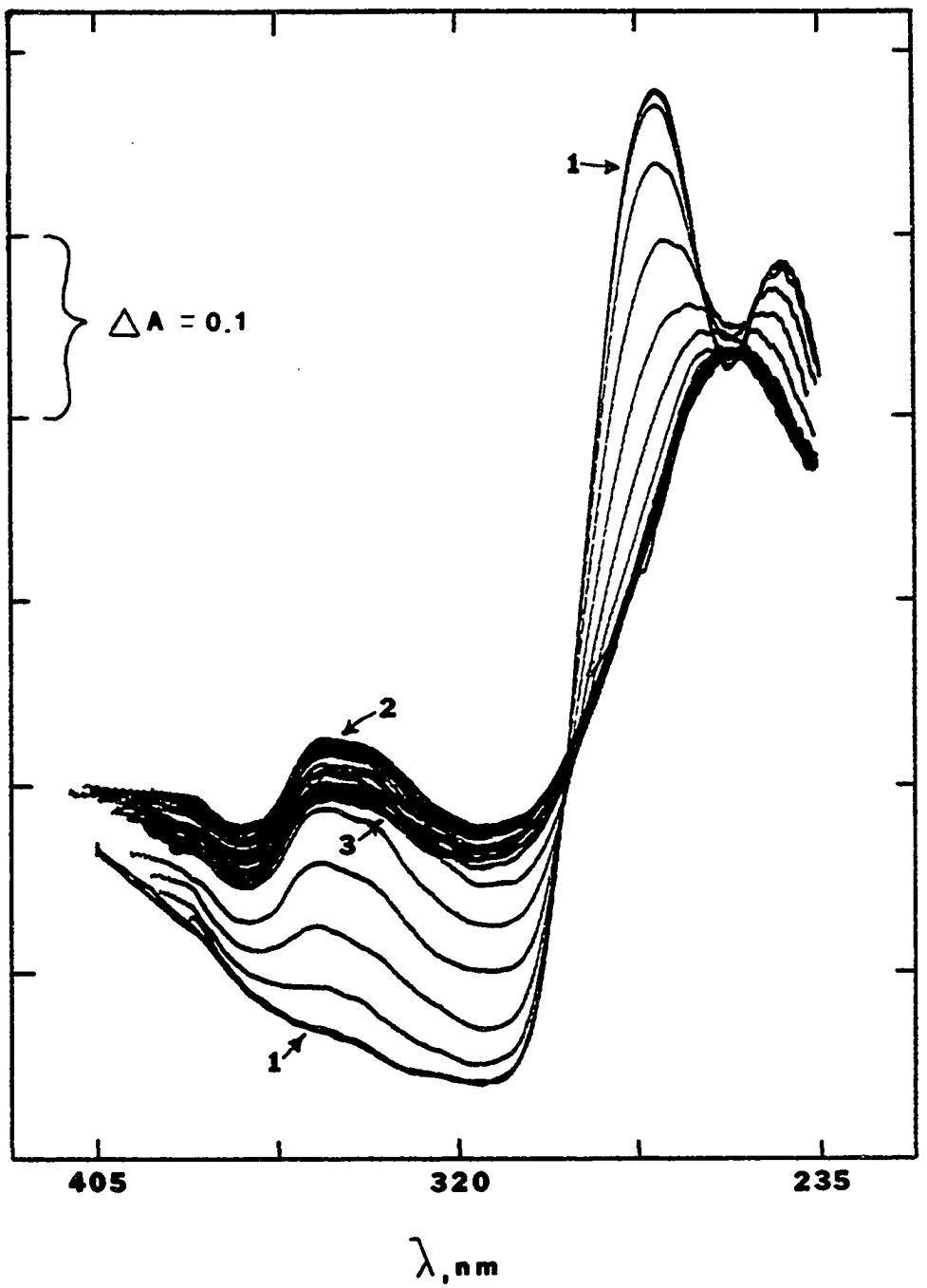

Figure 17. Spectrum of 10 mM 9-methylxanthine electrolyzing at 1.2V at pH 8 at gold minigrid electrode in a thin-layer cell. Curve (1) is spectrum before electrolysis. Electrolysis stopped at Curve (2). Curve (3) is spectrum after decay of intermediate. Repetitive scans are 9.4 sec.

increasing concentration. This suggests, therefore, that perhaps 9-methylxanthine forms a primary electrochemical product which undergoes a second-order reaction such as dimerization. A comparison of the ratios of the maximum absorbance of the peak at 340 nm to the initial absorbance at 277 nm for 9-methylxanthine with those of the peak at 304 nm to the absorbance at 287 nm for uric acid (Chapter 3), i.e., $(A_{max})_{340}/(A_{init})_{277}$ with $(A_{max})_{304}/(A_{init})_{287}$ are given in Table 7. It was pointed

TABLE 7

Comparison of $(A_{max})_{intermediate}/(A_{initial})$ for Uric Acid and 9-Methylxanthine

Compound	Concentration, mM	$(A_{max})_{intermed}/(A_{init})^a$
Uric Acid[b]	0.5	0.23
	1.0	0.25
	5.0	0.23
	10.0	0.25
9-Methylxanthine[c]	2.0	0.32
	5.0	0.42
	10.0	0.52
	20.0	0.90

[a] $(A_{max})_{304}/(A_{init})_{287}$ for uric acid, $(A_{max})_{340}/(A_{init})_{277}$ for 9-methylxanthine.

[b] pH 7.0 phosphate buffer.

[c] pH 8.0 phosphate buffer.

out in Chapter 3 that the species giving rise to $(A_{max})_{304}$ in the uric acid system was formed in a first-order (or

pseudo first-order) process. It can be easily seen from Table 7 that for uric acid the ratio of absorbance values are essentially constant over a wide range of concentration while for 9-methylxanthine the ratio increases with increasing concentration. This is clearly indicative of a second-order process (e.g., dimerization), since higher concentrations of reactant(s) greatly increases the relative extent of this type of process.[90]

When studying the thin-layer spectroelectrochemical oxidation of 10 mM and 20 mM solutions of 9-methylxanthine at pH 8, a small decrease in absorbance at ca. 284 nm was observed when the electrolysis was terminated. This corresponds to the λ_{max} of the observed intermediate for 9-methyluric acid. Unfortunately, this decay was too small to allow meaningful kinetic data to be obtained. At lower concentrations, it was difficult to observe any significant decay.

Studies of 9-methylxanthine at pH 8 at various applied potentials (0.8 V to 1.4 V, corresponding to peak II_a and V_a, respectively) also showed the formation of the u.v. peak at ca. 340 nm. However, at the less positive potentials (e.g., 0.8 V) no absorbance decay in the region 330-360 nm was observed over at least a 30 minute period upon electrolysis. As the potential was made more positive up to 1.4 V, greater decay was observed in this wavelength region. This is in agreement with the

behavior observed in controlled potential coulometric experiments at the PGE (vide supra).

The thin-layer spectroelectrochemical behavior of 9-methylxanthine at pH 6, 7, and 9 was essentially identical to that reported above for pH 8. However, at pH 6 a smaller absorbance at 340 nm was observed. Moreover, the maximum solubility of 9-methylxanthine at pH 6 was between 2 and 5 mM. Below pH 6 it became increasingly difficult to observe the spectrum of the intermediate species at 340 nm until at pH 3, for example, it was not possible to observe any absorption at 340 nm. In addition, below pH 6 the solubility of 9-methylxanthine decreases (< 1 mM) such that thin-layer spectroelectrochemical studies became very difficult, if not impossible.

Kinetic measurements

The kinetics of the decomposition reaction of the u.v.-absorbing intermediate species formed on electro-oxidation of 9-methyluric acid (i.e., at 284 nm) was studied by thin-layer spectroelectrochemistry. The absorbance of the intermediate species was monitored at 284 nm as a function of time during electrooxidation of 9-methyluric acid at 0.8 V, just positive of peak I_a, and continued after the electrolysis was stopped. A typical plot of absorbance versus time throughout the course of such an experiment with 9-methyluric acid is

shown in Figure 18. The electrolysis was stopped when approximately one-half to three-fourths of the 9-methyluric acid had been electrooxidized as indicated by an appropriate decrease in its u.v. absorbance at 292 nm. The decrease of the absorbance of the intermediate species with time was used to study the kinetics of its decomposition reaction. A typical rate plot obtained for the intermediate formed on electrooxidation of 9-methyluric acid at pH 7 is presented in Figure 19. Clearly the plot of log $A-A_\infty$ vs. time is linear indicating that the reaction of the absorbing intermediate species follows first-order kinetics. The value of the observed first-order solution rate constant for reaction of the u.v.-absorbing intermediate formed on electrochemical oxidation of 9-methyluric acid at pH values between 6 and 9 are presented in Table 8. Thus, the value of the observed rate constant is essentially independent of concentration and of pH. Accordingly, it was concluded that the observed rate constant for the reaction of the u.v.-absorbing intermediate is 0.018 ± 0.002 sec^{-1}.

The kinetics of the decomposition reaction of the intermediate species (λ_{max} = 340 nm) formed on electrooxidation of 9-methylxanthine at potentials corresponding to peaks IV_a/V_a was also studied by thin-layer spectroelectrochemistry. The absorbance was monitored at 340 nm

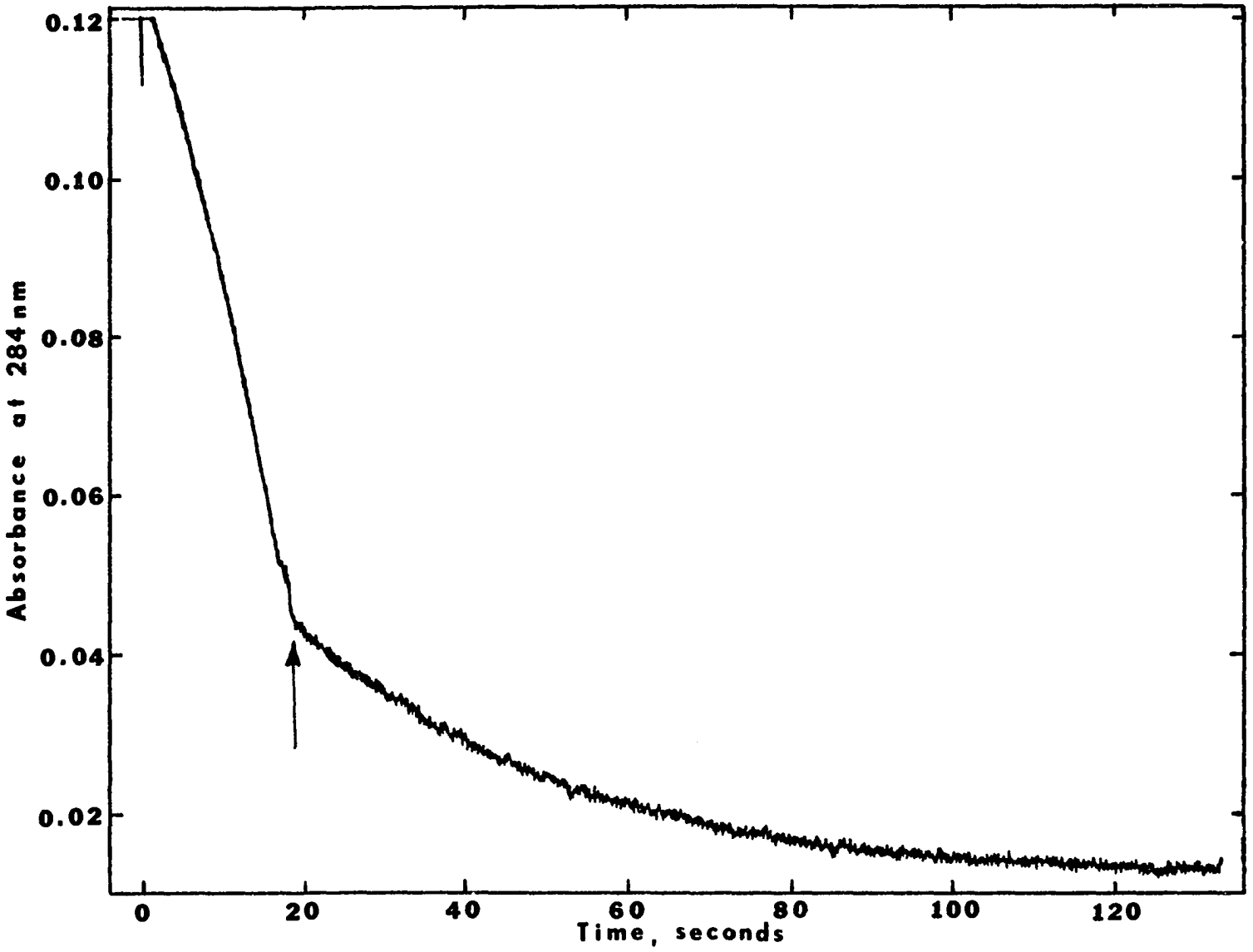

Figure 18. Absorbance vs. time for electrooxidation of 5mM 9-methyluric acid at pH 7 at 284 nm. Electrolysis stopped at arrow.

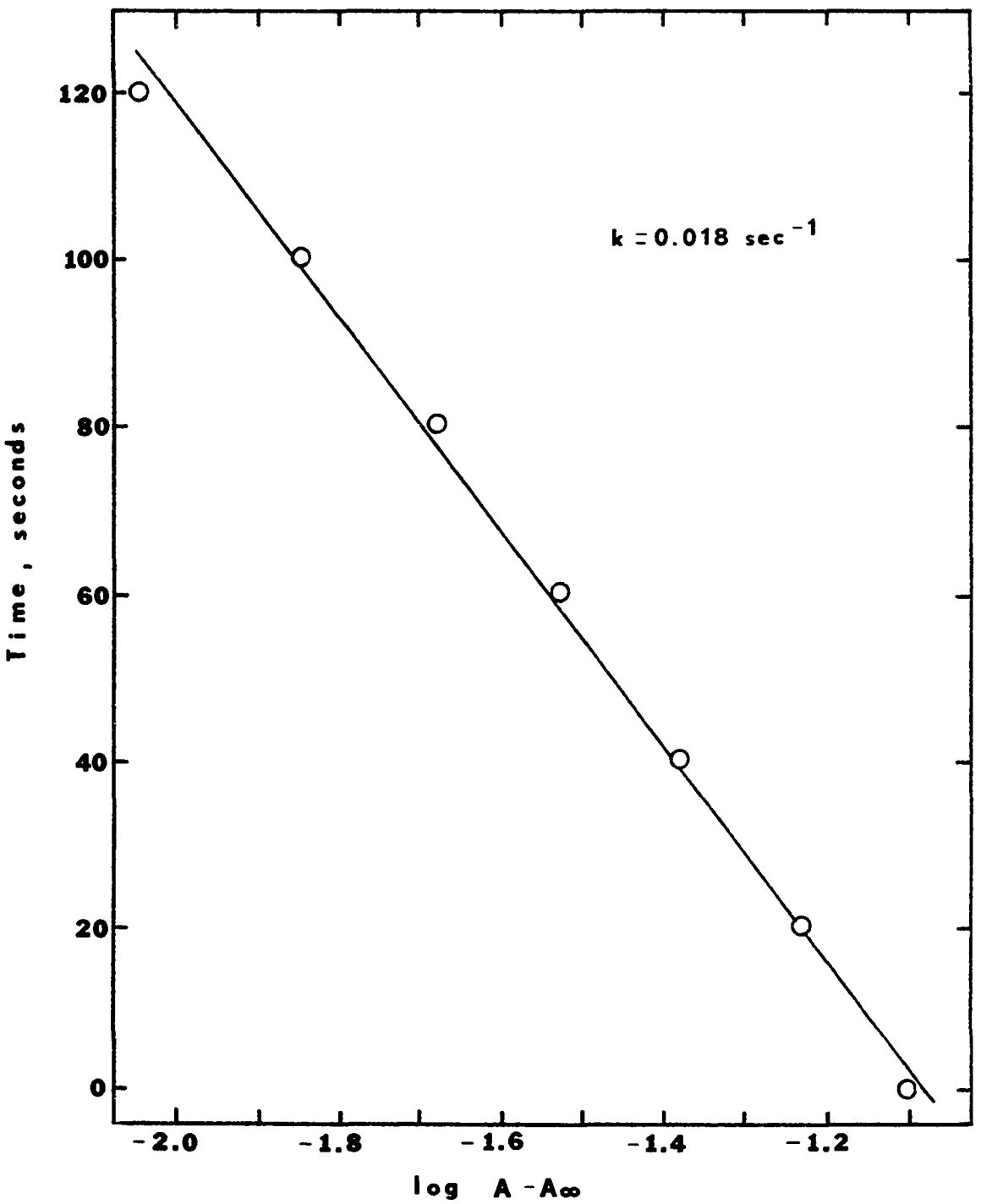

Figure 19. Kinetic plot of time vs. log absorbance at 284 nm. Absorbance data taken from Figure 18.

TABLE 8

Observed First-Order Rate Constants for Reaction of the U.v.-absorbing Intermediate Formed on Electrochemical Oxidation[a] of 9-Methyluric Acid at a Gold Minigrid Electrode

pH[b]	Initial Concentration, mM	k_{obs}, sec^{-1}
6	5	0.017
7	1	0.019
	2	0.016
	5	0.018
	10	0.018
8	5	0.018
9	5	0.02

[a]Applied potentials were 0.8 V, at or positive of peak I_a.

[b]Phosphate buffers containing K_2SO_4, ionic strength of 0.5.

while 9-methylxanthine was oxidized at a constant potential at the gold minigrid electrode. The electrolysis was stopped when the peak at 340 nm reached its maximum absorbance. Figure 20 shows a typical absorbance versus time experiment for 9-methylxanthine at pH 8. Curves such as this were used to determine the rate constant for the reaction of the absorbing intermediate species which was also found to follow first-order kinetics. Values of the observed first-order solution rate constant for the intermediate formed on electrochemical oxidation of

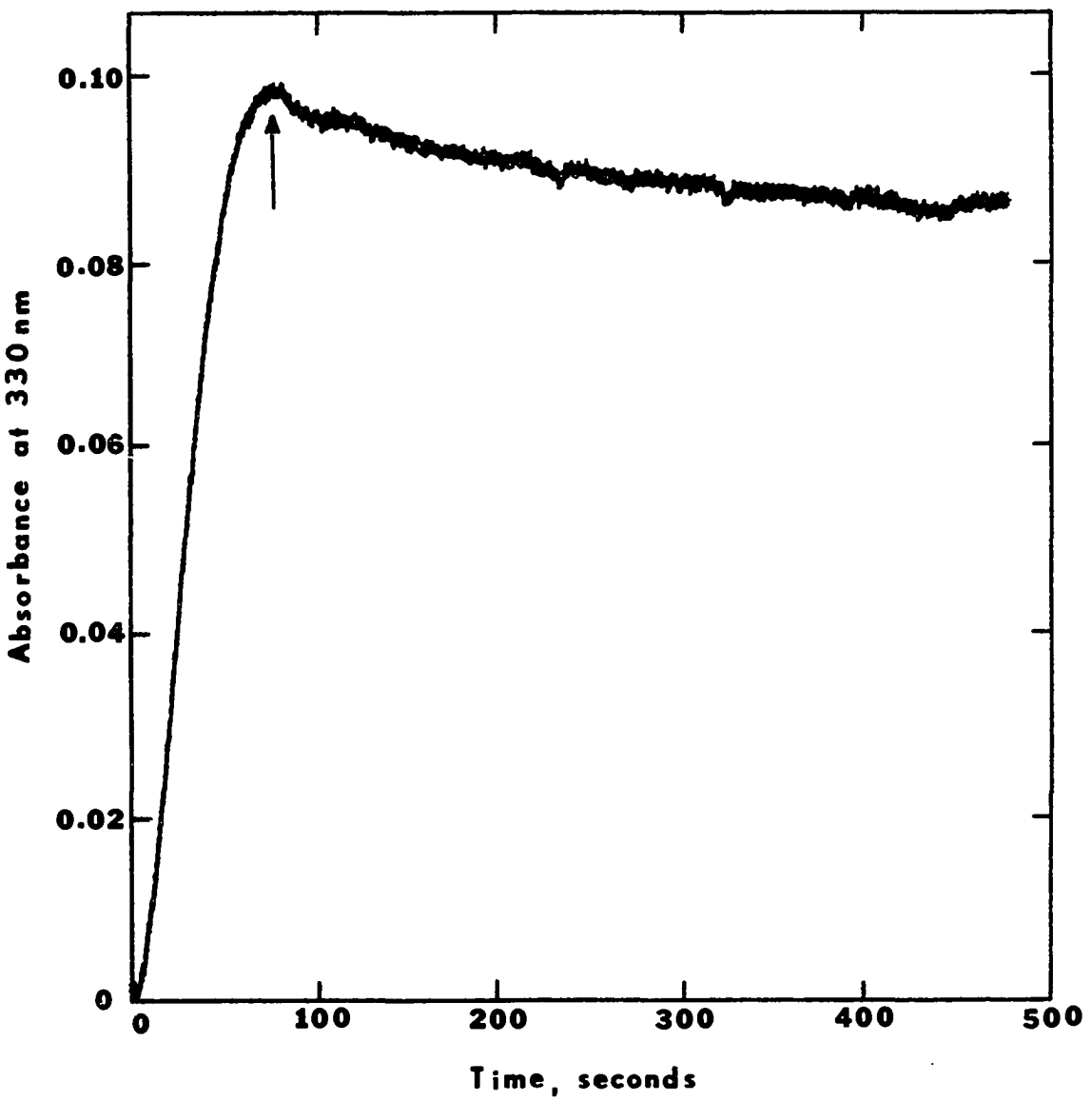

Figure 20. Absorbance vs. time for electrooxidation of 10mM 9-methylxanthine at pH 8 at ca. 340 nm. Electrolysis (at 1.2V) stopped at arrow.

9-methylxanthine between pH 7 and 9 are given in Table 9.

TABLE 9

Observed First-Order Rate Constants for Reaction of the Intermediate (340 nm) Formed on Electrochemical Oxidation[a] of 9-Methylxanthine at a Gold Minigrid Electrode

pH[b]	Initial Concentration, mM	k_{obs}, sec^{-1}
7	10	0.0066
8	2	0.0059
	5	0.0061
	10	0.0054
	20	0.0060
9	10	0.0060

[a]Applied potentials were 1.2 V, corresponding to peaks IV_a/V_a.

[b]Phosphate buffers containing K_2SO_4, ionic strength of 0.5.

The value of the observed rate constant is independent of concentration and pH. It was therefore concluded that the observed rate constant for the intermediate species (λ_{max} = 340 nm) formed on thin-layer spectroelectrochemistry of 9-methylxanthine is 0.006±0.0006 sec^{-1} over the pH range 7-9.

Owing to the very small absorbance decay at 284 nm observed on the electrochemical oxidation of 9-methylxanthine it was not possible to obtain any meaningful

kinetic data.

Conclusions

The voltammetric experiments reported above indicate that at graphite and gold electrodes 9-methyluric acid is electrochemically oxidized to a very short-lived primary product analogous to that proposed for uric acid. This product is also reducible as evidenced by peak I_c on cyclic voltammetry of 9-methyluric acid. However, it is possible to observe reduction peak I_c at relatively slow sweep rates (ca. 200 mV sec^{-1}) only at graphite electrodes which have a rough surface. At a gold electrode or graphite electrodes resurfaced such that their surface is highly polished and smooth, peak I_c can only be observed at fast sweep rates ($\geq$ 10 V sec^{-1}). Therefore, the primary product of electrooxidation of 9-methyluric acid is very unstable in homogeneous solution but when adsorbed at graphite electrodes it is attacked more slowly. (See Chapter 3 for further details.)

Thin-layer spectroelectrochemical experiments reveal that electrooxidation of 9-methyluric acid gives rise to a further intermediate that exhibits a u.v. absorption peak at 284 nm between pH 6-9. This species then undergoes a first-order decomposition reaction with an apparent rate constant of about 18×10^{-3} sec^{-1} (half-life ca. 40 sec). As in the uric acid system this inter-

mediate species cannot be the same species responsible for peak I_c.

Accordingly, it is proposed that the intermediate species giving rise to peak I_c on the electrooxidation of 9-methyluric acid is a diimine species (VIII) similar to that proposed in the uric acid system (II, equation 1, Chapter 1). This species is then postulated to undergo

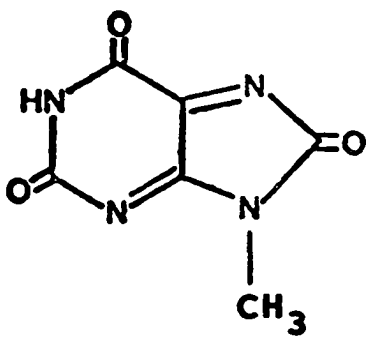

VIII

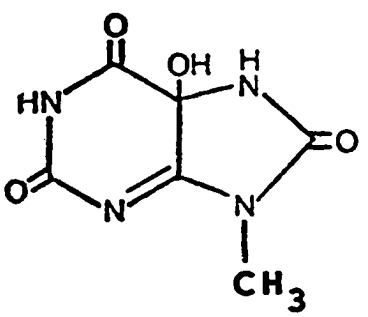

IX

partial hydration to the corresponding imine-alcohol (e.g., IX), which then is further attacked by water yielding the 4,5-diol species similar to IV (equation 1, Chapter 1). It is this latter reaction which is responsible for the observed spectroelectrochemical behavior. The structures just proposed are based primarily on the similarities of the voltammetric, coulometric, and spectroelectrochemical behavior of uric acid and 9-methyluric acid. Thus, 9-methyl substitution appears to have no effect on the electrochemical oxidation of uric acid as studied by

voltammetry; however, in spectroelectrochemical experiments a shift in λ_{max} of the proposed imine-alcohol intermediate towards shorter wavelengths was observed.

The electrochemical oxidation of 9-methylxanthine appears to be more complex. However, as with uric acid, xanthine, and 9-methyluric acid, a very short-lived primary product or intermediate species is formed which is reducible as evidenced by peak I_c on cyclic voltammetry of 9-methylxanthine. Peaks I_c and I_a have peak potentials corresponding to those of the I_c/I_a couples for uric acid, xanthine, and 9-methyluric acid. As mentioned earlier in the voltammetry section, though, peaks I_c and I_a (as well as peak II_c) of 9-methylxanthine are not observed without first scanning past peaks IV_a and/or V_a. In addition, the species responsible for peak I_c also appears to be stabilized by adsorption since its voltammetric behavior at rough and smooth electrodes is identical to that of the other compounds investigated (i.e., very unstable in homogeneous solution; much more stable when adsorbed to a rough electrode surface).

Evidence given in earlier sections of this chapter indicate that two additional intermediate species, one with λ_{max} = 284 nm and one with λ_{max} = 340 nm, are formed on the electrochemical oxidation of 9-methylxanthine. The results of controlled potential coulometry and

spectroelectrochemistry experiments reveal that the species with λ_{max} = 340 nm is formed in the peak II_a process (the first oxidation peak of 9-methylxanthine). This material is yellow, has a u.v. peak with λ_{max} ca. 340 nm, and is further oxidizable as evidenced by the peak III_a process. Controlled potential coulometry experiments show that oxidation of 9-methylxanthine at potentials corresponding to peak II_a results in an accumulation of the yellow material and an increase in peak III_a with corresponding decreases in peaks II_a, IV_a, V_a, I_c, and I_a. These results indicate that the processes responsible for peaks IV_a and V_a are independent of peaks II_a and III_a and are probably due to oxidation of 9-methylxanthine itself.

That the formation of the yellow species in the peak II_a process is probably second-order has been shown by spectroelectrochemical studies of 9-methylxanthine as a function of its concentration (Table 7). Moreover, controlled potential coulometry of 9-methylxanthine at high concentrations resulted in much lower n-values than at lower concentrations. This behavior is typical of second-order reactions, e.g., dimerization.[90] Moreover, the cyclic voltammetry at varying concentrations of 9-methylxanthine discussed earlier further supports this behavior. It was observed that at low concentrations of 9-methylxanthine (0.5 mM) peak III_a was small in relation to peak II_a while at high concentrations (20 mM)

peak III_a was very large. These results show that the amount of the yellow material formed from the peak II_a oxidation of 9-methylxanthine (and which is responsible for peak III_a) is greatly increased at high concentrations of initial reactant.

It is not unreasonable to propose, therefore, that the yellow, u.v.-absorbing material formed in the initial oxidation process (peak II_a) of 9-methylxanthine is some kind of dimeric species formed in a second-order process. Additionally, the lower n-values obtained in controlled potential electrolyses at higher concentrations of 9-methylxanthine support this proposal.[90] Hansen and Dryhurst[91] in their account of the electrochemical oxidation of theophylline (1,3-dimethylxanthine) report the formation of a dimeric species, 1,3-(dimethylxanthyl-8)-1,3-dimethylxanthine (X) which has several characteristics similar to

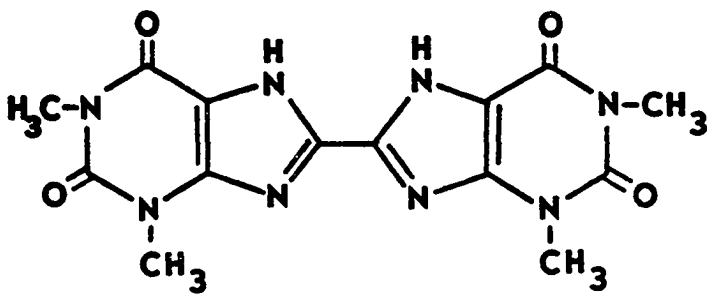

X

the 9-methylxanthine peak II_a oxidation product. Species

X is also a yellow material, and it has a u.v. absorption peak centered at ca. 340 nm. In all known xanthine electrooxidations the site of primary attack is the C(8) position.[91] It would seem probable that a similar position of oxidation would also occur in the case of 9-methylxanthine. Carbon (8) would not be totally oxidized to a carbonyl moiety, but a 1-electron oxidation would occur followed by dimerization (which would result, as was observed, in coulometric n-values lower than the expected value of 4). Moreover, rather poor quality mass spectral results to date[92] show several m/e peaks in the range 320-350, near that expected for a dimer of 9-methylxanthine. A dimer of 9-methylxanthine similar to the theophylline dimer (X) would have m/e = 330.

Thin-layer spectroelectrochemical studies have demonstrated that if the applied potential is positive enough to include peak III_a (the oxidation of the proposed dimer) a decay of the u.v.-absorbing material (λ_{max} = 340 nm) may be observed, even when the electrolysis is stopped at $(A_{max})_{340}$. If, however, the potential is much less positive (corresponding to the rising portion of peak II_a) no decay may be observed. These results indicate that peak III_a represents a further oxidation of the proposed dimeric material. The electrooxidation product then chemically reacts further to form one or more products

which do not absorb (at least to the same extent) at 340 nm.

Moreover, spectroelectrochemical studies at potentials corresponding to peaks IV_a/V_a at high concentrations of 9-methylxanthine show a small increase and then decay (when the electrolysis was stopped) at 284 nm, corresponding to the observed decay for 9-methyluric acid. Unfortunately, the extent of this decay was too small to determine a numerical value for the corresponding rate constant. Owing to the complicating oxidative processes of peaks II_a and III_a, high concentrations of 9-methylxanthine are required to observe the A_{284} decay. However, high concentrations also enhance the second-order process which causes more of the initial material to proceed via this route rather than the 9-methylxanthine to diimine to imine-alcohol, etc., process (as monitored at 284 nm).

These investigations provide considerable insight into the effect of 9-methyl substitution on the electrochemical oxidation of uric acid and xanthine. These studies should prove very helpful in investigations of electrochemical oxidations of xanthosine (9-ribosylxanthine) and other purine nucleosides.

EXPERIMENTAL

Chemicals

9-Methyluric acid and 9-methylxanthine were ob-

tained from Adams Chemical Company. Buffer solutions were constituted as described in Chapter 3.

Apparatus and Procedures

The apparatus and procedures employed have been described in previous chapters.

SUMMARY

The effect of 9-methyl substitution on the electrochemical oxidation of uric acid and xanthine has been studied and compared to the results for uric acid and xanthine. These studies were carried out at rough and smooth graphite electrodes and at a gold electrode by cyclic voltammetry, controlled potential coulometry, and thin-layer spectroelectrochemistry. It was shown that the electrooxidation of 9-methyluric acid proceeds similarly to that of uric acid forming first a very reactive and reducible diimine species which is further hydrated to the corresponding imine-alcohol. This diimine is strongly adsorbed at rough electrode surfaces and is appreciably more stable than in solution. The imine-alcohol may be observed as a further intermediate by thin-layer spectroelectrochemistry. However, the imine-alcohol of 9-methyluric acid appears to absorb at shorter wavelengths than for the imine-alcohol of uric acid. The kinetics of hydration of this species was determined by spectroelectro-

chemistry.

The electrooxidation of 9-methylxanthine apparently proceeds by two processes. In the first, 9-methylxanthine is very likely oxidized to some dimeric species (via peak II_a) which can be further oxidized (via peak III_a). The product of this latter oxidative process is unstable and decomposes chemically which can be monitored by spectroelectrochemistry. The kinetics of this chemical decomposition was studied and a rate constant determined by thin-layer spectroelectrochemistry. The second oxidation process proceeds via peak IV_a and/or peak V_a similar to that for xanthine and ultimately results in formation of 9-methyluric acid diimine (peak I_c). This diimine is then partially hydrated to the corresponding imine-alcohol which can be further hydrated to 9-methyluric acid-4,5-diol.

CHAPTER 5

ELECTROCHEMICAL OXIDATION OF XANTHOSINE (9-RIBOSYLXANTHINE)

INTRODUCTION

Xanthosine (I) is an example of a purine nucleoside. Since the electrochemical oxidation of xanthine and 9-methylxanthine had been investigated in some detail, xanthosine was chosen as the first purine nucleoside to be studied. Accordingly, the present study was undertaken to investigate the electrochemical oxidation of xanthosine using cyclic voltammetry, controlled potential coulometry, and thin-layer spectroelectrochemistry.

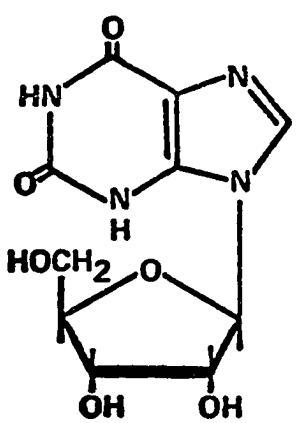

I

RESULTS AND DISCUSSION

pK_a for xanthosine

A plot of λ_{max} vs. pH for the two u.v.-absorbing peaks of xanthosine is shown in Figure 21. As in the case for 9-methylxanthine the λ_{max} for both peaks are essentially constant over a wide range of pH until pH 5-6 where a drastic shift is observed in λ_{max} for both peaks. Indeed, the reported value for the pK_a of xanthosine is 5.7.[93]

Voltammetry at carbon and gold electrodes

The voltammetry of xanthosine at the RPGE (Figure 22) is almost identical to that of 9-methylxanthine. Between pH 1-7 the peak potential for electrooxidation peak II_a is described by the equation $E_p = 1.2-0.063$ pH at a sweep rate of 5 mV sec^{-1}. At pH > 7 the peak potential becomes independent of pH with $E_p = 0.81\pm0.02$ V between pH 7-10. The peak potential for electrooxidation peak IV_a is described by the equation $E_p = 1.33-0.055$ pH between pH 1-7 and becomes independent of pH with $E_p = 0.97\pm0.03$ between pH 7-10. Below pH 7, peak V_a is too close to background discharge potentials to obtain any meaningful data on its pH dependence, but between pH 7-10 peak V_a is also independent of pH with $E_p = 1.15\pm0.05$ V. Peak III_a is only detectable at concentrations $\geq$ ca. 5 mM.

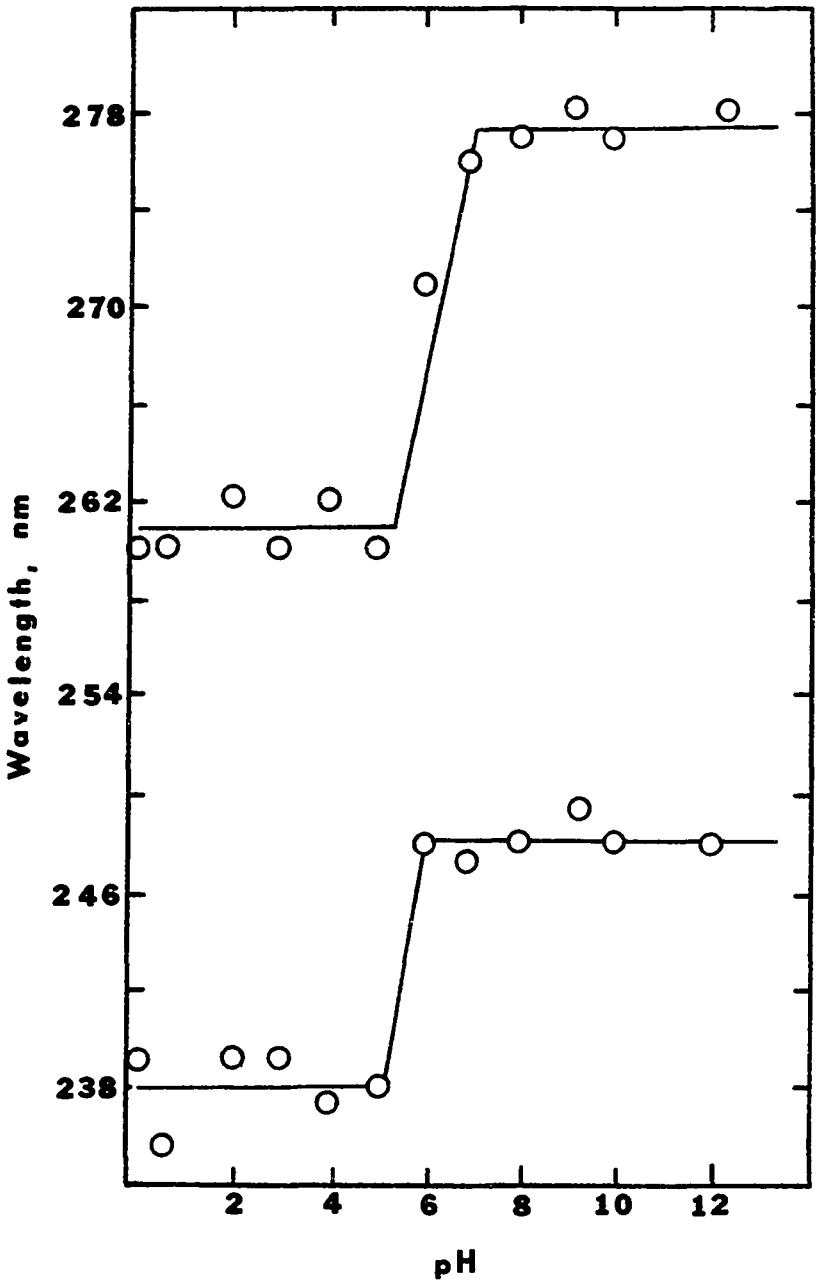

Figure 21. Wavelength versus pH for the two u.v.-absorbing peaks of xanthosine.

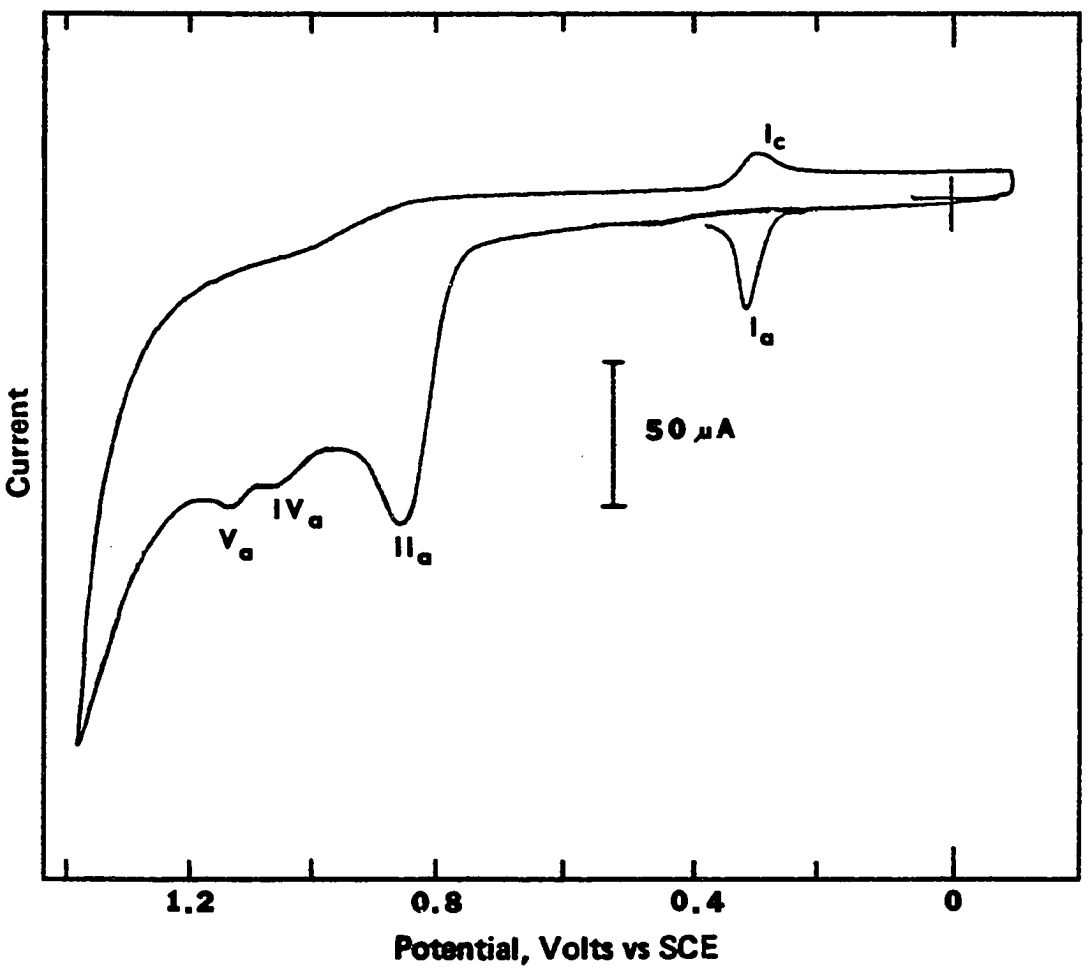

Figure 22. Cyclic voltammogram of 0.5mM xanthosine at pH 7 at the RPGE. Initial scan towards positive potentials. Scan rate 200 mV sec^{-1}.

At lower values of concentration (e.g., 0.5 mM, Figure 22) no peak III_a is present. The electrooxidation peaks of xanthosine were designated in the same fashion as those for 9-methylxanthine to allow meaningful comparison.

As shown in Figure 22, the cyclic voltammetric behavior of xanthosine is very similar to that for 9-methylxanthine except that the electrooxidation peaks of xanthosine are ca. 0.2 V more positive. Another difference is the absence of peak III_a at low concentrations of xanthosine.

Peaks I_c and I_a of xanthosine correspond to peaks I_c and I_a for uric acid, xanthine, 9-methyluric acid, and 9-methylxanthine. In addition, the peak I_c-I_a couple may also be observed only after sweeping into the peak IV_a/V_a region. Though not shown in Figure 22, peak II_c also corresponds to peak II_c for the other compounds previously described, and is also observed only after sweeping into the peak IV_a/V_a region.

The effect of decreasing the electrode roughness on the cyclic voltammetry of xanthosine also parallels that observed for 9-methylxanthine (Chapters 3 and 4). That is, at a smooth electrode surface peak I_c does not appear at slow sweep rates (e.g., 200 mV sec^{-1}) but only at much faster sweep rates ($\geq$ 5 V sec^{-1}).

The peak potential for oxidation peak II_a of xanthosine at the gold foil electrode follows the relation-

ship E_p = 1.4-0.06 pH from pH 1-7 at a voltage sweep rate of 5 mV sec^{-1}, after which the peak becomes independent of pH with E_p = 1.03±0.05 V between pH 7-10. Cyclic voltammetry of xanthosine at the gold electrode is impossible owing to the formation of gold oxide(s) at very positive potentials. Consequently, peaks IV_a and V_a were not discernible and peak potential relationships could not be obtained.

The effect of pH on the cyclic voltammetry of xanthosine at the PGE parallels that of 9-methylxanthine, i.e., peak I_c cannot be observed at slow sweep rates below ca. pH 5 and is most pronounced at pH 6-7. At higher pH peak I_c becomes smaller until at pH 9 at 200 mV sec^{-1} it completely disappears. Thus, the species responsible for peak I_c is most stable at pH 6-7.

Controlled potential coulometry

Over the pH range 2-8 a faradaic n-value of about 4 (3.4-4.4) was obtained for the electrochemical oxidation of xanthosine at the PGE at a constant applied potential positive enough to include peaks IV_a and V_a. The concentrations utilized for coulometric experiments usually ranged from 0.14-2.0 mM. Table 10 presents some typical results of the experimental n-value. It was observed that coulometry of xanthosine at concentrations above ca. 5 mM showed a systematic decrease in the n-value with

TABLE 10

Coulometric n-Values for the Electrochemical Oxidation of Xanthosine at the PGE

pH[a]	Initial Concentration mM	Controlled Potential, V vs. SCE	n-value
2[b]	2	1.2	3.4
2[b]	2	1.2	3.6
2[b]	2	1.2	3.7
2.3[c]	2	1.2	4.1
2.3[c]	2	1.2	3.8
3	0.5	1.2	4.1
3	0.25	1.2	4.0
4	0.4	1.1	4.3
4	0.4	1.1	3.8
4	0.4	1.1	3.9
5	0.4	0.99	3.95
5	0.4	1.05	3.7
5	0.4	0.98	3.8
6	0.4	1.0	4.1
6	0.14	1.0	4.1
7	0.5	1.05	3.7
7	0.5	1.05	4.1
7	2.0	1.05	4.2
8	0.4	0.98	4.2
8	0.4	0.96	4.01

[a]Unless otherwise noted, phosphate buffers containing K_2SO_4, ionic strength 0.5.

[b]1 M hydrochloric acid.

[c]1 M acetic acid.

increasing concentration. For example, at pH 8 at potentials corresponding to peaks IV_a/V_a (1.2 V) the n-value for a 5 mM solution of xanthosine is ca. 3.8. At 20 mM, however, under the same conditions, the n-value is ca. 3.0. This behavior was also observed for 9-methylxanthine (Chapter 4).

Coulometric n-values for electrooxidation of xanthosine by controlled potential electrolysis in a thin-layer cell using a gold minigrid electrode at 1.4 V (corresponding to peaks IV_a/V_a) ranged from 3.25-3.85. These values are in close agreement with those obtained at the PGE.

The phenomenon observed during controlled potential electrolysis of 9-methylxanthine at pH 7 at the PGE, i.e., the formation of the u.v.-absorbing, yellow intermediate species, was also observed in the case of xanthosine. At potentials $\geq$ 1.0 V (peak III_a) the yellow color would appear, remain for a long period of time, and then gradually fade. Moreover, the u.v. spectrum was nearly identical to that observed in the 9-methylxanthine electrolyses, i.e., λ_{max} = 330-340 nm, and was associated with the appearance and disappearance of the yellow material. When the applied potential corresponded to values negative of the peak potential for peak II_a ($\leq$ 0.84 V) of xanthosine, the yellow color (and $A_{max}(335)$) remained indefinitely,

especially when the electrolysis was stopped and the solution was allowed to set for 2-3 days. This behavior paralleled that of 9-methylxanthine.

The effect of pH on the appearance of the yellow color and u.v. peak at 335 nm during an electrolysis of xanthosine is the same as that in the case of 9-methylxanthine. For example, electrolyses at pH 2 and 3 produced no color change, but as the pH was increased the intensity of the yellow color and the u.v. absorbance peak (335 nm) also increased.

Electrolyses at potentials corresponding to peak II_a of xanthosine resulted in a decrease of all other voltammetric peaks as peak III_a increased and the yellow color and u.v. peak appeared. This is also similar to the observed behavior for 9-methylxanthine (see Figure 15, Chapter 4).

Thin-layer spectroelectrochemical studies

Thin-layer spectroelectrochemical studies of xanthosine were conducted utilizing a rapid scan spectrometer and gold minigrid working electrode. Based on a comparison of the voltammetric and coulometric behavior at both gold and graphite electrodes it was judged that the basic electrode reaction schemes for xanthosine at both electrodes were essentially the same.

A typical u.v. spectrum obtained prior to

electrolysis of xanthosine at pH 8.0 at the gold minigrid electrode in a thin-layer cell is shown in Figure 23A where it can be observed that xanthosine exhibits two absorption peaks with λ^1_{max} = 248 nm and λ^2_{max} = 271 nm. Upon application of a potential of 1.2 V, corresponding to peaks IV_a/V_a, the u.v. peaks of xanthosine decrease with time and, correspondingly, a broad peak (λ_{max} ca. 330-340 nm) appears and grows (Figure 23B). This behavior is identical to that observed for 9-methylxanthine except that the λ_{max} for the intermediate occurs at a slightly shorter wavelength.

The electrolysis shown in Figure 23B was stopped at the point when the peak at ca. 335 nm had reached its approximate maximal value. Unlike the behavior observed with 9-methylxanthine, however, no absorbance decay was observed.

Thin-layer spectroelectrochemical studies of xanthosine over a range of concentrations (1-20 mM) at pH 8 gave similar results to that shown in Figure 23. The behavior observed with 9-methylxanthine (increase of the ratio $(A_{max})_{335}/(A_{init})_{271}$ with increasing concentration) is also observed with xanthosine, again suggesting a second-order process.

Studies of xanthosine at varying applied potentials (0.9 V to 1.4 V, corresponding to peaks II_a-V_a) also

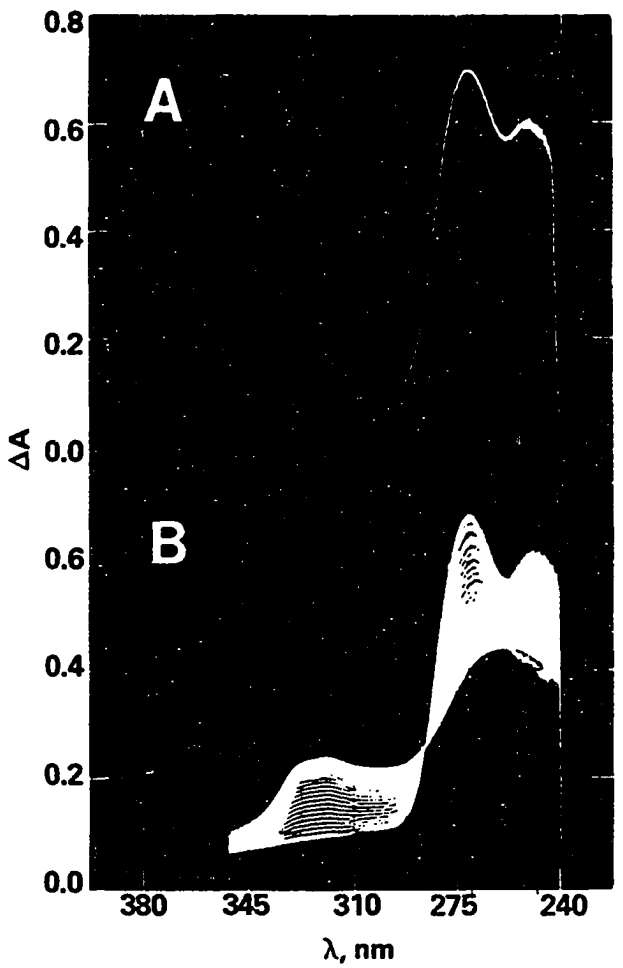

Figure 23. Spectrum of 10mM xanthosine electrolyzing at 1.2V at pH 8 at gold minigrid electrode in a thin-layer cell (A) before electrolysis; (B) during electrolysis. Repetitive scans are 1 second.

gave results similar to those shown in Figure 23. However, at applied potentials more negative than peaks II_a or III_a (< ca. 1.1 V) the rate of electrooxidation was significantly slower.

The thin-layer spectroelectrochemical behavior of xanthosine at pH 6 and 7 was essentially identical to that reported above at pH 8. However, below pH 6 it became increasingly difficult to observe the spectrum of the intermediate species until at pH 2 and 3, for example, it was not possible to observe any absorption due to any species other than xanthosine. This parallels the behavior of xanthosine in the controlled potential coulometry studies, and also parallels that of 9-methylxanthine.

Kinetic measurements

Owing to the lack of any appreciable absorbance decay at 330-340 nm upon electrochemical oxidation of xanthosine, it was not possible to obtain any meaningful kinetic data.

Conclusions

The experiments reported above indicate that xanthosine is electrochemically oxidized in much the same way as is 9-methylxanthine. Thus, one route of xanthosine electrooxidation occurs via the peak II_a process. The initial product of the peak II_a process, as in the peak

II_a process for 9-methylxanthine, is yellow, has a u.v. peak with λ_{max} ca. 330-335 nm, and is further oxidized via the peak III_a process. The peak II_a-III_a oxidation process is apparently independent of the peak IV_a-V_a-I_c-I_a processes, as was true for 9-methylxanthine.

The evidence presented in this study supports the proposal that formation of the yellow species as a result of the peak II_a oxidation is a second-order process, and that this material is probably some dimeric species. This material has certain characteristics of the dimer identified by Hansen and Dryhurst[91] which was discussed in more detail in Chapter 4. The u.v. absorbance at λ_{max} = 335 nm of the product of the peak III_a electro-oxidation of xanthosine decays very slowly when the electrolysis is stopped at $(A_{max})_{335}$. However, if the solution is allowed to stand over a period of time the absorbance at 335 nm does decay eventually to about one-third $(A_{max})_{335}$. This time period is ca. 20-30 minutes in the thin-layer cell and ca. 2-4 hours (with continued electrolysis) in a large-scale electrolysis cell. In the latter case, the yellow color fades along with the decrease in A_{335}. This implies that the peak III_a electrooxidation product of xanthosine is much more stable than the corresponding product of 9-methylxanthine. Owing to the extremely slow decay of the peak III_a product of xanthosine,

meaningful kinetic measurements were not feasible.

Furthermore, a short-lived intermediate species, which is evidently not formed without first scanning (in cyclic voltammetry) past peaks IV_a and/or V_a or electrolyzing (in controlled potential coulometry) at potentials corresponding to these peaks, is produced which is reducible as shown by the peak I_c process. This species also appears to be stabilized by adsorption as shown by its voltammetry at rough electrode surfaces.

These investigations show that the electrochemical oxidation of xanthosine, as studied by cyclic voltammetry, controlled potential coulometry, and thin-layer spectroelectrochemistry, is very similar to that of 9-methylxanthine. These studies should provide considerable insight into the reaction schemes for the electrooxidation of other purine nucleosides.

EXPERIMENTAL

Chemicals

Xanthosine was obtained primarily from Vega-Fox Biochemicals. Buffer solutions were constituted as described in Chapter 3.

Initial samples of xanthosine were found to be contaminated with a small amount (3-5%) of xanthine. A method was developed to screen xanthosine samples so that

only those free of xanthine were used in the investigation. This method is described in detail in Chapter 6.

Apparatus and Procedures

The apparatus and procedures employed have been described in previous chapters.

Electrolysis of xanthosine in HOAc and HCl

Lyophilization of solutions of xanthosine electrolyzed in acetic acid and hydrochloric acid resulted in a dark green-black and very mucilaginous substance, which hardens when exposed to air. When xanthosine is electrolyzed in phosphate buffers and then lyophilized, this behavior is not observed. Solutions of free D-ribose were electrolyzed at the same potential as xanthosine in acetic acid and when lyophilized also formed a blackish, very sticky substance. These results certainly seem to imply that acidic solutions (e.g., acetic and hydrochloric acids) cause polymerization or some other reaction of the ribose moiety of xanthosine.

SUMMARY

The electrochemical oxidation of xanthosine (9-ribosylxanthine) was shown to be nearly identical to that of 9-methylxanthine. Xanthosine is apparently electro-oxidized in two independent processes. In the first,

the oxidation proceeds via peak II_a and may involve formation of some dimeric species which can then be further oxidized via peak III_a. The peak III_a electro-oxidation product of xanthosine is much more stable than the corresponding product of 9-methylxanthine as observed by its slower absorbance decay at ca. 330-340 nm.

In the second process, the oxidation occurs via peaks IV_a and/or V_a in a process that may be somewhat similar to that for xanthine and resulting in the corresponding diimine which further reacts chemically and electrochemically in a manner similar to that of uric acid diimine (equation 1, Chapter 1).

CHAPTER 6

ANALYTICAL APPLICATIONS

During the course of the work described in previous chapters, it was often necessary to utilize various analytical methods. These methods included many chromatographic, spectroscopic, classical, and electroanalytical techniques. Most of these methods were established and recognized procedures, or were modifications of existing ones. However, there were occasions where new methods were needed in order to successfully carry out the intended goals of this work.

The subject of this chapter is to describe in more detail two new analytical methods which were developed and utilized. One of these methods is the screening of xanthosine samples for xanthine by electrochemical methods. The second describes procedures for removing inorganic phosphate material from low molecular weight organic compounds by a column chromatographic method.

A. Detection and Determination of Xanthine in Xanthosine by Electrochemical Methods

Introduction

Preliminary studies of the electrochemical and spectroelectrochemical oxidation of xanthosine (I) at the pyrolytic graphite electrode (PGE) revealed several voltammetric oxidation peaks (Chapter 5). The first, least positive, voltammetric oxidation peak occurred at the same peak potential as the single peak observed for xanthine (II) at the PGE. Controlled potential electrolysis and coulometry of commercial samples of xanthosine at potentials corresponding to its first voltammetric oxidation

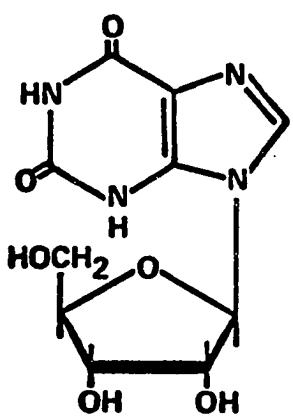

(I)

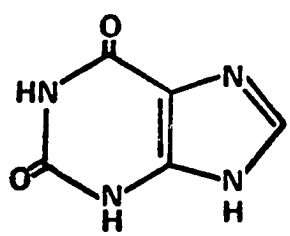

(II)

peak revealed that the latter peak could be completely eliminated without affecting the more positive xanthosine peaks. The experimental n-value was found to be 0.2 to

0.25. If the first voltammetric peak observed with commercial samples of xanthosine was an adsorption pre-peak, it would not have been eliminated without total electrooxidation of xanthosine (with an n-value of 3-4). It was concluded, therefore, that some commercial samples of xanthosine may be contaminated with the parent base xanthine. Further studies of the electrochemical behavior of the first peak observed with commercial xanthosine samples revealed that it exhibited identical behavior to the peak of pure xanthine.[54]

Because the interfacial[94] and electrooxidation behavior of xanthine is quite different from that of xanthosine it was therefore necessary to devise an analytical method to screen xanthosine samples so that only those free of xanthine were used in the investigations. Since the ultraviolet absorption spectra of xanthine and xanthosine are virtually identical the conventional, simultaneous analysis of such a mixture is impossible.

Several qualitative methods based on paper and thin-layer chromatography for the detection of xanthine in the presence of xanthosine have been described[95-98] but they did not possess the speed and sensitivity required. Gerlach et al.[99] reported a paper chromatographic method for the quantitative determination of many purine and pyrimidine bases and their corresponding nucleosides. This method involved eluting the paper

chromatogram after separation and determining the concentration of each species individually by a u.v. spectrophotometric method. This paper chromatographic method suffers from being very time-consuming and utilizes fairly large solution concentrations of the test materials (ca. 0.01 M). Tortolani and Colosi[100] employed a similar method utilizing thin-layer chromatography on Sephadex G-10/cellulose or Sephadex G-10/silica gel mixed beds.

A recent application of high pressure liquid chromatography[101] has been reported with fairly good results. However, poor peak resolution in mixtures of xanthine and xanthosine would render this method unacceptable for analytical determinations of these compounds.

Since xanthine and xanthosine give well-separated voltammetric oxidation peaks at the PGE the use of electrochemical techniques for analysis of small quantities of xanthine in the presence of xanthosine was investigated. The present study describes a rapid and reliable method for the qualitative detection of xanthine in xanthosine as well as a convenient and dependable method for the quantitative determination of xanthine.

Results and Discussion

Linear sweep voltammetry

Over the pH range 3-8 xanthine exhibits a single, well-defined voltammetric oxidation peak at the PGE with

the peak potential, E_p, being described by the equation $E_p = 1.11-0.063$ pH at a sweep rate of 0.2 V sec^{-1}. Under the same conditions the first and major peak of xanthosine exhibits a peak at $E_p = 1.24-0.063$ pH between pH 3-6. At higher pH values the peak potential for xanthosine is independent of pH, $E_p = 0.86 \pm 0.1$ V. The difference between the peak potentials of xanthine and xanthosine is more clearly seen in Figure 24. The optimal separation in the peak potentials for xanthine and xanthosine obviously occurs at pH 7-8 (Fig. 24). A typical linear sweep voltammogram of xanthosine containing about 3% by weight of xanthine is shown in Figure 25.

The electrochemical oxidation of xanthine is a 4e process[54] while the oxidation of xanthosine involves between 3-4e (Chapter 5). The reason that the peak current for xanthine in Figure 25 is so large is that xanthine is very strongly adsorbed at the PGE.[54,102] This results in a very pronounced enhancement of the xanthine peak current at low concentrations compared to that expected for a diffusion controlled process.

Controlled potential coulometry

The voltammetric oxidation peak of xanthine exhibits a non-linear peak current versus concentration relationship[102] owing to the strong adsorption of this compound. In addition, the xanthine peak current is

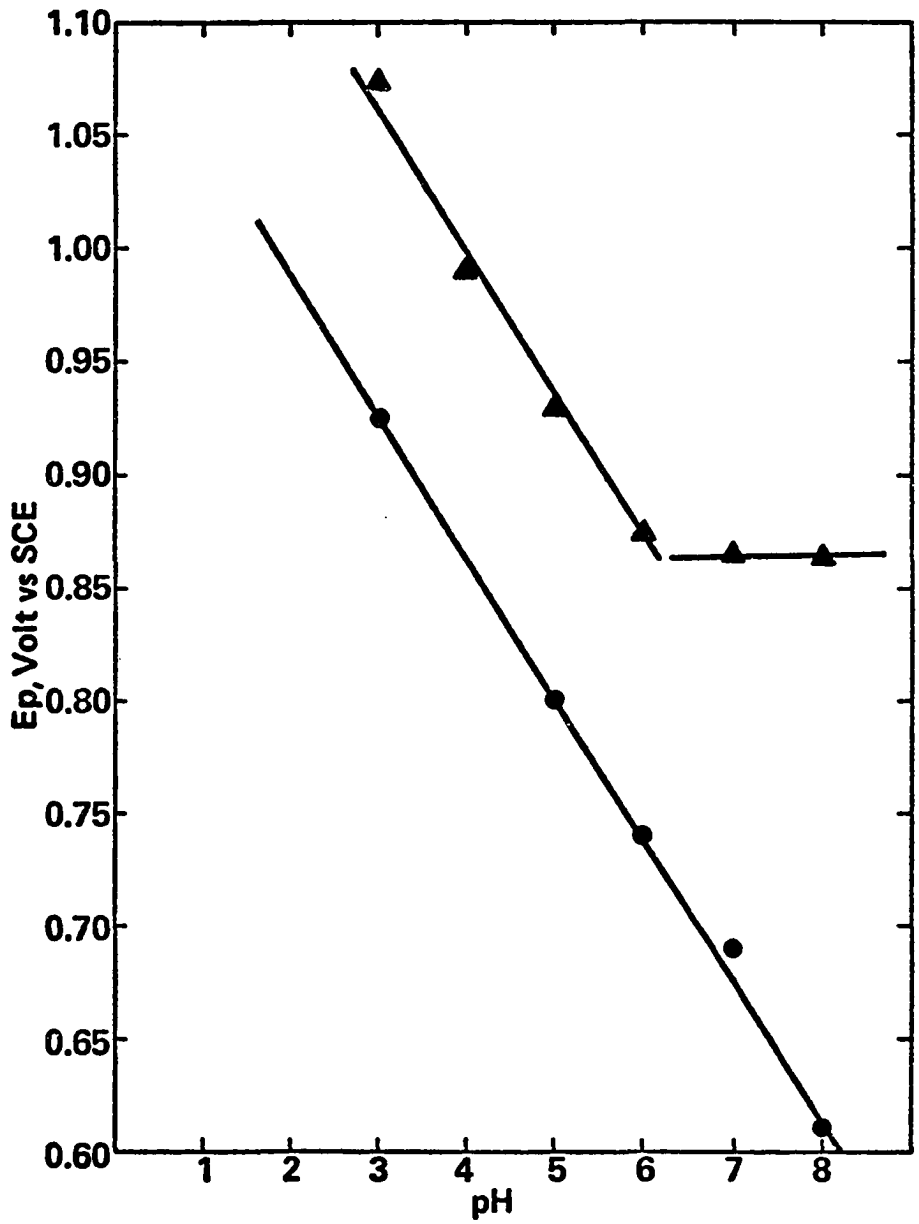

Figure 24. Variation of E_p with pH for xanthine (●—●) and xanthosine (▲—▲) at the PGE. Scan rate 200 mV sec^{-1}.

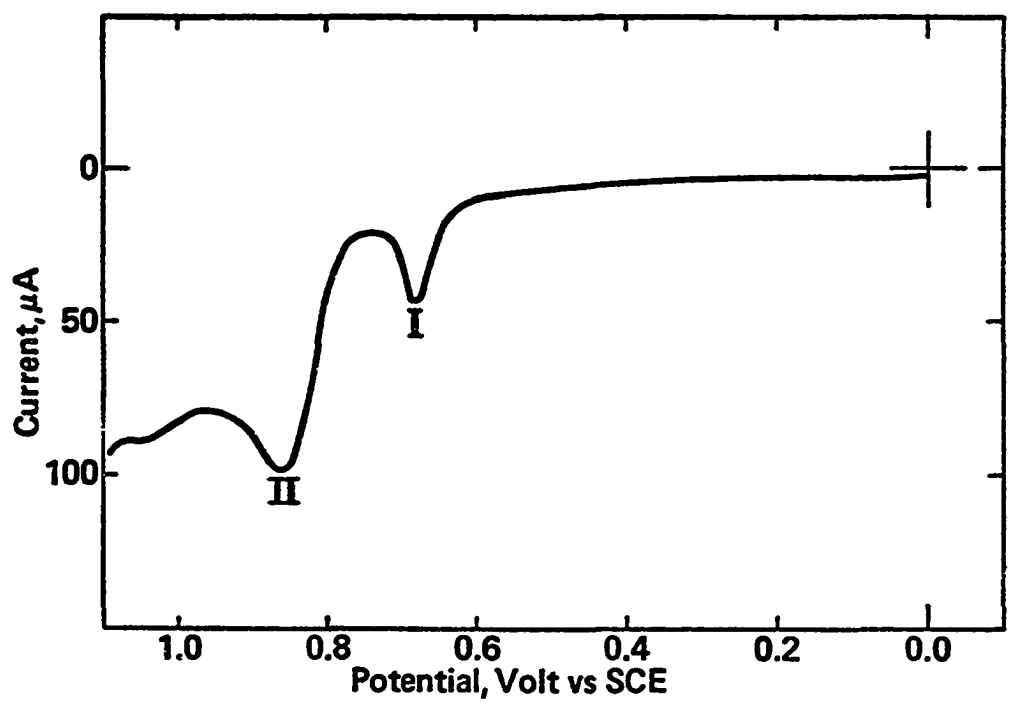

Figure 25. Linear sweep voltammogram of 0.5 mM xanthosine (peak II) containing ca. 0.03 mM xanthine (peak I) in pH 7.0 McIlvaine buffer at the PGE. Scan rate 200 mV sec^{-1}.

probably dependent on the concentration of other adsorbable species in solution such as xanthosine.[103,104] It was concluded, therefore, that a conventional voltammetric method for the determination of xanthine in the presence of xanthosine would not be satisfactory.

The voltammetric oxidation peak of xanthine in xanthosine-xanthine mixtures can be eliminated by controlled potential electrolysis at potentials at, or slightly positive of, the xanthine peak potential, particularly at pH 7-8 where the peak separation is greatest. Under these conditions negligible electrooxidation of xanthosine takes place. Accordingly, a controlled potential coulometric method was developed to analyze for xanthine in the presence of xanthosine (see Experimental). The optimum pH for such a coulometric analysis is between 7 and 8 where the xanthine and xanthosine peaks show their greatest peak separation (Fig. 24). However, lower pH values may be employed if necessary (vide infra).

Some typical analytical results for a sample of pure xanthosine to which known amounts of xanthine were added are shown in Table 11. Clearly, at pH 7 and 8 the amount of xanthine taken and that found is in good agreement, even when xanthine occurs at 1% or less of the xanthosine concentration. At pH 5 the analytical results are significantly poorer. This is due to partial electrooxidation of small amounts of xanthosine at the

TABLE 11

Typical Results for Coulometric Determination of Xanthine in Xanthosine[a]

McIlvaine buffer	Xanthine (mg) Taken	Found
pH 7	0.65	0.70
	1.22	1.16
	1.76	1.79
	0.13	0.13
pH 8	0.63	0.61
	1.03	1.03
pH 5	0.22	0.31
	0.51	0.73
	0.73	1.12

[a]In each case 14-15 mg pure anhydrous xanthosine in *ca.* 100 ml of the buffer was used.

potentials used to electrolyze xanthine (more peak overlap, see Fig. 24).

Linear sweep voltammetry of solutions of several commercial samples of xanthosine at the PGE revealed that the voltammetric oxidation peak of xanthine was present. Quantitative analysis of these samples by controlled potential electrolysis indicated that appreciable quantities of xanthine were present (Table 12).

Stability of xanthosine

To determine whether the xanthine present in commercial xanthosine samples was due to hydrolysis or other decomposition processes, xanthosine solutions at pH values between 5 and 8 were allowed to stand at room temperature for 2-4 days after first removing all xanthine by controlled potential electrolysis. Under none of these conditions did the voltammetric oxidation peak of xanthine reappear. Accordingly, it is unlikely that hydrolysis or other decomposition processes are responsible for the formation of xanthine from xanthosine.

Experimental

Chemicals

Xanthosine was obtained from Calbiochem and from Vega-Fox. Xanthine was purchased from Nutritional Biochemicals Corporation.

TABLE 12

Coulometric Determination of Xanthine in

Commercial Xanthosine Samples

Sample	Wt. Sample Taken,[a] mg	Wt. Xanthine Found, mg	Xanthine % by weight
pH 7 McIlvaine Buffer			
I[b]	18.66	0.56	3.0
	18.50	0.59	3.2
	17.13	0.56	3.2
	223.50	6.63	3.0
	17.54	0.59	3.3
II[c]	15.80	0.79	5.0
	16.80	1.05	6.0
	17.12	0.96	5.6
pH 8 McIlvaine Buffer			
I[b]	16.12	0.45	2.8
	16.72	0.53	3.1
II[c]	17.16	0.85	5.0
	15.27	0.87	5.7
	15.89	0.91	5.7

[a]Dissolved in ca. 100 ml buffer solution.

[b]Sample obtained from Vega-Fox, lot number H-1415.

[c]Sample obtained from Calbiochem.

Buffer solutions were prepared from reagent grade chemicals and had an ionic strength of 0.5.

Apparatus

Earlier chapters contain descriptions of the instrument used to obtain the linear and cyclic sweep voltammograms, the X-Y recording device, the thermostated three-compartment electrochemical cell, and the pyrolytic graphite electrodes.

Controlled potential coulometry utilized a Wenking Model LT73 Potentiostat and a Koslow Scientific Model 541 Coulometer. A two-compartment cell (each compartment ca. 130 ml capacity) was employed with a set of large pyrolytic graphite electrodes (area ca. 42 cm^2) and a Fisher Fiber-Tip saturated calomel reference electrode (SCE) in one compartment and a platinum foil counterelectrode in the other. The two compartments were separated by a KCl-agar salt bridge. The usual volume of the electrolysis solution ranged from 100-125 ml and was stirred magnetically. The counterelectrode compartment was filled with the appropriate buffer solution. All potentials are referred to the SCE at 25°C.

Procedure for qualitative detection of xanthine in the presence of xanthosine

A 1-2 mg sample of the xanthosine to be tested

is placed in a 10 ml volumetric flask and diluted to the mark with the desired buffer solution. A buffer in the pH range 7-8 is the most suitable. If there is a substantial amount of xanthine in the sample ($\geq$ 5%) it is often necessary to stir the solution for ca. 10-20 minutes in order to dissolve all of the sample. A voltammogram of the resulting solution is then run at a clean, resurfaced PGE starting at 0.0 V and sweeping towards positive potentials. The sweep rate for the voltammogram is not critical although in the interest of speed a sweep rate of 0.2 V sec^{-1} is recommended. The appearance of a single peak at E_p = 0.86-0.88 V at pH 6-8 indicates that there is no significant xanthine present in the sample. In certain buffers (e.g., phosphate pH 7) some additional, small, ill-defined peaks may be observed at more positive potentials (Chapter 5). These are due to additional electrochemical oxidations of xanthosine and are of no particular interest in the present context.

The appearance of an additional voltammetric peak prior to the first xanthosine peak at E_p = 1.11-0.063 pH indicates the presence of xanthine in the sample. Owing to the very strong adsorption of xanthine at the PGE the xanthine peak is readily observable even when the latter compound is present at concentrations of 1% or lower.

Procedure for quantitative determination of xanthine in the presence of xanthosine

Once the presence of xanthine in the xanthosine sample has been established a quantitative analysis for xanthine may be carried out by controlled potential coulometry. Typically, a 10-20 mg sample is dissolved in 100-125 ml of the appropriate buffer solution and an electrolysis carried out at a potential ca. 50 mV positive of E_p for xanthine as determined from the linear sweep voltammogram. The electrolysis is continued until the current decreases to a low, constant value and the number of coulombs is then recorded. A similar experiment is carried out in the absence of xanthosine and the coulombs recorded for this blank solution is subtracted from that obtained for the sample electrolysis. (Note: it is not necessary to run the blank for each electrolysis. An average over several runs is quite sufficient.) The weight of xanthine present in the sample may be calculated from the equation:

1 coulomb = 0.3938 mg xanthine

This equation is obtained from the expression

$$Q = nFN^{\circ}$$

where Q = total number of coulombs passed during electrolysis

n = number of electrons involved in electrode reaction

F = 96,500 coulombs

N° = number of moles of test material

Since the faradaic n-value for xanthine is 4[54] and its molecular weight is 152.1, the amount of xanthine required for passage of one coulomb can be readily determined. A simple way to check that the electrolysis of xanthine is complete is to run a single sweep voltammogram of a small aliquot of the electrolyzed solution when only the xanthosine peak(s) should be observed. A typical electrolysis takes ca. 2-3 hours.

At pH 7 and 8 the total concentration of xanthine and xanthosine in a mixture can be determined spectrophotometrically because their molar absorptivities, ε, are essentially identical for their u.v.-absorbing peaks at ca. 277 nm.[105,106] Thus, the total xanthine plus xanthosine concentration can be calculated from the expression

$$C = A_{277}/8900 \text{ } \ell \text{ moles}^{-1} \text{ cm}^{-1}$$

where

C = total concentration of xanthine and xanthosine in the mixture

A_{277} = total absorbance at 277 nm at pH 7 or 8

The concentration of xanthine can be determined by the controlled potential coulometric method previously described. Then by subtracting the concentration of xanthine from the total concentration of xanthine and xanthosine, the amount of xanthosine can be determined. Analysis of several unknown mixtures by these methods yielded values for both xanthine and xanthosine well within 5% of the original sample weight.

Summary

Xanthine and xanthosine are voltammetrically oxidized at the pyrolytic graphite electrode (PGE) at different potentials. The difference between the peak potentials of xanthine and xanthosine becomes most pronounced at pH 7-8. The presence of small amounts of xanthine in xanthosine samples is readily detected using linear sweep voltammetry at the PGE. Quantitative analysis of xanthine present in xanthosine may be accomplished by controlled potential coulometric oxidation of the xanthine. The reproducibility of the method is ±5-10%.

B. Separation of Some Low Molecular Weight Organic Compounds from Phosphate Buffers

Introduction

The electrochemical oxidation of biologically important purine derivatives and the relationship between the electrochemical products and mechanisms and the biological oxidations of these compounds was discussed in Chapter 1. One of the major problems encountered in such studies is the separation and identification of the relatively large number of electrooxidation products that are formed. In the past several different separations and/or analytical techniques have been utilized for identification and quantitation of purine electrooxidation products.

Recently, investigations have commenced on the electrochemical oxidation of purine nucleosides and nucleotides. It became obvious that the methods used for qualitative and quantitative analysis of simple purine electrooxidation product mixtures were inadequate for analysis of the products from electrooxidation of the more complex nucleosides, nucleotides, and oligonucleotides. A series of investigations were begun to develop better methods for product separation. Recently, a column

chromatographic technique was developed which could quantitatively separate milligram quantities of typical purine electrooxidation products such as allantoin, alloxan, oxaluric acid, parabanic acid, ribose, and urea.[107] This procedure utilized series coupled Sephadex G-10 and QAE A-25 column packings and aqueous KH_2PO_4 solutions as the eluant. In order to properly identify the products separated by the latter technique it became necessary to remove the aqueous phosphate eluant from each component. This would then allow techniques such as mass, infrared and u.v.-visible spectroscopy, elemental analysis, etc., to be used to identify the various components.

A search of the literature revealed that there have been no methods reported for adequately separating small quantities of low molecular weight organic compounds from relatively large excesses of inorganic phosphate. However, desalting of high molecular weight compounds and biopolymers by gel filtration chromatography has been reported.[108,109]

Another method for removing some inorganic salts from organic compounds has employed cation exchange resins eluted with various mixtures of water and non-aqueous solvents.[110,111]

The present study describes two column chromatographic methods which may be used for removal of inorganic

phosphate from low molecular weight organic compounds.

Results and Discussion

In the column chromatographic separation scheme developed for the purine electrooxidation products,[107] KH_2PO_4 solutions were used as eluant. Each component was eluted in a volume of about 40-50 ml of, usually, 0.025 M KH_2PO_4. By freeze-drying the latter solutions to about 1 ml, each organic component would be present in a solution of ca. 1 M inorganic phosphate. Accordingly, the experiments reported here utilized 1.6-30 mg of the organic species dissolved in 1 ml of 1 M KH_2PO_4.

Sephadex G-10

Some typical chromatograms showing the separation of phosphate from D-ribose, allantoin, and urea using water as the eluant are presented in Figure 26. Clearly, a satisfactory separation of the organic component from inorganic phosphate can be achieved. The yield of the organic component was exactly the same as the amount initially added to the column, i.e., a quantitative recovery of the organic material was possible.

Chromatograms for alloxan and parabanic acid under identical conditions are shown in Figure 27 where it can be observed that using water as the eluant a broad, ill-defined peak occurs between the phosphate and alloxan

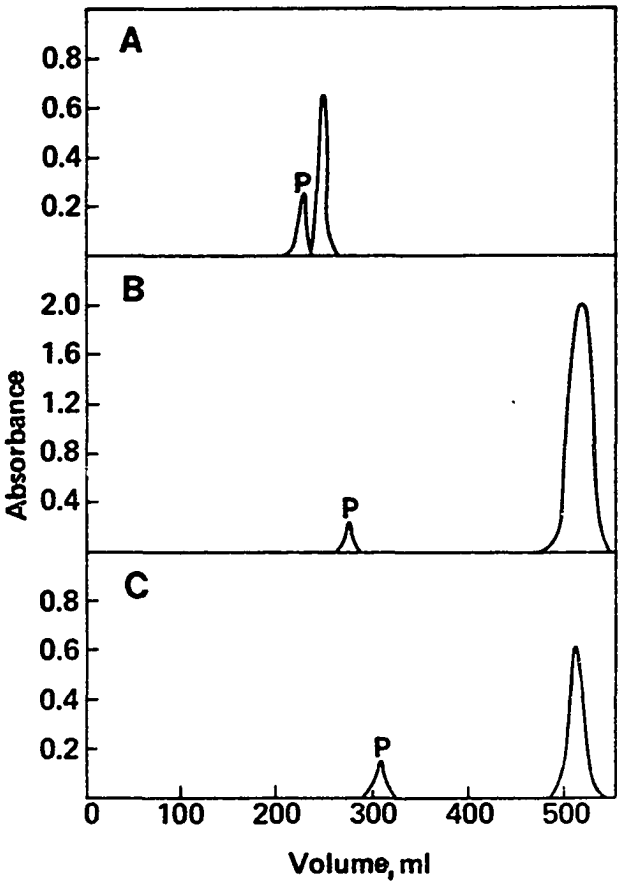

Figure 26. Chromatograms obtained for 1 ml 1 M KH_2PO_4 containing (A) 30 mg D-ribose, (B) 6 mg allantoin, and (C) 10.6 mg urea using water as the eluant. Flow rate for (A) 24 ml h^{-1}, (B) 51 ml h^{-1}, and (C) 48 ml h^{-1}. Absorbance monitored at (A) 195 nm, (B) 215 nm, and (C) 201 nm. P refers to phosphate peak.

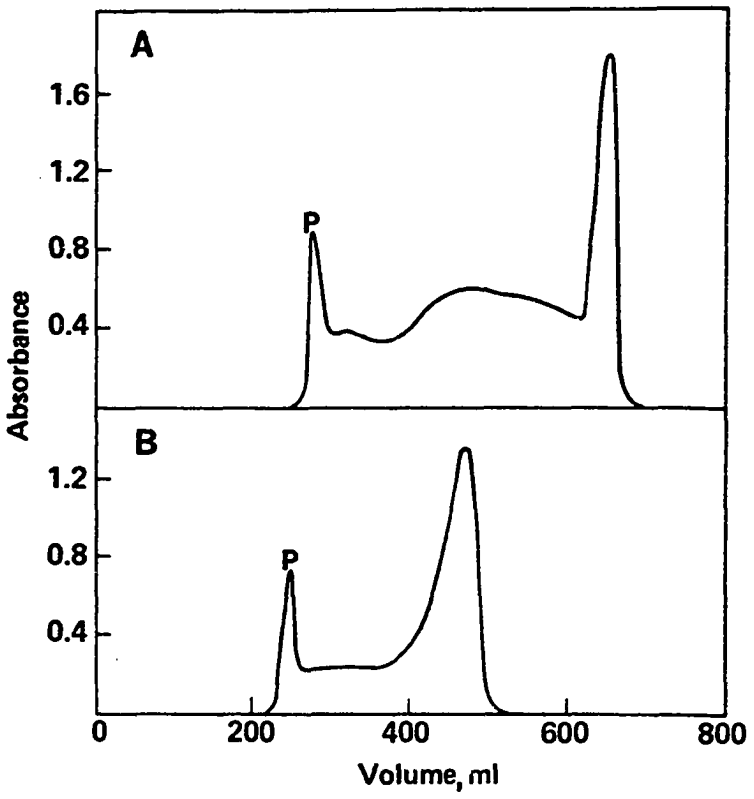

Figure 27. Chromatograms obtained for 1 ml 1 M KH_2PO_4 containing (A) 10 mg alloxan and (B) 10 mg parabanic acid using water as the eluant. Flow rate 54 ml h^{-1}. Absorbance monitored at (A) 206 nm and (B) 210 nm. P refers to phosphate peak.

or parabanic acid peaks. The amount of alloxan or parabanic acid recovered was significantly lower than the original amount of these compounds added to the column. The low yields of these components and the distorted form of the chromatograms suggested that both alloxan and parabanic acid decompose to some extent as the separation proceeds. It is well-known that above about pH 4-5 alloxan decomposes to alloxanic acid.[112,113] In addition, at neutral pH parabanic acid hydrolyzes to oxaluric acid.[114]

Attempts to separate oxaluric acid from inorganic phosphate on Sephadex G-10 using water as the eluant were unsuccessful even after passage of in excess of 1200 ml of water. This behavior suggested that oxaluric acid, which would be in its anionic form at neutral pH,[115] is strongly retained on the column.

In order to satisfactorily elute alloxan, parabanic acid, or oxaluric acid from a Sephadex G-10 column and to separate these compounds from phosphate it was found that the pH of the eluant has to be significantly lowered. This was accomplished by using dilute HCl (0.001 M, pH 3) as the eluting solvent. Hydrochloric acid was used because it is subsequently easily removed from the organic component by lyophilization.

Figure 28 shows chromatograms for alloxan, parabanic acid, and oxaluric acid in mixtures with phosphate

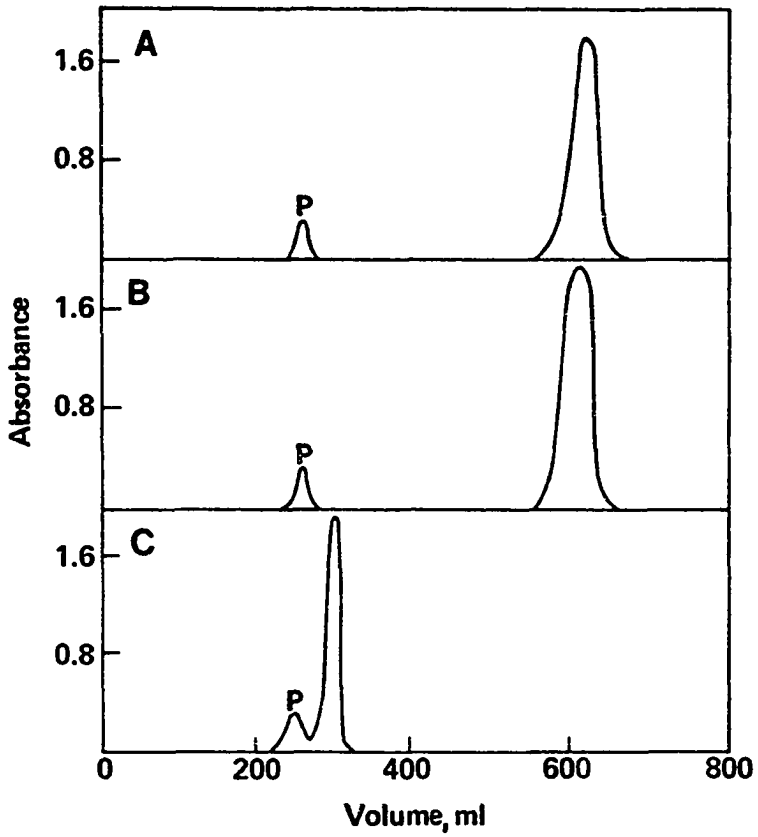

Figure 28. Chromatograms obtained for 1 ml 1 M KH_2PO_4 containing (A) 1.8 mg alloxan, (B) 1.8 mg parabanic acid, and (C) 1.7 mg oxaluric acid. Flow rate in each case 54 ml h^{-1}. Eluant 0.001 M HCl. Absorbance monitored at (A) 206 nm, (B) 210 nm, and (C) 220 nm. P refers to phosphate peak.

using dilute HCl as the eluant. Clearly, in each case, a very good separation between inorganic phosphate and the organic component is noted with no distortion of the chromatographic peaks.

The chromatograms shown in Figures 26 and 28 indicate that in most cases the resolution of the phosphate and organic component peaks are excellent. For comparative purposes some peak resolution values (R_s) between each of the six organic components and phosphate based on equation (1)

$$R_s = \frac{2(V_p - V_o)}{W_p + W_o} \qquad (1)$$

are presented in Table 13. In equation (1) V_p and V_o are the retention volumes for the phosphate and organic component peaks, respectively, while W_p and W_o are their baseline bandwidths.[116] A resolution of 1.5 or greater indicates virtually complete, or baseline, separation. A resolution of 1.0 corresponds to about 98% complete separation.[116] Clearly, four of the compounds exhibit excellent resolution ($\geq$ 1.5). In the case of D-ribose a resolution of 0.67 was observed at a flow rate of 54.0 ml hr^{-1} (Table 13). However, when the flow rate was decreased to 24.0 ml hr^{-1} the resolution increased to 1.0 (Table 13). Accordingly, for D-ribose or oxaluric acid an enhanced resolution between these components and

TABLE 13

Resolution Between Phosphate and Organic Component Chromatographic Peaks on Sephadex G-10 Column[a]

Compound	Eluant	Resolution[b]
D-Ribose	H_2O	0.67
D-Ribose	H_2O	1.0[c]
Oxaluric Acid	Dilute HCl[d]	1.04
Allantoin	H_2O	2.0
Parabanic Acid	Dilute HCl[d]	4.2
Urea	H_2O	4.3
Alloxan	Dilute HCl[d]	4.6

[a]Flow rate 54.0 ml hr^{-1}, except as noted otherwise.

[b]See equation 1 for definition.

[c]Flow rate 24.0 ml hr^{-1}.

[d]0.001 M HCl in water.

phosphate can, if so required, be readily accomplished by appropriate decrease of the eluant flow rate.

All fractions under component peaks under conditions similar to those shown in Figures 26 and 28 gave no evidence for the presence of any phosphate.

During the course of this work the solid organic components after elution and freeze-drying were tested for their authenticity. Typically, melting points were taken and comparative thin-layer chromatography was carried out. Often u.v. spectra were also taken. In each case the eluted organic compounds were found to be analytically pure and free from inorganic phosphate.

Methanolic AG 50W-X8

Following dissolution of the organic component/ KH_2PO_4 mixture in methanol and application to the methanolic AG 50W-X8 column, it was found that the phosphate formed a white crust at the top of the column and was not eluted. Accordingly, only a single peak due to the organic component was eluted from the column. Some typical data for allantoin, alloxan, parabanic acid, D-ribose, and urea are shown in Table 14. The recovered organic components were pure and free of any inorganic phosphate (methanol does not interfere with the phosphate test, but care must be exercised in heating the test tube). Oxaluric acid is almost completely insoluble in methanol and hence cannot

be desalted by this method.

TABLE 14

Retention Volumes for Methanol AG 50W-X8 Column

Compound	Sample weight,[a] mg	Flow rate, ml hr^{-1}	Wavelength monitored, nm	Retention Volume ml
Allantoin	4	120	224	55
Alloxan	1.7	90	230	42
Parabanic acid	1.6	90	225	45
D-Ribose	30	90	216	42
Urea	12	90	225	51

[a]This weight of sample was dissolved in 1 ml 1 M KH_2PO_4, freeze-dried, dissolved in 3-8 ml methanol, and passed through the methanol-washed AG 50W-X8 column.

The white phosphate crust which forms at the top of the methanolic cation exchange column may be readily removed during regeneration of the column with water and hydrochloric acid (see Experimental).

Other ion exchange systems

A number of other ion exchange resins (see Experimental) were also examined as chromatographic stationary phases for separation of organic purine electro-oxidation products from inorganic phosphate. For each resin several column parameters were examined, e.g.,

type of eluant and flow rate. Partial success was achieved with Amberlite MB-3 mixed bed ion exchange resin. However, generally two or three passes through relatively long, freshly washed columns were required to accomplish a satisfactory separation.

The principal difficulty noted with most separations was the tendency for the organic species to be very strongly retained by the strong anion exchange resins even though the exchange of phosphate anion with hydroxide ion was complete. When weak anion exchange resins were utilized, however, both the organic sample and phosphate eluted together. Therefore, it was not possible to develop any useful separation techniques with the anion exchange resins.

Other considerations

An advantage of desalting with Sephadex G-10 or methanolic cation exchange columns in combination with the separation scheme previously mentioned[107] is that it lends itself to the separation and identification of products of small scale electrolyses. Previously, repetitive large scale electrolyses requiring long times ($\geq$ 4-5 days) were necessary to obtain significant quantities of reaction products for characterization.

Moreover, phosphate buffers have an advantage in covering a fairly wide pH range for electrolyses. Citric

acid buffers (McIlvaine) could not be employed in electrolyses for product isolation due to the difficulty in removing the citric acid in the desalting process. In addition, phosphate buffers have an increased oxidation potential background limit compared to those of citric acid and most other buffer systems. Solutions of hydrochloric acid and acetic acid have, in the past, been employed as electrolytes due to their ease of removal by lyophilization but their major drawback is the low pH of such supporting electrolyte systems.

The desalting techniques outlined in this study should provide a basis for removal of inorganic material from a variety of organic compounds. The methods should be particularly useful for desalting solutions formed from electrochemical reactions where reaction products are normally contaminated with large excesses of inorganic buffer/electrolyte materials.

Experimental

Chemicals

Chemicals were obtained from the sources indicated: parabanic acid and allantoin (Eastman), alloxan and oxaluric acid (Nutritional Biochemicals Corporation), urea (Merck), and D-ribose (Calbiochem).

The following ion exchange resins and gels were used: AG11A8 ion retardation, AG 50W-X8 strong cation,

AG 501-X8 mixed bed, and AG 21K strong anion (Bio Rad); Amberlite MB-3 mixed bed, and Amberlite IR-4B weak anion (Mallinckrodt); Dowex 2-X8 strong anion (J. T. Baker); Sephadex QAE-A25 strong anion and Sephadex G-10 gel permeation (Pharmacia).

Thin-layer chromatography was carried out with Brinkman MN-Polygram Polyamide-6-UV_{254} and Eastman Chromogram 6060 silica gel precoated sheets impregnated with fluorescent indicator.

Apparatus

Chromatographic columns for Sephadex G-10 were 75 cm long and 2.75 cm in diameter. A Mariotte flask system was utilized to obtain constant and reproducible flow rates.

Columns for the AG 50W-X8 and the AG11A8 packings were 40 cm long and 2.5 cm in diameter. Most of the other ion exchange columns ranged from 20 x 1.3 cm to 30 x 2.0 cm.

ISCO Golden Retriever and or ISCO Model 1200 fraction collectors were utilized for sample collection (Instrument Specialties Company, Lincoln, Nebraska). Ultraviolet spectra and monitoring of chromatographic fractions utilized a Hitachi-Perkin Elmer Model 124 Spectrophotometer using 1.00 cm quartz cells.

Column Packing Conditions

Sephadex G-10

Two hundred grams of the dry resin were allowed to swell in excess water by heating on a boiling water bath for at least one hour with constant stirring. The slurry was then allowed to cool to room temperature (ca. 1 1/2 hr.). The column was mounted as vertically as possible with the aid of a bubble level. Excess water was removed from the gel in order to form a thick slurry. Then, by means of a long glass rod, the slurry was carefully poured into the column which contained about 100 ml of water. The column flow was started immediately since this was found to give the most even packing. An extension reservoir was placed on the top of the column so that all the required gel could be added at one time. This also aids in obtaining an evenly packed bed. The G-10 packing filled all but the upper 4-8 cm of the column. This space was filled with the eluant and a Mariotte flask fitted to ensure a constant flow rate. Several bed volumes of eluant were passed through the column in order to stabilize and equilibrate the gel bed. The homogeneity of the packed bed was checked by visual inspection in transmitted light from an incandescent light held behind the column. Such columns were operated at room temperature with flow rates of 42.0-54.0 ml hr^{-1}, except as otherwise noted.

Methanolic AG 50W-X8

The appropriate amount of dry AG 50W-X8 strong cation exchange resin necessary to give about 150 ml of swelled resin was hydrated with excess deionized water for several hours with gentle stirring. The resin was then allowed to settle and excess water removed by decantation to form a thick slurry. This slurry was poured into the vertically mounted column in several portions allowing each portion of resin to settle before the next was added. The slurry was washed into the column with small quantities of water. This method of adding the packing gives a more uniform and reproducible column. If all the packing is added at one time the resin tends to gradate according to size giving a less reproducible column.[117] The remaining space at the top of the column was filled with water and a Mariotte flask system was attached. Several bed volumes of water were passed through the column to completely equilibrate the resin. The column was then washed with 1-2 bed volumes of 1 M HCl to ensure that all the resin was in the hydrogen ion form. Then, the column was washed with water until the effluent was free of chloride (as tested with 0.1 M $AgNO_3$). Distilled methanol was then passed through the column (1-2 bed volumes). Owing to the lower swelling of the resin in methanol compared to water, significant

channeling occurred at this stage.[110] In order to remove such channels the column was inverted several times until the resin settled uniformly. It should be noted that if the cation exchange resin remains in contact with methanol for extended periods of time, then apparently a u.v. absorbing component of the resin is dissolved by the methanol. This results in a large background absorbance which can, on occasion, obscure sample peaks. For this reason the methanol wash of the column usually preceded the sample application by at most 1-2 hours. Following sample elution the methanol was washed off the column with several bed volumes of water. This cation exchange column was operated at room temperature at flow rates typically between 90.0-180.0 ml hr^{-1}.

Other Ion Exchange Resins

Other ion exchange resins were packed into columns in an analogous manner to that of the AG 50W-X8 resin described above.

Procedures for removal of phosphate

Sephadex G-10 Columns

The test component (typically about 1.7-30 mg) dissolved in 1 ml of 1 M KH_2PO_4 was carefully applied to the top of the column of Sephadex G-10 after first draining the excess eluant above the surface of the column. (The upper surface of the gel bed was protected with a

disc of Whatman No. 1 filter paper.) The sample was carefully absorbed into the top of the column, and the column walls and gel surface were washed several times with 1-2 ml of eluant, allowing each wash to drain into the column. The column was then filled with eluant and connected to a Mariotte flask. Fractions of 3 ml volume were collected with the fraction collector. These fractions were monitored at an appropriate wavelength (see Figs. 26 and 28). As a general rule, however, for monitoring unknown components of purine electrooxidations as they are eluted a wavelength of ca. 200 nm is the most widely applicable. Every fourth fraction was monitored except in regions where absorbing components were eluted; then the absorbance of every second fraction was measured. In the case of each organic compound studied the first peak to be eluted was that of phosphate which at high concentrations gives a readily detectable u.v. absorption at wavelengths below ca. 220 nm. The presence of phosphate in this peak was confirmed by testing with ammonium molybdate (vide infra). Those fractions containing the organic component were combined and freeze-dried. The resulting residue was confirmed as the authentic material by melting point, thin-layer chromatography, or u.v. spectrophotometry.

Methanolic AG 50W-X8 columns

The test components, dissolved in 1 ml of 1 M KH_2PO_4, were first freeze-dried. The resultant residue was then extracted with the minimum amount of distilled methanol (typically 3-8 ml) and applied to the top of the column in exactly the same way as described for the Sephadex G-10 column except that methanol was employed as the eluant. Again, 3 ml fractions of the column effluent were collected and each fraction was monitored by u.v. spectrophotometry at a suitable wavelength (see Table 14). The fractions containing the organic component were combined and the methanol removed by evaporation under reduced pressure.

Detection Methods

Thin-layer chromatography

In order to detect alloxan, parabanic acid, and urea in column effluents various thin-layer chromatographic procedures were employed. Alloxan was best detected using a polyamide thin-layer plate (see Chemicals) developed with methanol + acetic acid (95:5). The bright red-brown spot developed upon air drying (R_f = 0.7) is characteristic of alloxan.[67] The detection of parabanic acid was accomplished using silica gel plates developed with n-butanol + acetic acid + water (12:3:5). A blue-black spot observed under u.v. light (254 nm) with an R_f of

about 0.55 is characteristic of parabanic acid.[118] Urea was detected with the same system used for parabanic acid except that it was visualized as a yellow spot (R_f = 0.55) by spraying the plate with Ehrlich's reagent (10% w/v p-dimethylaminobenzaldehyde in concentrated HCl).[119]

Detection of phosphate

The presence of phosphate in the chromatographic effluent was detected by adding a few drops of 3 M nitric acid to ca. 1 ml of test solution followed by 100-200 mg of ammonium molybdate. The resulting solution was gently heated. The presence of phosphate was indicated by formation of a bright yellow precipitate of ammonium phosphomolybdate, $(NH_4)_3PO_4 \cdot 12MoO_3$.[120]

Detection of D-ribose

Under the same conditions used for detection of phosphate D-ribose gives a blue color. This is probably due to reduction of molybdate to blue Mo(III).[121] This method was quite selective for free D-ribose. Tests of several purine nucleosides (e.g., xanthosine, guanosine) produced no color change.

Summary

Two rapid and simple chromatographic methods

have been developed to quantitatively separate a number of organic compounds such as alloxan, urea, allantoin, parabanic acid, oxaluric acid, and D-ribose from relatively large excesses of inorganic phosphate. These organic compounds are representative of typical products expected upon electrochemical oxidation of various purine derivatives which may be themselves separated from each other by liquid chromatography using phosphate buffers. The phosphate may subsequently be separated from the organic components either by use of a Sephadex G-10 gel permeation column using water or very dilute hydrochloric acid as the eluant or by use of a methanol washed column of a strong cation exchange resin using methanol as the eluant.

CHAPTER 7

SUMMARY

These investigations were concerned primarily with the application of thin-layer spectroelectrochemistry at a gold minigrid electrode to the electrochemical oxidation of various biologically important purines. Compounds studied included 5,6-diaminouracil, uric acid, xanthine, 9-methyluric acid, 9-methylxanthine, and xanthosine.

The study of the electrochemical oxidation of 5,6-diaminouracil was undertaken because this molecule serves as a model for uric acid. Electrooxidation of 5,6-diaminouracil yields an intermediate species which can be detected by its u.v. absorption spectrum. The kinetics of the apparent hydrolysis of this species has been measured and is first-order. This intermediate has been proposed to be a diimine or quinoneimine species.

It has been confirmed that the primary electro-oxidation product of uric acid and xanthine is a diimine species. This diimine is very unstable in solution and is rapidly hydrated to an imine-alcohol in a first-order

reaction. The imine-alcohol may be observed as a further intermediate by its u.v. absorption spectrum. The hydration of this species to uric acid-4,5-diol was determined to be first-order and the solution rate constant was measured.

The effect of 9-methyl substitution on the electrochemical oxidation of uric acid and xanthine has been studied and the results compared to those for uric acid and xanthine. The electrooxidation of 9-methyluric acid proceeds similarly to that of uric acid except that the corresponding imine-alcohol absorbs at shorter wavelengths than that of uric acid. The kinetics of hydration of this species was also measured. The electrooxidation of 9-methylxanthine is more complex and proceeds by two processes. The first process apparently occurs in a manner similar to that for xanthine. The second process very likely involves oxidation of 9-methylxanthine to some dimeric species which can be further oxidized to an unstable species.

The electrochemical oxidation of xanthosine (9-ribosylxanthine) was shown to be nearly identical to that of 9-methylxanthine.

These electrooxidations were studied using cyclic voltammetry, double potential step chronoamperometry, controlled potential coulometry, and thin-layer spectro-

electrochemistry. Methods for screening commercial samples of xanthosine for xanthine and for removing inorganic phosphate from organic electrooxidation products were also developed and described.

CHAPTER 8

REFERENCES

1. E. Fischer, Ber. Dtsch. Chem. Ges., 17, 329 (1884).
2. E. Fischer, Ber. Dtsch. Chem. Ges., 30, 558 (1897).
3. R. K. Robins, Heterocyclic Compounds, 8, 162 (1967).
4. G. Dryhurst, Electrochemistry of Biological Molecules, Academic Press, New York, 1977, pp. 71-74.
5. A. Albert and D. J. Brown, J. Chem. Soc., 157, 2060 (1954).
6. "Properties of Nucleic Acid Derivatives," 5th rev. ed., Calbiochem, Los Angeles, California, 1964.
7. F. Bergmann and S. Dikstein, J. Am. Chem. Soc., 77, 691 (1955).
8. C. L. Angell, J. Chem. Soc., 164, 504 (1961).
9. C. H. Willits, J. C. Decius, K. L. Dille, and B. E. Christiensen, J. Am. Chem. Soc., 77, 2569 (1955).
10. C. W. Scheele, Opuscula, 2, 73 (1776).
11. Marcet, "An Essay on the Chemical History and Medical Treatment of Calculous Disorders," London, 1817, pp. 95-107 (Cited in Robins[3]).

12. F. B. Brown, J. C. Cain, D. E. Grant, L. F. J. Parker, and E. L. Smith, Biochem. J., 59, 82 (1955).

13. Runge, "Neuste Phytochemische Entdeckungen," Vol. I, p. 144, Berlin, 1820, (Cited in Robins[3]).

14. A. Woskresensky, Ann. Chem. Pharm., 41, 125 (1942).

15. A. Kossel, Ber. Dtsch. Chem. Ges., 21, 2164 (1888).

16. E. H. Rodd, ed., Chemistry of Carbon Compounds, Vol. IVc, Elsevier Publishing Co., New York, 1959, pp. 1663-1671.

17. F. G. Mann and J. W. Porter, J. Chem. Soc., 148, 751 (1945).

18. V. Papesch and E. F. Schroeder, Med. Chem. (N.Y.), 3, 175-237 (1956).

19. L. S. Goodman and A. Gilman, eds., The Pharmacological Basis of Therapeutics, 3rd ed., Macmillan, New York, 1967, p. 355.

20. E. E. Conn and P. K. Stumpf, Outlines of Biochemistry, 2nd ed., Wiley, New York, 1967.

21. G. Dryhurst, Electrochemistry of Biological Molecules, Academic Press, New York, 1977, pp. 1-5.

22. R. S. Nicholson and I. Shain, Anal. Chem., 36, 706 (1964).

23. J. Pech, Collect. Czech. Chem. Commun., 6, 126 (1934).

24. J. C. Heath, Nature, 158, 23 (1946).

25. D. Hamer, D. M. Waldron, D. L. Woodhouse, Arch. Biochem. Biophys., 47, 272 (1953).

26. D. L. Smith and P. J. Elving, J. Am. Chem. Soc., 84, 1412 (1962).

27. G. Dryhurst, Electrochemistry of Biological Molecules, Academic Press, New York, 1977, pp. 80-127.

28. G. Dryhurst, Electrochemistry of Biological Molecules, Academic Press, New York, 1977, pp. 71-185.

29. P. J. Elving, W. A. Struck, and D. L. Smith, Mises Point Chim. Anal. Org. Pharm. Bromatol., 14, 141 (1965).

30. R. N. Adams, Electrochemistry of Solid Electrodes, Marcel Dekker, Inc., New York, 1969, p. 19-42.

31. A. L. Beilby, W. Brooks, and G. L. Lawrence, Anal. Chem., 36, 22 (1964).

32. F. J. Miller and H. E. Zittel, Anal. Chem., 35, 1866 (1963).

33. L. Chuang, I. Fried, and P. J. Elving, Anal. Chem., 36, 2426 (1964).

34. R. E. Panzer and P. J. Elving, J. Electrochem. Soc., 119, 864 (1972).

35. G. Dryhurst, Anal. Chim. Acta, 57, 137 (1971).

36. D. Keilin and E. F. Hartree, Proc. R. Soc. London, Ser. B, 119, 114 (1936).

37. R. Bentley and A. Neuberger, Biochem. J., 52, 694 (1952).

38. K. Agner, Acta Physiol. Scand., Suppl., 8, 5 (1941).

39. K. Agner, Acta Chem. Scand., 12, 89 (1958).

40. K. G. Paul and Y. Avi-Dor, Acta Chem. Scand., 8, 637 (1954).

41. E. S. Canellakis, A. L. Tuttle, and P. P. Cohen, J. Biol. Chem., 213, 397 (1955).

42. R. R. Howell and J. B. Wyngaarden, J. Biol. Chem., 235, 3544 (1960).

43. G. Soberon and P. P. Cohen, Arch. Biochem. Biophys., 103, 331 (1963).

44. T. Matsuura and I. Saito, Chem. Commun., 693 (1967).

45. T. Matsuura and I. Saito, Tetrahedron, 24, 6609 (1968).

46. M. I. Simon and H. Van Vanukis, Arch. Biochem. Biophys., 105, 197 (1964).

47. K. Zenda, M. Saneyoshi, and G. Chihara, Chem. Pharm. Bull., 13, 1108 (1965).

48. E. C. B. Anmann and V. H. Lynch, Biochim. Biophys. Acta, 120, 181 (1966).

49. J. Holian and W. M. Garrison, J. Phys. Chem., 71, 462 (1967).

50. J. Holian and W. M. Garrison, Chem. Commun., 676 (1967).

51. F. Fichter and W. Kern, Helv. Chim. Acta, 9, 429 (1926).

52. D. L. Smith and P. J. Elving, Anal. Chem., 34, 930 (1962).

53. W. A. Struck and P. J. Elving, Biochemistry, 4, 1343 (1965).

54. G. Dryhurst, J. Electrochem. Soc., 119, 1659 (1972).

55. G. Dryhurst, Electrochemistry of Biological Molecules, Academic Press, New York, 1977, p. 130.

56. G. Dryhurst, Top. Curr. Chem., 34, 47 (1972).

57. G. Dryhurst, J. Electrochem. Soc., 116, 1411 (1969).

58. B. H. Hansen and G. Dryhurst, J. Electroanal. Chem., 30, 417 (1971).

59. R. Brdička and E. Knoblock, Z. Elektrochem., 47, 721 (1941).

60. J. R. Merkel and W. J. Hickerson, Biochim. Biophys. Acta, 14, 303 (1954).

61. J. J. Lingane and O. L. Davis, J. Biol. Chem., 137, 567 (1941).

62. J. Pinson and J. Armand, Collect. Czech. Chem. Commun., 36, 585 (1971).

63. S. Kwee and H. Lund, Acta Chem. Scand., 25, 1813 (1971).

64. P. Zuman, Chem. Listy, 46, 688 (1952).

65. P. L. Pickard and S. H. Jenkins, J. Am. Chem. Soc., 75, 5899 (1953).

66. L. Holleck and B. Kastening, Z. Elektrochem., 60, 127 (1956).

67. B. M. Visinski and G. Dryhurst, J. Electroanal. Chem., 70, 199 (1976).

68. W. V. Childs, J. T. Maloy, C. P. Keszthelyi and A. J. Bard, J. Electrochem. Soc., 118, 874 (1971).

69. R. W. Murray, W. R. Heineman, and G. W. O'Dom, Anal. Chem., 39, 1666 (1967).

70. R. N. Adams, Electrochemistry at Solid Electrodes, Marcel Dekker, Inc., New York, 1969, p. 276.

71. L. Meites, Polarographic Techniques., 2nd ed., Wiley, New York, 1965, p. 441.

72. A. T. Hubbard and F. C. Anson, Electroanalytical Chemistry, Vol. 4, p. 179, A. J. Bard, ed., Marcel Dekker, New York, 1970.

73. G. B. Barlin and W. Pfleiderer, J. Chem. Soc. (B), 1425, 1971.

74. K. A. Connors, Reaction Mechanisms in Organic Analytical Chemistry, Wiley, New York, 1973, p. 76.

75. R. N. Adams, Electrochemistry at Solid Electrodes, Marcel Dekker, Inc., New York, 1969, p. 356.

76. R. N. Adams, Electrochemistry at Solid Electrodes, Marcel Dekker, Inc., New York, 1969, p. 23.

77. W. R. Heineman, B. J. Norris, and I. F. Goelz, Anal. Chem., 47, 79 (1975).

78. R. C. Weast, ed., Handbook of Chemistry and Physics, 52nd ed., Chemical Rubber Co., Cleveland, 1971-72, p. C-205.

79. G. Dryhurst, M. Rosen, and P. J. Elving, Anal. Chim. Acta, 42, 143 (1968).

80. J. W. Strojek, G. A. Gruver, and T. Kuwana, Anal. Chem., 41, 481 (1969).

81. M. S. Denton, T. P. DeAngelis, A. M. Yacynych, W. R. Heineman, and T. W. Gilbert, Anal. Chem., 48, 20 (1976).

82. J. L. Owens and G. Dryhurst, J. Electroanal. Chem., 80, 171 (1977).

83. G. Dryhurst and P. K. De, Anal. Chim. Acta, 58, 183 (1972).

84. H. A. Marsh, Jr. and G. Dryhurst, unpublished work.

85. R. N. Adams, Electrochemistry at Solid Electrodes, Marcel Dekker, Inc., New York, 1969, p. 194.

86. E. A. Johnson, Biochem. J., 51, 133 (1952).

87. L. F. Cavalieri, J. J. Fox, A. Stone, and N. Chang, J. Amer. Chem. Soc., 76, 1119 (1959).

88. R. N. Adams, Electrochemistry at Solid Electrodes, Marcel Dekker, Inc., New York, 1969, p. 207.

89. Jordan, The Nucleic Acids, Vol. 1, p. 447, E. Chargaff and J. N. Davidson, eds., Academic Press, New York, 1955.

90. L. Meites, Polarographic Techniques, 2nd ed., Wiley, New York, 1965, p. 527.

91. B. H. Hansen and G. Dryhurst, J. Electroanal. Chem., 32, 405 (1971).

92. M. T. Cleary and G. Dryhurst, work in progress.

93. H. A. Sober, ed., Handbook of Biochemistry, 2nd ed., Chemical Rubber Co., Cleveland, 1970, p. G-52.

94. H. Kinoshita and G. Dryhurst, unpublished work.

95. K. Fink and W. S. Adams, J. Chromatog., 22, 118 (1966).

96. K. Fink, R. E. Cline and R. M. Fink, Anal. Chem., 35, 389 (1963).

97. L. Rossi and C. Rossi, J. Chromatog., 30, 278 (1967).

98. N. Kolassa, H. Roos, and K. Pfleger, J. Chromatog., 66, 175 (1972).

99. E. Gerlach, R. H. Dreisbach, and B. Deuticke, J. Chromatog., 18, 81 (1965).

100. G. Tortolani and M. E. Colosi, J. Chromatog., 70, 182 (1972).

101. P. R. Brown, S. Bobick, and F. L. Hanley, J. Chromatog., 99, 587 (1974).

102. G. Dryhurst, Bioelectrochem. Bioenergetics, 1, 49 (1974).

103. G. Dryhurst, Anal. Chim. Acta, 57, 137 (1971).

104. G. Dryhurst, Talanta, 19, 769 (1972).

105. R. C. Weast, ed., Handbook of Chemistry and Physics, 53rd ed., Chemical Rubber Co., Cleveland, 1972-73, p. C-539.

106. H. A. Sober, ed., Handbook of Biochemistry, 2nd ed., Chemical Rubber Co., Cleveland, 1970, pp. G-21, G-52.

107. M. T. Cleary and G. Dryhurst, Anal. Chim. Acta, submitted, 1977.

108. P. Flodin, J. Chromatog., 5, 103 (1961).

109. M. W. Neal and J. R. Florini, Anal. Biochem., 55, 328 (1973).

110. F. C. Saville, Comprehensive Analytical Chemistry, Vol. IIB, p. 241, C. L. Wilson and D. W. Wilson, eds., Elsevier, Amsterdam, 1968.

111. S. Kato, B. M. Visinski, and G. Dryhurst, J. Electroanal. Chem., 66, 21 (1975).

112. G. M. Richardson and R. R. Cannon, Biochem. J., 23, 68 (1929).

113. D. Seligson and H. Seligson, J. Biol. Chem., 190, 647 (1951).

114. G. Dryhurst, B. H. Hansen, E. B. Harkins, J. Electroanal. Chem., 27, 375 (1970).

115. J. C. Andrews, I. T. Sell, Arch. Biochem. Biophys., 56, 405 (1955).

116. B. L. Karger, L. R. Snyder, and C. Horvath, An Introduction to Separation Science, Wiley, New York, 1973, p. 147.

117. Materials, Equipment and Systems for Chromatography, Electrophoresis, and Membrane Technology, Bio-Rad Laboratories, Richmond, California, 1975, p. 13.

118. G. Dryhurst and G. F. Pace, J. Electrochem. Soc., 117, 1259 (1970).

119. I. Smith, ed., Chromatographic and Electrophoretic Techniques, 2nd ed., Vol. 1, Interscience, New York, 1960, pp. 41-65.

120. C. H. Sorum, Introduction to Semimicro Qualitative Analysis, 3rd ed., Prentice-Hall, Englewood Cliffs, New Jersey, 1960, p. 200.

121. A. I. Vogel, A Textbook of Macro and Semimicro Qualitative Inorganic Analysis, 4th ed., Longman, London, 1960, p. 577.